



Norwegian University of
Science and Technology

Quantification of Bacterial Adhesion and Characterization of Polymeric Pristine and Modified UF Membranes

Anissa Hasane

Civil and Environmental Engineering

Submission date: July 2016

Supervisor: Cynthia Halle, IVM

Norwegian University of Science and Technology
Department of Hydraulic and Environmental Engineering

Quantification of Bacterial Adhesion and Characterization of Polymeric Pristine and Modified UF Membranes

Anissa Hasane

July 2016

MASTER'S THESIS

Department of Hydraulic and Environmental Engineering

Norwegian University of Science and Technology

Supervisor: Associate Professor Cynthia Halle (Norwegian University of Science and Technology)

Co-Supervisor: Associate Professor Santiago Romero Vargas Castrillón (University of Minnesota)

Preface

This Master's thesis is the final part of the Civil and Environmental Engineering program at The Norwegian University for Science and Technology (NTNU). It was carried out during the spring semester of 2016. The research was done at the Department of Civil, Environmental, and Geo- Engineering at the University of Minnesota (UMN) in Minneapolis. It was enabled through a cooperation between UMN and NTNU.

I always had a great interest in membrane technology, as I believe they are important processes that will contribute in solving the future's water issues. When this project was sent to me, I was first intimidated by its complexity. I had never heard of the techniques that I was to apply and had little experience in laboratory work. Luckily, I convinced myself on taking on this challenge, and did not regret. This project has taught me a lot, and being able to use state-of-the-art techniques as well as doing research in the United States has been an unforgettable experience.

This thesis is oriented towards readers that have an interest in membrane technology. I have tried to break down and explain the different topics to a level that does not require expertise in the field by covering the necessary background in Chapters 2, 3 and 4.

Trondheim, 2016-07-21

A handwritten signature in black ink that reads "Anissa Hasane". The signature is written in a cursive style with a white background behind the text.

Anissa Hasane

Acknowledgment

First and foremost I would like to express my humble gratitude to all those involved in the work culminating this thesis, for taking interest in my project and sharing their knowledge.

I would like to acknowledge my supervisor Associate Professor Cynthia Halle (Norwegian University of Science and Technology) for her valuable inputs on my writing and her thoughtful and much appreciated advices for guiding and pushing me towards the fulfilment of this thesis.

Further, I would like to thank my co-supervisor Associate Professor Santiago Romero Vargas Castrillón (University of Minnesota) for welcoming me to his lab with open arms, providing excellent support and pushing me to strive for good work in the lab.

If there is someone I could not have done it without, it's Phd. student Sara BinAhmed (University of Minnesota). Thank you for teaching me all you knew about AFM and bacteria, for spending all those long hours in the lab, for always providing a granola-bar snack and for innumerable laughs about things only we could find funny.

I would also like to thank graduate student Nathan Karp (University of Minnesota) for showing me how to make membranes and doing contact angle measurements.

Post-doc Mehdi Jeddi-Karzar (University of Minnesota) also deserves a warm thank you for being a great office-buddy, always making me laugh, providing help with Latex and of course sharing his knowledge about fluid mechanics.

I am grateful for the opportunity I had to travel to the United States through the UMN-NTNU project thanks to the Norwegian center for international cooperation in education (SIU)'s partnership program with North America.

I am also thankful for the generous scholarship I was granted by Norsk Vannforening and for all the help the Department of Hydraulic and Environmental Engineering has provided over the years.

I was lucky to travel with Ida Engan who made it easier to be far away from home. Thank you for all the laughs and for attempting to make me speak "trøndersk".

I would also like to thank Mohammed Harrak for helping me through those five years of hard studies, I could not have asked for greater support.

Finally, I must express my very profound gratitude to my parents, and to my little brother for providing me with unfailing support and continuous encouragement throughout my years of study and through the process of researching and writing this thesis. This accomplishment would not have been possible without them. Thank you.

Anissa Hasane

Abstract

Membrane filtration is an important technology that might help solving future challenges regarding the access to potable drinking water. One of the main challenges in membrane operations is biofouling. Biofouling is the formation of a biofilm on the membrane surface. It deteriorates the system performance, leads to higher operating pressure and a reduced life of the membrane (Ridgway and Flemming, 1996). Bacteria accumulate on surfaces by adhesion and growth, feeding on easily assimilable organics present in the feed stream (Machenbach, 2007). In order to make this technology more accessible and cost-efficient, an optimization is necessary.

Membrane surface modification can reduce fouling by altering the surface properties and weakening the membrane-foulant interactions. In this study, the efficiency of polydopamine (PDA) as an anti-foulant was studied. PDA is naturally found in mussels and is a result of the oxidization of dopamine (Lee et al., 2007).

Polysulfone (PSF) ultrafiltration (UF) membranes were fabricated using wet phase-inversion process and coated with 4g/L PDA. The membranes were characterized both before (PSF) and after coating (PSF-PDA). The hydrophobicity, permeability and roughness were determined using contact angle measurements, finding the pure water flux and Atomic Force Microscopy (AFM) respectively. The bacterial adhesion was then quantified using AFM and single cell force spectroscopy (SCFS). A single *P.fluorescens* was immobilized on a PDA-coated cantilever and measurements were taken over both membrane types. The applied force was 600 pN for all the curves, and the contact time varied between 0s, 2s and 5s.

The hydrophilicity increased significantly when coating. Not only does this have a positive effect on the reduction of bacterial adhesion, but it also might have contributed in increasing the permeability.

The roughness did not increase much, but when scanning over larger areas, some nanoaggregates could be observed.

The obtained force curves showed that the force of adhesion (F_{adh}) increased with an

increasing contact time. The contact time did not have a statistical significant impact on the rupture length (L_{rup}), one can therefore conclude that bond strengthening does not involve a sequence of different adhesins, but rather an increasing number of adhesins increasing the interaction.

The adhesion force decreased drastically when obtained on modified membranes. These results are promising in regards of using PDA as an anti-foulant on UF membranes.

However, the tests were performed under highly simplified conditions and the coating should be subject to further testing.

Sammendrag

Membranfiltrering er en viktig teknologi som kan bidra til å løse fremtidens utfordringer når det gjelder tilgang til rent drikkevann. En av hovedutfordringene i membranoperasjoner er biofouling. Biofouling er dannelsen av en biofilm på membranoverflaten. Den forringer systemets ytelse, fører til høyere driftstrykk og en redusert levetid for membranen (Ridgway and Flemming, 1996). Bakterier samler seg på overflaten, setter seg fast og gror. De skaffer næring fra lett assimilerbare organiske stoffer som er tilstede i vannet (Machenbach, 2007). For å gjøre denne teknologien mer tilgjengelig og kostnadseffektiv, er en optimalisering nødvendig.

Membranoverflatemodifikasjon kan redusere biofouling ved å endre overflateegenskapene og svekke interaksjonene mellom membranen og bakteriene. I dette studie ble effektiviteten av polydopamine (PDA) som en "anti-foulant" undersøkt. PDA finnes naturlig i blåskjell, og er et resultat av oksidering av dopamin (Lee et al., 2007).

Polysulfone (PSF) ultrafiltreringsmembraner (UF) ble fabrikkert ved hjelp av våt fase-inversjon prosess og belagt 4 g/L PDA. Membranene ble karakterisert både før (PSF) og etter belegging (PSF-PDA). Hydrofobiteten, permeabiliteten og ruheten ble bestemt ved hjelp av kontaktvinkelmålinger, finne "pure water flux" og "Atomic Force Microscopy (AFM)". Bakterienes festeevne ble deretter kvantifisert ved hjelp av AFM og "single cell force spectroscopy" (SCFS). En *P. fluorescens* celle ble immobilisert på en PDA-belagt probe og målinger ble tatt over begge membrantypene. Den tilførte kraften var 600 pN for alle kurvene, og kontakttiden varierte mellom 0s, 2s og 5s.

Hydrofobiteten sank betydelig med PDA belegging. Dette har ikke bare en positiv effekt på reduksjon av bakteriell adhesjon, men det også kan ha bidratt til å øke permeabiliteten.

Ruheten økte ikke mye, men under skanning av større områder, kunne noen nanoaggregater ses. linje De oppnådde kurvene viste at styrken av adhesjonen (F_{adh}) økte med økende kontakttid. Kontakttiden hadde ikke en statistisk signifikant innvirkning på bruddlengden (L_{rup}), man kan derfor konkludere med at bindingens styrking ikke

involverer en sekvens av forskjellige adhesiner, men snarere et økende antall adhesin. Adhesjonskraften reduseres drastisk på modifiserte membraner. Disse resultatene er lovende i forhold til å bruke PDA som en ”anti-foulant” på UF-membraner. Testene ble utført under sterkt forenklede forhold, og PDA-beleggingen bør derfor være gjenstand for ytterligere testing.

Contents

Preface	ii
Acknowledgment	iii
Abstract	v
Sammendrag	vii
List of Figures	xiii
List of Tables	xvii
Abbreviations	xviii
1 Introduction and Conceptual Framework	1
1.1 Background and Motivation	1
1.2 Project Description	2
1.3 Goals and Questions	3
1.4 Thesis Structure	4
2 Membrane Technology	5
2.1 Introduction and History	5
2.2 Membrane Types and Separation Mechanisms	6
2.3 Flow Regime and Operation	9
2.4 Hydraulics of Flow Through Porous Membranes	10
2.5 Polymeric Membranes	12

2.5.1	Immersion Precipitation and the Wet Phase Inversion Process	12
2.5.2	Polysulfone and Polyvinylpyrrolidinone Membranes	16
2.6	Membrane Fouling	17
2.6.1	Biofouling	18
2.7	Membrane Modification to Prevent Biofouling	19
3	Bacterial Adhesion	22
3.1	Bacterial Cell Structure	22
3.1.1	Cell Wall	22
3.1.2	Capsule and slime layers	23
3.1.3	Flagella	24
3.1.4	Fimbriae and Pili	24
3.2	Interaction With Membrane Surfaces	25
3.2.1	Biofilm	25
3.2.2	Factors influencing bacterial adhesion	27
4	Atomic Force Microscopy	31
4.1	Single Cell Force Spectroscopy	33
5	Methodology	37
5.1	Membrane Fabrication by Phase Inversion	37
5.2	Membrane Modification: PDA coating	38
5.3	Membrane Characterization	39
5.3.1	Hydrophobicity	39
5.3.2	Permeability	40
5.3.3	Roughness	41
5.4	Quantification of Adhesion	41
5.4.1	The Experimental Set-Up	41
5.4.2	AFM calibration	46
5.4.3	AFM force measurements with bacterial probe	48

<i>CONTENTS</i>	xi
5.4.4 Viability assay of the immobilized bacteria	50
5.4.5 Data Analysis	50
5.4.6 Control Measurements	54
6 Results and Discussion	56
6.1 Membrane characterization	56
6.1.1 Hydrophobicity	56
6.1.2 Permeability	57
6.1.3 Roughness	58
6.2 Quantification of Bacterial Adhesion	60
6.2.1 Adhesion profiles	60
6.2.2 Statistical significance	66
6.2.3 Control measurements	67
6.2.4 Adhesion force and rupture length	69
6.2.5 PDA as an anti-foulant	73
7 Conclusion and Further Work	75
7.1 Conclusion	75
7.2 Recommendations for Further Work	76
Bibliography	78
A Protocols for conducted laboratory work	84
A.1 Protocol for fabricating and modifying the polymeric membranes	84
A.1.1 Making the dope solution	84
A.1.2 Making the membranes	86
A.1.3 Coating the membranes with Polydopamine	88
A.2 Protocol for bacterial culture	90
A.2.1 Preparing the culture	90
A.2.2 Diluting the solution	92

<i>CONTENTS</i>	xii
A.2.3 Collecting the bacteria and preparing the fluorescent dye	95
A.3 Protocol for preparing the probe	96
A.4 Protocol for gluing the sample of membrane	99
A.5 Protocol for determining the flux and permeability of a membrane . . .	100
B Pressure on a single cell on a membrane surface	103
C T-tests	105

List of Figures

2.1.1 Schematic of a membrane treatment process	6
2.2.1 Hierarchy of membrane processes. (Hand et al., 2012)	7
2.2.2 Mechanisms for rejection in membrane filtration. (a) Straining (b) Adsorption (c) Cake filtration (Hand et al., 2012)	8
2.3.1 Illustration of dead-end and cross-flow regimes (Ødegaard et al., 2012).	9
2.4.1 Schematic representation of the simplification to parallel cylindrical pores perpendicular to the membrane surface.	11
2.5.1 Schematic representation of immersion precipitation; P, polymer; S, solvent; NS, non-solvent.	13
2.5.2 Composition paths of a cast film after immersion featuring instantaneous and delayed mixing for $t < 1s$	13
2.5.3 Different membrane morphologies caused by different types of demixing. the figure is adapted from Guillen et al. (2011) and has been modified by the author.	15
2.5.4 The principle of screen filtration in anisotropic membranes (Richard et al., 2004).	16
2.5.5 The molecular structure PSF	16
2.5.6 The molecular structure of PVP.	17
3.1.1 Cell walls of bacteria (Madigan et al., 2015).	23
3.1.2 LPS structure (Madigan et al., 2015).	23

4.0.1 A schematic illustration of AFM.	32
4.1.1 A schematic illustration of SFCS with an immobilized cell.	34
4.1.2 Illustration of the process of making a single-cell bacterial probe (Zeng et al., 2014).	36
5.1.1 Illustration of the process of wet phase inversion using NMP as a solvent, and PSF+PVP as polymers.	38
5.2.1 Illustration of the PDA coating of membranes.	39
5.3.1 Illustration of contact angles (θ) formed by a water droplet on a smooth surface.	40
5.4.1 The cantilever placed in its holder.	43
5.4.2 This picture shows the cantilever and a rod shaped <i>P.fluorescens</i> (circled in green) right before immobilization.	44
5.4.3 <i>P.fluorescens</i> immobilized on a cantilever looked at through a 60x lens and fluorescent microscopy.	45
5.4.4 (a) The cell is placed too far in, and the cantilever is touching the surface when doing measurements. (b) The cell is positioned properly and is the only thing in contact with the surface when doing measurements.	45
5.4.5 A force curve taken on a PSF membrane with a bacterial probe, at a force of 600 pN and a contact time of 0s. The red curve shows the extraction, and the blue curve the retraction. The red curve has a sinusoidal shape due to optical interference.	46
5.4.6 Cantilever C, MLCT0. The laser beam was placed on the triangle's leg to avoid optical interference	47
5.4.7 Illustration explaining how a force curve was obtained.	49
5.4.8 A force curve taken with a <i>P.fluorescens</i> cell at a set point of 600 pN, 5s contact time over a PSF membrane.	51

5.4.9 Illustration of the performed modifications on a force vs. separation curve. The measurement was taken with a <i>P.fluorescens</i> cell at a set point of 600 pN, 5s contact time and over a PSF membrane. (a) Raw force vs separation curve. (b) After line subtract (c) Only displaying the retraction after x and y offset.	53
6.1.1 The mean and standard deviation of contact angle measurements performed on PSF and PSF-PDA membrane. The measurements were performed by Nathan Karp and obtained through personal communication.	57
6.1.2 AFM images of (a) PSF and (b) PSF-PDA membranes.	59
6.1.3 AFM images of (a) 20-by-20 μm and (b) 10-by-10 μm PSF-PDA membranes. The white spots on the images are PDA nanoaggregates and the black lines are artifacts	60
6.2.1 A force-separation curve obtained with a single <i>P.fluorescens</i> cell at a set point of 600 pN, 2s contact time and over a PSF membrane	61
6.2.2 Three force-separation curves obtained at the same spot with a single <i>P.fluorescens</i> cell at a set point of 600 pN, 0s contact time and over a PSF membrane	62
6.2.3 Force-separation curve obtained at a set point of 600 pN, 2s contact time and over a PSF membrane. No cell was immobilized.	68
6.2.4 Force-separation curve obtained at a set point of 600 pN, 2s contact time and over a PSF-PDA membrane. No cell was immobilized.	68
6.2.5 The mean of F_{adh} for both membrane types and the three contact times. No cell was immobilized.	69
6.2.6 The mean of L_{rup} for both membrane types and the three contact times. No cell was immobilized.	69
6.2.7 Normalized histograms of F_{adh} for (a) PSF membrane and (b) PSF-PDA membrane.	70

6.2.8 Normalized histograms of L_{rup} for (a) PSF membrane and (b) PSF-PDA membrane.	71
6.2.9 (a) The mean of F_{adh} for both membrane types and the three contact times. (b) The mean of L_{rup} for both membrane types and the three contact times.	72
A.1.1 The membranes in the casting frame	89
A.2.1 The Necessary equipment	91
A.2.2 Blank LB	93
A.2.3 Taped flask in the incubator	94
A.3.1 AFM probe soaked in Polydopamine	97
A.3.2 Desiccator with Nitrogen flow	98
A.5.1 The set-up for determining the flux and permeability.	102

List of Tables

5.4.1	Calibrated parameters	47
5.4.2	Distribution and the amount of obtained force curves.	51
6.1.1	Measured permeability of PSF and PSF-PDA samples.	58
6.1.2	R_{RMS} of PSF and PSF-PDA membranes. The roughness was found using AFM in topography mode. 6 1-by-1 μm images were obtained for PSF membranes, and 5 1-by-1 μm images for PSF-PDA	59
6.2.1	Typical patterns observed for force-curves on PSF membranes.	64
6.2.2	Typical patterns observed for force-curves on PSF-PDA membranes.	65
6.2.3	T-tests of F_{adh} and L_{rup} with regards to contact time. <i>OK</i> means that there is a statistically significant difference between the two groups, whereas <i>Failed</i> means that there is not a statistically significant difference.	66
6.2.4	T-tests of F_{adh} and L_{rup} with regards to the membrane type. <i>OK</i> means that there is a statistically significant difference between the two groups, whereas <i>Failed</i> means that there is not a statistically significant difference.	67

Abbreviations

AFM Atomic force microscopy

L-DOPA L-3,4-dihydroxyphenylalanine

MF Microfiltration

NF Nanofiltration

NOM Natural organic matter

PSF Polysulfone

PDA Polydopamine

PVP Polyvinylpyrrolidone

P.fluorescence Pseudomonas fluorescence

RO Reverse osmosis

SCFS Single cell force spectroscopy

UF Ultrafiltration

Chapter 1

Introduction and Conceptual Framework

1.1 Background and Motivation

Water is crucial for all aspects of life, but fresh, accessible water is a scarce and unevenly distributed resource (Corcoran, 2010). Approximately 97,5 % of all water is found in the sea and oceans, of the remaining water, only 0,50-1 % are considered as exploitable freshwater resources (Ødegaard et al., 2012).

The quality of water is a fundamental part to all the roles that water plays in our lives. Access to safe water has been classified as a human right by the United Nations in 2010, but today, this necessity is not yet accessible to everyone. In 2014, water-borne diseases caused by inadequate drinking water sanitation and hygiene have been estimated to cause 842 000 diarrheal disease death. The scarcity of clean and potable water, combined with both climate change and an exponential population growth are important challenges that today's society needs to address (United-Nations, 2010).

Water treatment, for treating or reclaiming wastewater and treating drinking water,

is therefore of great importance. Most developed nations have built treatment plants collecting and treating wastewater before releasing it. However, other countries have taken this even further. Singapore and the US are examples of countries that have adopted the practice of reclaiming wastewater. Singapore's first NEWater plant, distributing recycled wastewater, was completed in May 2000 (PUB, 2015), followed by The Orange County District in California in 2008, which recycles wastewater for potable use (Monks, 2014). In both those examples, membrane filtration is a key step in the treatment. These processes are very energy demanding, and costly especially due to fouling. Fouling is a major challenge for water purification membranes. Fouling occurs when solutes or particles in a feed solution accumulate in the membrane pores or on the membrane surface, thus reducing the membrane's permeability and performance. In order to make it more accessible, especially to developing countries, an optimization is necessary. Membrane surface modification can reduce fouling by altering the surface properties and weakening the membrane-foulant interactions (Kasemset et al., 2016).

1.2 Project Description

Remark: The following description was written by Associate Professor Santiago Romero Vargas Castrillon.

The colonization of membrane surfaces by microbial communities, a process known as biofouling, constitutes a major technical problem in water treatment processes such as seawater desalination and wastewater reuse by reverse osmosis. Biofouling results in a decreasing permeate flux, selectivity and useful life of the membrane. Biofilm formation begins with the reversible adhesion of bacterial cells on the surface of the membrane. Consequently, efficient biofouling mitigation and prevention strategies should focus on gaining a fundamental understanding of, and formulating strategies to interrupt, the

reversible forces underlying bacterial cell adhesion.

In the study proposed herein, we will elucidate the mechanism of adhesion between bacterial cells and polymeric membrane surfaces. Toward this goal, we will use single-cell force spectroscopy (SCFS), an atomic force microscopy-based technique providing direct, quantitative information on the forces between extracellular appendages in bacteria and membrane surfaces. This investigation will allow us to understand and formulate effective coatings to prevent bioadhesion and biofouling.

1.3 Goals and Questions

Goals:

- Fabricate and modify polymeric membranes.
- Characterize the membranes before and after modification:
 - Permeability
 - Hydrophobicity
- Use AFM to find the topography and roughness before and after modification
- Use AFM to find the bacterial adhesion forces before and after modification

Hypothesis:

- PDA modification does not negatively affect the UF membrane's function and performance.
- PDA modification and the contact time have an impact on bacterial adhesion.

1.4 Thesis Structure

Chapter 1 This chapter introduces the thesis and presents its motivation as well as the hypothesis.

Chapter 2 This chapter presents the theoretical framework for membrane technology. Hydraulics of flow, membrane types, fabrication, modification and modules will be covered.

Chapter 3 This chapter will present bacterial adhesion and factors influencing it.

Chapter 4 Here, Atomic Force Microscopy will be presented. Both topography measurements and force spectroscopy will be introduced.

Chapter 5 The methodology chapter aims to present and describe the work conducted in the laboratory.

Chapter 6 In this chapter, the results from laboratory work will be presented and discussed.

Chapter 7 Here, the thesis will be concluded and recommendations for further work will be given.

Appendix In the appendix, detailed protocols, calculations and spreadsheets are attached.

Chapter 2

Membrane Technology

2.1 Introduction and History

Membrane processes are modern physiochemical separation techniques that cover the entire size range of water constituents, from particulate matter to dissolved organics and mineral salts. During membrane treatment, water is pumped against the surface of a membrane (see Figure 2.1.1). The incoming stream (Q_{In}) can either contain particulate (two-phased) or dissolved matter (single-phased). The pressure drives permeable matter (permeate) through the semipermeable membrane, whereas impermeable matter (retentate) is rejected through a waste stream (Q_w).

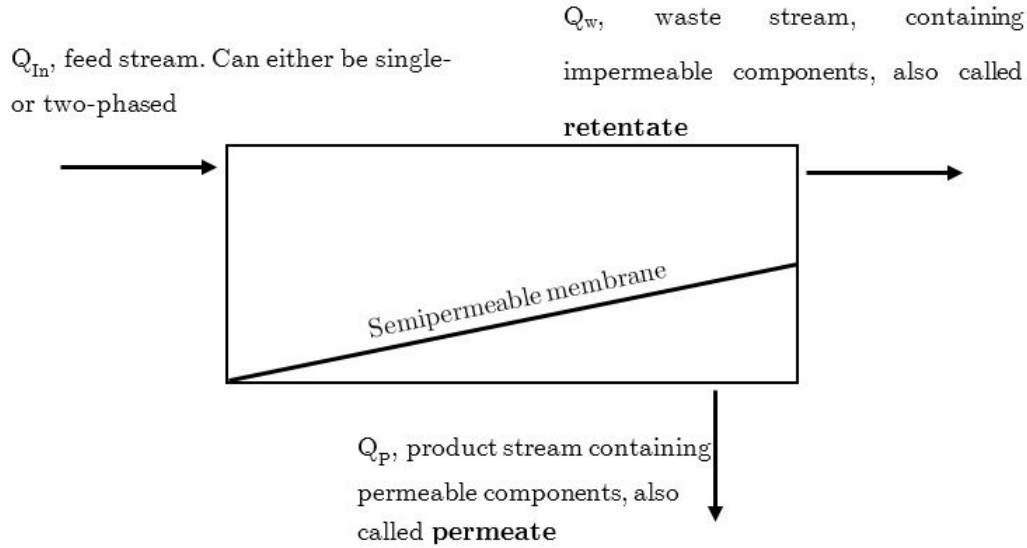


Figure 2.1.1: Schematic of a membrane treatment process

Microporous membranes were first patented in the 1920s and were mostly limited to laboratory purposes until the 1950s (Belfort et al., 1994). They were primarily used for identifying and enumerating bacteria and macromolecules. In the 1950s multiple industrial users began applying membrane filtration for treating waste water and sterilizing water. It is not until the 1980s that the first interest in membrane filtration for drinking water treatment arisen. New technology and treatment configuration made those processes more effective than the classical rapid granular filter (Hand et al., 2012). Their ability to separate both particulate and dissolved matter is one of the reasons for their popularity. Today, membrane processes are widely used in many industries, such as drinking water treatment and reclaiming waste water (Ødegaard et al., 2012).

2.2 Membrane Types and Separation Mechanisms

Membranes are divided into two categories: porous membranes and dense membranes. Porous membranes function by pore flow. This filtration process can be broadly defined

as a process separating particulate matter from a liquid phase (a two-phased system). Dense membranes, on the other hand, function by solution-diffusion. This process, also called reverse osmosis, is the separation of dissolved matter from a liquid phase (a single-phased system).

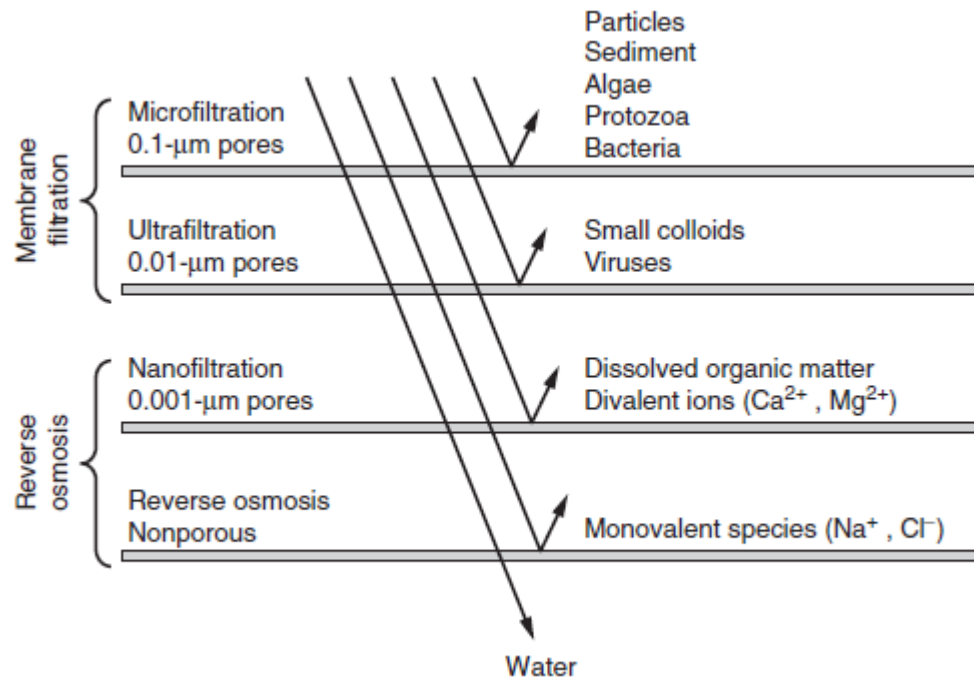


Figure 2.2.1: Hierarchy of membrane processes. (Hand et al., 2012)

As illustrated in Figure 2.2.1, there are four types of processes distinguished by the size and type of contaminants removed. Microfiltration (MF) and Ultrafiltration (UF) are so-called low-pressure processes operated typically at a pressure up to 3 bar (Machenbach, 2007). They both utilize straining through porous membranes as the separation mechanism. Reverse Osmosis (RO) is a high-pressure process operating at a pressure range from 30 to 85 bar (Hand et al., 2012). This process relies on semipermeable membranes and the principle of solution diffusion as a separation mechanism (Geise et al., 2010). Nanofiltration (NF) membranes are situated in between dense and porous membranes. Their pores are extremely small, causing a low or moderate rejection of higher valent ions, but a low rejection of monovalent ions (Geise et al., 2010).

The primary mechanism for removing particles in porous membranes is straining, but removal is also affected by two other mechanisms known as adsorption and cake formation.

Straining, also called sieving means that particles larger than the pores will be retained on the surface, while water and smaller particles will flow through Figure 2.2.2 (a) illustrates this process (Hand et al., 2012).

Natural organic matter (NOM) can adsorb to membrane surfaces and is the prime cause of membrane fouling by NOM (Jucker and Clark, 1994). Thus, particles that have a smaller diameter than the pores can also be rejected through adsorption (Figure 2.2.2 (b)). Adsorption is an important mechanism during early stages of filtration with a clean membrane, but its full capacity is quickly reached. This process on its own will not be efficient, but adsorbed material can reduce the size of voids through the membrane and therefore increase the ability of the membrane to retain smaller particles by straining (Hand et al., 2012).

As the filtration process goes, a clean membrane will quickly accumulate a cake of solids at the surface due to straining. This surface cake will act as an additional filter (Figure 2.2.2 (c)). This surface cake is often referred to as a "dynamic membrane" because it grows in thickness over time, and is partially or wholly removed during backwashing.

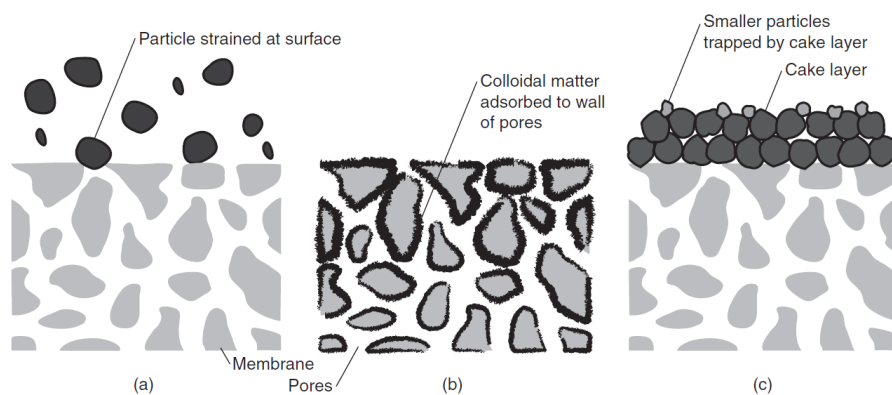


Figure 2.2.2: Mechanisms for rejection in membrane filtration. (a) Straining (b) Adsorption (c) Cake filtration (Hand et al., 2012)

2.3 Flow Regime and Operation

There are two methods to bring the water in contact with the membrane: dead-end and cross-flow regime. In dead-end filtration (Figure 2.3.1), the water is perpendicularly pressed towards the surface of the membrane. All the filtered material will therefore deposit on the surface, leading to increased fouling (Ødegaard et al., 2012). In cross-flow filtration, the feed water is pumped parallel to the membrane surface (Figure 2.3.1). The water is pumped at a high rate and velocity into the system. The velocity parallel to the surface creates a high shear force that reduces the development of a surface cake and reduces fouling. Typically, the permeate flow is less than 25% of the feed flow. Thus, big recirculation systems are required, but on the other hand, the membranes can have longer filtration cycles.

Whether or not one should choose a cross-flow over a dead-end configuration depends on the quality of the feed water. If the concentration of solids is low, the advantages of cross-flow filtration become less-significant. In addition, the pumping of recycling great amounts of water can triple the operating costs over dead-end flow (Glucina et al., 1998). In Norway, UF membranes are mainly used as the separation step after a coagulation/flocculation process, resulting in a high turbidity in the feed water. A dead-end flow would require more backwashing yielding short filtration cycles (Ødegaard et al., 2012). Cross-flow regimes are therefore the most common (Hem and Thorsen, 2008).

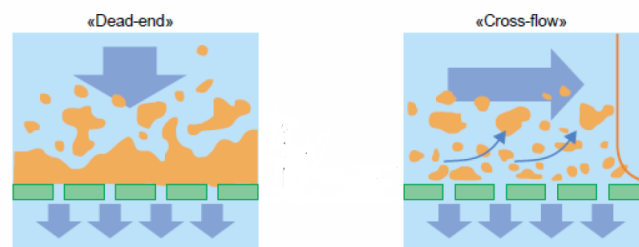


Figure 2.3.1: Illustration of dead-end and cross-flow regimes (Ødegaard et al., 2012).

2.4 Hydraulics of Flow Through Porous Membranes

This thesis brings into focus ultrafiltration membranes. Thus, only transport through porous membranes is presented. As mentioned in Section 2.5, there is a large variety in the possible pore geometries. Different models have been developed to adequately describe the transport in these different geometries. A simplification illustrated in Figure 2.4.1, is to consider the membrane as a number of equal, parallel cylindrical pores perpendicular to the membrane surface. The length of each of those pores is almost equal to the thickness of the membrane. The volume flux through the membrane can hence be described by the Hagen-Poiseuille equation (Mulder, 1991):

$$J = \frac{\epsilon}{r^2 8\mu\tau} \frac{\Delta P}{\Delta x} \quad (2.4.1)$$

The equation indicates that the solvent flux is proportional to the driving force, which in this case is ΔP across a membrane of thickness Δx and pore radius r . The factors η and τ are, respectively, the viscosity and the pore tortuosity (for cylindrical perpendicular pores, the tortuosity is equal to 1). The quantity ϵ is the surface porosity and is equal to the ratio of pore area to membrane area, A_m :

$$\epsilon = \frac{n_b \pi r^2}{A_m} \quad (2.4.2)$$

n_b is the total amount of pores.

The flux J is proportional to the membrane's resistance R_m (Hand et al., 2012):

$$J = \frac{\Delta P}{\mu} R_m \quad (2.4.3)$$

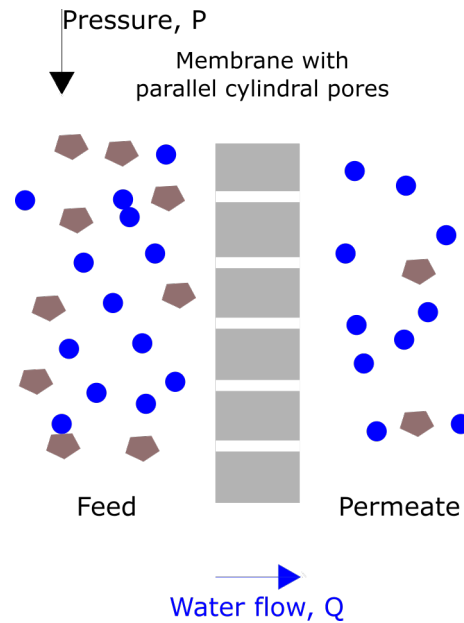


Figure 2.4.1: Schematic representation of the simplification to parallel cylindrical pores perpendicular to the membrane surface.

Where the membrane's resistance is defined as:

$$R_m = \frac{1}{\mu A} \quad (2.4.4)$$

A is defined as the membrane's permeability. The resistance is also a value utilized in the Resistance-in-Series model. Several factors can contribute to resistance to flow. As mentioned, there is the membrane's own resistance due to the pores, however when the membrane begins to foul, as covered in Section 2.6, each component of membrane fouling will add a new layer that is resistive to flow. It is assumed that each of these layers act independently from one another. The model can then be expressed as:

$$J = \frac{\Delta P}{\mu(R_m + R_c + R_i + R_p)} \quad (2.4.5)$$

Where R_c is the cake layer resistance coefficient, R_i the irreversible fouling resistance coefficient and R_p the pore construction resistance coefficient. Depending on the fouling type and the membrane, different resistance coefficients can be added. (Hand et al.,

2012)

2.5 Polymeric Membranes

There are two main types of membranes: ceramic and polymeric. Polymeric membranes are the most common membrane type for large-scale membrane applications such as municipal drinking water production and the treatment of waste water. They are cheaper and thereby more accessible than ceramic membranes, but are unfortunately more prone to fouling. Polymers such as polysulfone (PSF), polyvinylidene (PVDF), cellulose acetate, polyethersulfone (PES) and polypropylene (PP) are commonly used to produce MF or UF membranes (Pendergast and Hoek, 2011). In Norway, almost all the utilized membranes in drinking water treatment facilities are cellulose acetate membranes because they have a good resistance against fouling and are resistant to chlorine (Hem and Thorsen, 2008).

2.5.1 Immersion Precipitation and the Wet Phase Inversion Process

There are several techniques utilized to produce polymeric membranes. The oldest and most common is known as immersion precipitation (Figure 2.5.1). It consists of forming a concentrated layer of a polymer in a solvent followed by immersion into a liquid bath where the polymer will precipitate and form the membrane (Geise et al., 2010). Other methods such as thermally induced phase inversion, stretching and track etching have also been reported.

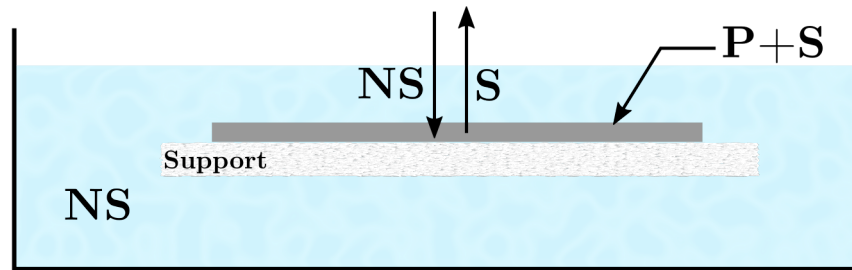


Figure 2.5.1: Schematic representation of immersion precipitation; P, polymer; S, solvent; NS, non-solvent.

In the immersion precipitation process illustrated in Figure 2.5.1, the speed of demixing is an important factor affecting the membrane's structure. Strathmann and Kock (1977) used the ternary phase diagram to discuss the thermodynamic aspects of the process. A typical diagram is illustrated in Figure 2.5.2.

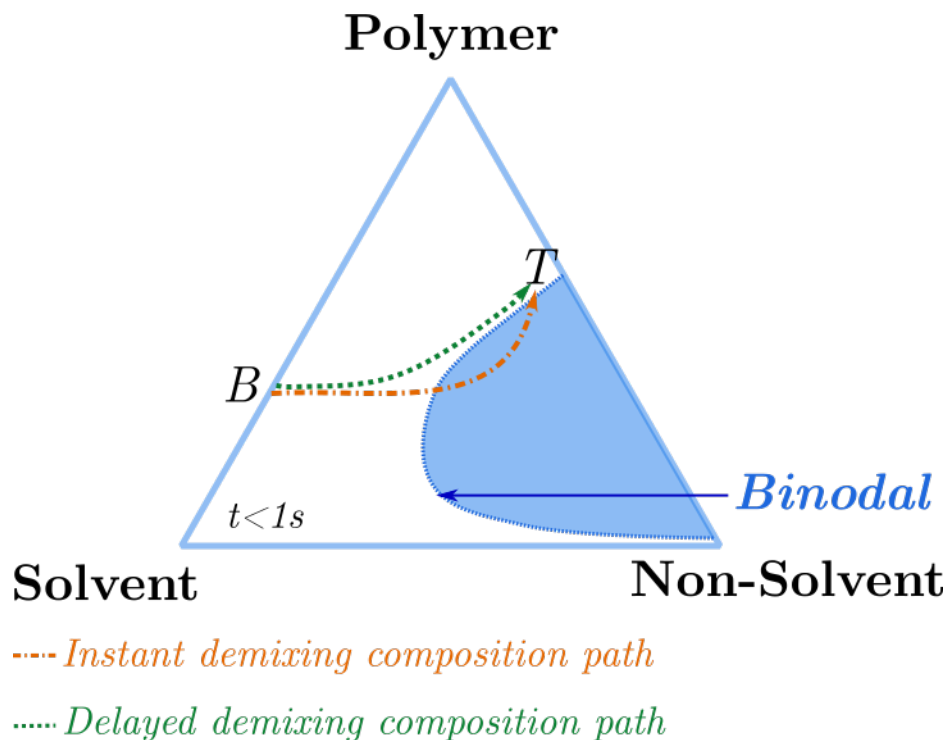


Figure 2.5.2: Composition paths of a cast film after immersion featuring instantaneous and delayed mixing for $t < 1s$.

The corners of the triangle represent the three components present in the system: polymer, solvent and non-solvent. Any point in the triangle represents a mixture of those three components. There are two regions present in the system: a one-phase region where all the components are soluble and a two-phase region where the system is divided into a polymer rich and polymer poor phase. The regions are divided by the binodal. Every composition within its boundaries will separate into two phases that may differ in composition, but that are in a thermodynamic equilibrium with each other.

A so-called composition path of the polymer film can be expressed schematically for a given time. The letters B and T in Figure 2.5.2 respectively represent the bottom and top of the film. It is important to mention that the composition path is for a given time (here, $t < 1s$), and not time dependant: it illustrates the composition of the film at a given time rather than it is change over time. For instantaneous demixing, the composition path will cross the binodal line at a time $t < 1s$, meaning that demixing will start immediately after immersion. For the delayed demixing, all the compositions beneath the top layer T will still be located in the homogeneous one-phase region, meaning that no demixing, and thereby no precipitation is yet occurring at $t < 1s$. After a longer time interval, the compositions beneath the top layer T will begin to cross the binodal. There are two rates involved in this process: the precipitation rate of the polymer in the non-solvent, and the rate at which the solvent dissolves in the non-solvent, and they both will have an impact on the membrane's structure. Membranes that demonstrate a "sponge-like" morphology (see Figure 2.5.3) have been subjected to a slow rate of solvent to non-solvent exchange, whereas membranes demonstrating "finger-like" morphology, often accompanied by macrovoids are results of a high rate of solvent to non-solvent exchange (Guillen et al., 2011). Macrovoids are defined by Van de Witte et al. (1996) as very large elongated pores that can extend over the entire membrane thickness.

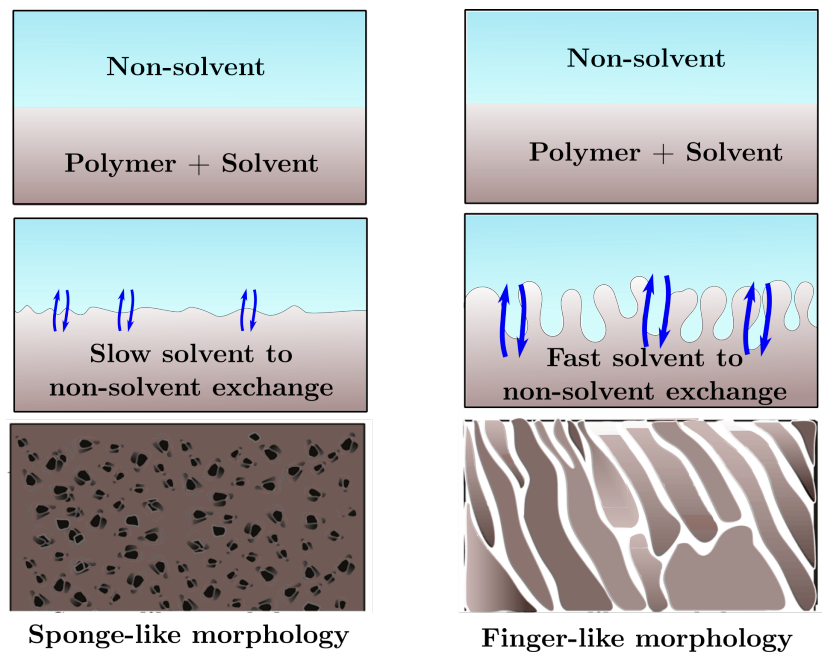


Figure 2.5.3: Different membrane morphologies caused by different types of demixing. the figure is adapted from Guillen et al. (2011) and has been modified by the author.

Wet phase inversion, also known as the Loeb-Sourirajan process, was described in 1963 by Loeb and Sourirajan and is a very commonly used process for fabricating both UF and MF membranes. It was originally made for RO membranes, but today, other techniques such as thin-film composite are applied. In the Loeb Sourirajan process, water is used as the non-solvent. Before applying the polymer film, the support layer is wetted with the solvent. This will create a concentration gradient within the film leading to a gradation of pore size upon the immersion. The membrane will become anisotropic: a thin skin with fine pores will form on the top, whereas larger pores with a lower resistance to water flux will form on the lower part (Geise et al., 2010). Anisotropic membranes will remove the pollutants at the surface acting as screen filters using straining (Figure 2.5.4). Typically, UF membranes will be fabricated to act as screen filters and MF membranes as depth-filter (i.e. the filtration step happens in the whole thickness of the membrane). The fouling of anisotropic UF membranes will therefore occur on the surface rather than inside the membrane (Richard et al., 2004). Coating the surface with anti-foulants would thus be a good method to prevent fouling in UF systems.

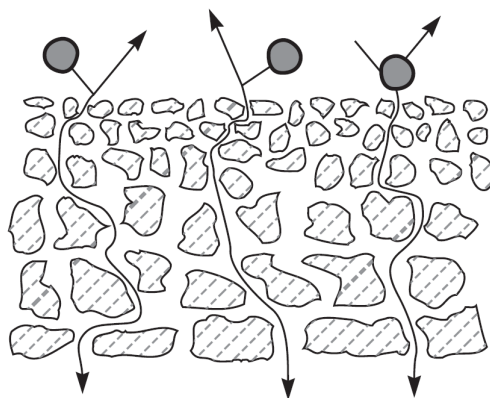


Figure 2.5.4: The principle of screen filtration in anisotropic membranes (Richard et al., 2004).

2.5.2 Polysulfone and Polyvinylpyrrolidinone Membranes

Polysulfone (PSF) (Figure 2.5.5) is the generic term for all sulfone-containing polymers and belongs to the family of thermoplastic polymers. It is a rigid and tough polymer that can withstand high temperatures and is highly resistant to alkali and oxidizing agents (Parker et al., 2002).

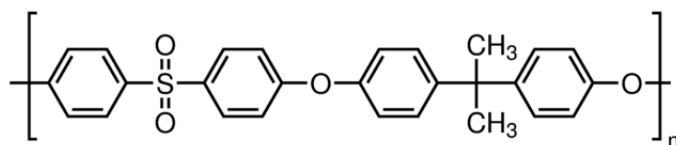


Figure 2.5.5: The molecular structure PSF

PSF is one of the most common polymers used to make membranes by phase inversion (Guillen et al., 2011). It is commercially available and simple to work with. However, macrovoids might form. These are usually undesirable because they might cause mechanical weaknesses in the membrane (Van de Witte et al., 1996). As an attempt to resolve this problem, additives such as polyvinylpyrrolidinone (PVP) have been utilized (Guillen et al., 2011).

PVP is a polymer formed by the polymerization of vinylpyrrolidone (Figure 2.5.6). It is

soluble in water and in other various solvents. PVP has many commercial use including applications as adhesives, textile auxiliaries and dispersing agents (Haaf et al., 1985).

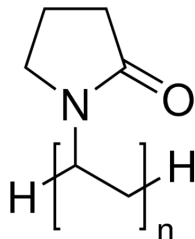


Figure 2.5.6: The molecular structure of PVP.

The addition of PVP to the membrane have been found to suppress the formation of macrovoids and increase the hydrophilicity of the membrane (Guillen et al., 2011). In a study by Chakrabarty et al. (2008), the addition of PVP to PSF/N-Methyl-2-pyrrolidone (NMP) membranes was studied. As PVP molecular weight increased from 24 to 360 kDa, membrane sublayers had denser structures with fewer macrovoids and the porosity and pore number increased.

2.6 Membrane Fouling

All membrane systems are prone to fouling. Fouling is a mechanism that Machenbach (2007) described as a decrease in permeability over time due to the accumulation of undesirable material on the membrane surface or within its pores. Fouling is considered as one the main challenges in membrane treatment (Escobar et al., 2005) and is characterized by: the mechanism, the ability to be removed and the foulant.

There are three fouling mechanisms applicable to UF membranes: pore blockage, pore constriction and cake formation. Pore blocking occurs when the entrance of a pore is completely sealed by a particle. Pore constriction is the reduction of the void volume within a membrane due to adsorption of material on the surface of a pore. Cake formation is the formation of a cake layer as described in Section 2.2. Although this layer

is beneficial for the membrane because it increases the separation and lowers the risk of pore constriction, it generates a high resistance to flow when becoming too thick, increasing the needed pressure of operation (Hand et al., 2012).

Fouling can be characterized as irreversible or reversible. Membranes operate in cycles: a filtration cycle and cleaning cycle. When cleaning, some of the fouling will be completely removed, whereas some will remain. The remaining foulants are causing irreversible fouling (Hand et al., 2012).

The foulants can be particles, such as clay or sand; biological due to the formation of a biofilm and organic due to the adsorption of NOM (Hand et al., 2012).

Fouling by particles can easily be removed by backwashing and rarely leads to irreversible fouling. In Norway, membrane systems are cleaned daily using solutions containing organic salts, tensides and chlorine. The use of chlorine is to reduce the bacterial growth in the system. Besides from the daily cleaning, plants also operate with a main cleaning. These are performed more rarely and their frequency depends on the membrane type and quality of the feed water (Ødegaard et al., 2012).

2.6.1 Biofouling

Biofouling is defined as fouling caused by biological matter. The formation of a biofilm on the membrane surface deteriorates the system performance, requires higher operating pressure, reduces the life of the membrane, as well as its selectivity. (Ridgway and Fleming, 1996). Bacteria accumulate on surfaces by adhesion and growth (Machenbach, 2007). They feed on easily assimilable organics present in the feed stream. Therefore, membranes used in treating wastewater are most prone to biofouling (Hand et al., 2012). The biofilm will grow over time due to the biosynthesis of extracellular polymeric substances (EPS) and cell growth. EPS can consist of polysaccharides or proteins and adhere to surfaces providing a trap for nutrients and dead cells thus providing favorable conditions for growth (Madigan et al., 2015).

Today, biofouling is addressed by the use of chemical disinfectant such as chlorine in the feed or backwash water (Hand et al., 2012), or by choosing a different system configuration (i.e. dead-end or cross-flow) (Ødegaard et al., 2012). In Norway, adding an additional filtration step prior to the membrane process has shown to improve resistivity against some foulants, such as NOM, but it has not been remarkably effective against biofouling (Hem and Thorsen, 2008). Apart from reducing the system performance, biofouling causes a higher demand of chemical cleansing and will likely reduce the lifetime of the membrane (Machenbach, 2007). In order to understand this process and be able to control it, one must first understand both the formation and function of a biofilm, this will be described in section 3.2.1.

2.7 Membrane Modification to Prevent Biofouling

A strategy to prevent biofouling is to change the membrane's surface and make it less favorable for microbial adhesion and growth, while maintaining the membrane's permeability and efficiency. Surface related factors such as roughness, electrical charge and most importantly hydrophobicity are highly influential on mediating bacterial adhesion, thus mediating biofouling formation (Friedlander et al., 2015). Their influence will be covered in Chapter 3. In general, obtaining smooth hydrophilic surfaces is the goal when modifying membrane surfaces. A bacterial cell attaching to a substrate will have to remove surface water molecules. Hydrophobic surfaces have fewer water molecules attached to them, making it easier for cells to adhere (Zeng et al., 2014). Numerous methods have been investigated over the years. One of them is polydopamine (PDA) coating. PDA is naturally found in mussels and is a result of the oxidization of dopamine. Dopamine is a neurotransmitter that is biosynthesized from L-3,4-dihydroxyphenylalanine (L-DOPA) by removal of its carboxyl group. When dopamine is dissolved in slightly alkaline conditions, it polymerizes to PDA by oxidation (Lee et al., 2007). PDA has the ability to deposit onto virtually any type and

shape of surface. This wide applicability, as well as the simplicity, explains the growing interest in its application. However, a fundamental understanding of the mechanism of formation and adhesion is still lacking (Lynge et al., 2011).

PDA is a good candidate for membrane surface modification due to its hydrophilicity. It only forms a very thin layer on the surface, so it is expected for the coating to have minimal impact on the membrane's permeability (Miller et al., 2012). The coating of membrane surfaces can also be biocidal, such as silver nanoparticles or graphene oxide.

Another membrane surface modification method was developed by Wood et al. (2016). Instead of trying to inhibit and prevent the formation of a biofilm, they engineered and beneficial benign biofilm on the membrane surface. The biofilm limited its own thickness by sensing the number of cells present through a quorum-sensing circuit. The benign biofilm also prevented the biofilm formation of deleterious bacteria by secreting nitric oxide, a general biofilm dispersing agent. Additionally, the bacteria strain used in the biofilm can be custom-made to enable the biodegradation of persistent organic pollutants.

The most ubiquitous type of fouling is biofouling (Geise et al., 2010) and researchers have therefore tried to engineer membranes that can reduce it. Studying and characterizing biofouling of membranes is challenging. Biofouling is not only affected by the by the membrane's physical and chemical properties, but the operating conditions and feed water characteristics such as its nature, source and microbial diversity are highly contributing factors that vary from plant to plant (Characklis et al., 2009; Hem and Thorsen, 2008). Most studies aiming at proving the biocidal effects of the new materials are carried over short incubation times that do not exceed few hours and do not mimic the operational parameters in a membrane treatment plant. Miller et al. (2012) found in their study that over time, the PDA coating lost its efficiency and the formation of biofilm was comparable to the pristine membranes. A challenge in the field is therefore

to be able to upscale these modifications from the experimental scale to real-life scale.

Chapter 3

Bacterial Adhesion

3.1 Bacterial Cell Structure

3.1.1 Cell Wall

The cytoplasm contained within the bacterial cell, maintains a high concentration of dissolved solutes. This leads to a significant osmotic pressure of about $2atm$. In order to withstand this pressure and resist osmotic lysis, cells of bacteria contain a wall (Madigan et al., 2015).

As illustrated in Figure 3.1.1, bacterial cell walls are divided into two major groups: Gram-negative and Gram-positive. The distinction between those two is based on the Gram stain reaction. During this reaction, bacteria are stained with a basic dye such as crystal violet. Gram-positive bacteria will appear purple-violet, whereas gram-negative bacteria will appear pink. This is due to the difference between both cell wall structures. Both cell walls contain a rigid layer of peptidoglycan.

Peptidoglycan is a polysaccharide composed of two sugar derivatives, and a few amino acids. Gram-positive cell walls are made of 90% peptidoglycan and are usually much thicker than gram-negative cell walls. Peptidoglycan sheets will often form and be

stacked upon another. Gram-negative cell walls are, on the other hand, only composed of a little amount of peptidoglycan. Most of the wall is made of the outer membrane, also called lipopolysaccharide (LPS) (Madigan et al., 2015). LPS, as illustrated in Figure 3.1.2, consists of an O-specific chain, a core oligosaccharide and a lipid component referred to as lipid A (Gutman et al., 2014).

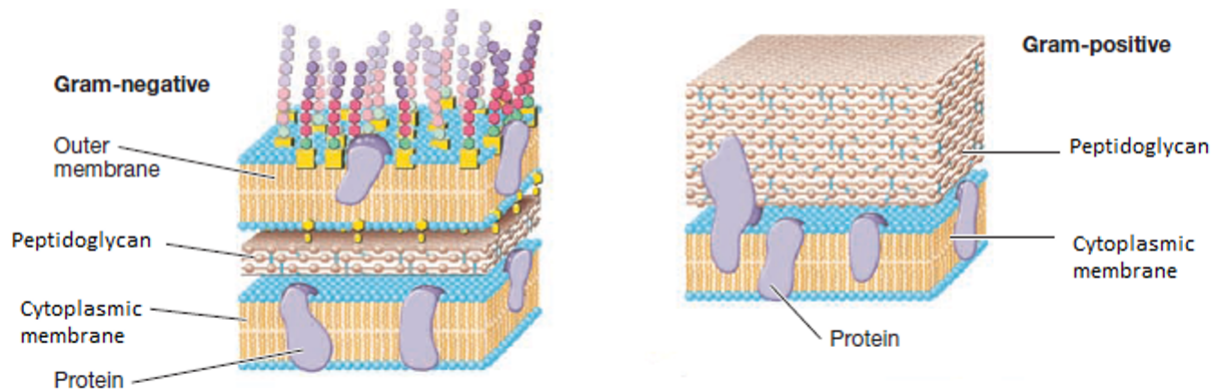


Figure 3.1.1: Cell walls of bacteria (Madigan et al., 2015).

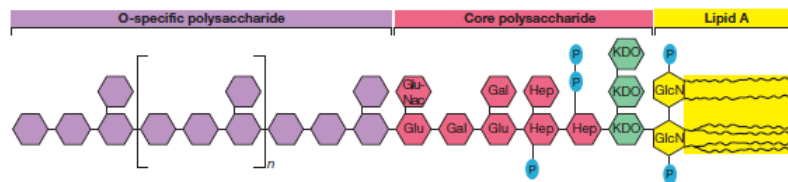


Figure 3.1.2: LPS structure (Madigan et al., 2015).

3.1.2 Capsule and slime layers

It is common for many microorganisms to secrete slimy, sticky materials on their cell surface. They usually consist of polysaccharide or protein and can be referred to as capsule or slime layer. The terms capsule and slime layer are often used interchangeably, but do not refer to the same thing. If the layer is organized in a tight matrix, excluding small particles such as India ink, it is called a capsule. By contrast, if the layer is

more deformable and is penetrated by small particles, like India ink, it is called a slime layer. Capsules will typically adhere strongly to the cell wall. Some capsules can even be covalently linked to peptidoglycan. As opposed to capsules, slime layers are loosely attached and can be lost from the cell surface. In addition to protecting the cell from dehydration, extracellular polysaccharides (also called extrapolymeric substances, EPS) play a key role in both the development and maintenance of biofilms (Madigan et al., 2015).

3.1.3 Flagella

Bacterial flagella are long, thin extracellular organelles that are free at one end and attached to the cell at the other end. They are from 15 to 20 nm thin and require staining in order to be seen with light microscopy. Flagella are not straight, but helical and are mostly made of several copies of a protein called *flagellin*.

They enable mobility of bacteria through swimming by rotating like a propeller. The flagellum motor is anchored in the cytoplasmic membrane and cell wall. Its rotation comes from the proton motive force (PMF) (Madigan et al., 2015).

Not only do these organelles improve cell motility and enable chemotaxis, but they have also been proved to increase the adhesion of bacterial cells to hydrophobic surfaces, while decreasing the adhesion on hydrophilic surfaces (Friedlander et al., 2015). They are also necessary for the biofilm development of several bacteria strains such as *P.aeruginosa* (O'Toole and Kolter, 1998).

3.1.4 Fimbriae and Pili

Fimbriae and pili are filamentous appendages that extend from the surface of a cell and can have multiple functions. Though some scientists distinguish fimbriae from pili, most scientists use the two words interchangeably (Isaacson, 1985).

There are two types of pili: the conjugative pili, also called "sex pili" and the Type

IV pili (T4P). The conjugative pili allows for the transfer of DNA between bacteria during the process of bacterial conjugation (Ou and Anderson, 1970). The T4P is an important bacterial appendage in adhesion and biofilm formation.

T4P are polymers composed of several thousand copies of identical protein subunits called *pilin*. The number of *pilin* subunits determine the molecular weight and length of the pilus. *Pilin* subunits are held together by noncovalent bonds, mostly hydrophobic and hydrogen bonds (Isaacson, 1985; Whitchurch, 2006). T4P usually have a diameter of 6-9 nm and are several micrometers long (Craig and Li, 2008).

They enable motility through twitching motility (Madigan et al., 2015). Twitching motility is a flagella-independent form of bacterial translocation over wet surfaces. It occurs by the extension and then retraction of the pili (Mattick, 2002). It has been reported by O'Toole and Kolter (1998) that *P.aeruginosa* mutants lacking T4P are deficient in biofilm formation. The twitching motility enables the cells to approach surfaces and increase the collision rate. The length of these appendages enables them to bind to targets that are at a distance of $1 - 6\mu m$ and thereby mediating adhesion (Isaacson, 1985).

3.2 Interaction With Membrane Surfaces

3.2.1 Biofilm

Bacterial cells can live in one of two states: freely moving in a solution known as planktonic bacteria, or attached to a surface as a unit or as part of a biofilm. A biofilm is defined as a community of colonies of microorganisms immobilized on a substrate or an interface and enclosed by extracellular polymeric substances (EPS) (Garrett et al., 2008).

Biofilm formation is a property of almost all bacterial species. For many microorganisms, adhesion and biofilm formation is a natural mode of living and survival mechanism

(Araújo et al., 2010) that provides protection from physical and chemical changes in the environment such as the presence of antibiotics and disinfectants, as well as declining nutrient supplies (Garrett et al., 2008). The biofilm enables a communication interchange and response among the cells. This phenomenon is called quorum sensing and is used to regulate gene expression to adapt to changes (Araújo et al., 2010). The biofilm also creates gradients to transport nutrients and other substances needed by the cells inwards while moving wastes outwards (Ødegaard et al., 2012).

The functions and structure of biofilms may differ from bacteria to bacteria, but the formation of a biofilm will, according to Boland et al. (2000), always follow these four steps:

Step 1: Reversible attachment A series of small molecules present in the medium, initially water and salt ions, will adsorb to the surface. Ultimately, the substrate is covered by a single layer of small, organic molecules and proteins that are present in the medium. This layer of water, ions, organic molecules and proteins is referred to as the conditioning film and is always present before the microorganisms adhere on the surface. It provides a support and nutrients for the formation of a biofilm (Dufrêne, 2015). This process is reversible (Boland et al., 2000).

Step 2: Cell adhesion to conditioning film Microorganisms will be exposed to the conditioning film through Brownian motion, gravitation, diffusion or motility. Before adhering to the conditioning film, they may adhere to each other forming microbial aggregates. Given the fact that the microorganisms first adhere to the conditioning film and not the surface itself, the strength of the initial biofilm will depend on the structure of the conditioning film. This reversible attachment is dominated by Van der Waals forces (farther than 50 nm) accompanied with nonspecific electrostatic forces at 10 – 20 nm. At a distance of 5 nm, short range forces including ionic, hydrophobic, hydrogen bonds, and dipole interactions dominate (Dufrêne, 2015). If repulsive forces overcome the attractive forces, the bacteria detaches and, consequently, no biofilm formation takes

place (Garrett et al., 2008).

Step 3: Irreversible attachment Quorum sensing in the second step will trigger biofilm-specific gene expression leading to the secretion of EPS (Madigan et al., 2015). The initially reversible attachment becomes then irreversible as the EPS will incorporate the conditioning film and strengthen its cohesiveness by enabling covalent and hydrogen bonding short range forces in addition to hydrophobic forces (Araújo et al., 2010).

Step 4: Further development Subsequently, the number of cells in the biofilm will grow. Nutrients will diffuse through the biofilm, creating a protected niche within the EPS matrix (Ødegaard et al., 2012).

3.2.2 Factors influencing bacterial adhesion

Bacterial adhesion is a complex process affected by the properties of all three phases involved: the adhering bacteria and the surface it adheres to, along with the suspending medium.

The medium

During membrane filtration, the medium is under a flowing condition. The flow pattern is an important factor in attachment of bacteria to a solid surface because of the shear stress it creates. Adhesion has been shown to be optimal under a shear stress of 6-8 N/m², but can still occur under shear forces up to 130 N/m² (Merritt and An, 2000). Studies with *S. epidermidis*, a Gram-positive bacteria part of the normal human flora, have shown that bacterial concentration plays a role in adhesion. The bacterial concentration and not the amount of microorganisms is the driving factor, thus indicating a surface hit phenomenon.

Concentrations of electrolytes like KCl or NaCl, as well as CO₂ and pH along with the presence of iron, cadmium, zinc and sugar have been shown to influence slime production and have therefore an impact on adhesion (Merritt and An, 2000). Bacteria and natural surfaces are mostly negatively charged, leading to a repulsive electrostatic interaction between cells and surfaces. This interaction depends on the Zeta potential (i.e. the thickness of the electrical double layer). This thickness depends on the medium's ionic strength. At high concentrations of electrolytes or polyvalent ions, the repulsion will therefore decrease, facilitating bacterial adhesion (Van Loosdrecht et al., 1987).

Bacterial hydrophobicity and surface charge

The nature of the bacteria species has big impact on adhesion to surfaces: for a given material surface, different bacterial species will adhere differently. This is due to the physiochemical characteristics of the microorganism.

The surface hydrophobicity of a bacteria is determined by cell surface components such as the cell wall, pilli and flagella. The bacterial hydrophobicity will not only vary according to the type of specie, but can also be influenced by the growth medium and the bacterial age. Bacterial hydrophobicity is an important physical factor especially when the surface they are adhering to are either hydrophobic or hydrophilic (Merritt and An, 2000). In general, hydrophobic bacteria will prefer hydrophobic surfaces, just as hydrophilic bacteria prefer hydrophilic surfaces. It has been demonstrated that hydrophobic bacteria will adhere better than hydrophilic bacteria (Van Loosdrecht et al., 1987).

Bacterial surface charge is usually negative due to the ionization or dissociation of the functional groups present on their surface, such as carboxyl and amino groups. Other factors contributing to bacterial surface charge are: bacterial species and concentration, age, surface structure, pH and ionic strength of the suspending environment (Araújo et al., 2010). The surface charge plays an important role because the initial step of bacterial colonization is governed by long-range Van der Waals forces. The negative

surface charge of the microorganisms will attract ions of positive charge. In colloidal chemistry, the surface charge is characterised by the Zeta potential. The higher the charge, the more stable the molecule. The higher the surface charge, the less likely is it for the bacteria to adhere. A high surface charge has been shown to be accompanied by a hydrophilic character although a hydrophobic bacteria might still have a high surface charge (Merritt and An, 2000).

Surface characteristics

Substrate related factors affecting bioadhesion include its roughness, morphology, electrical charge, and most importantly hydrophobicity (Araújo et al., 2010; Garrett et al., 2008; Friedlander et al., 2015).

Surface roughness is a two dimensional parameter of a material surface representing the distance between the peaks and valleys. Alternative terms can be surface finish or smoothness. A study demonstrated that roughening the surface of either glass or polystyrene with a grindstone increased the rate of biofilm development in a river environment. Other studies in the medical field have recommended striving for a low surface roughness in order to reduce bacterial colonization (Merritt and An, 2000). Merritt and An (2000); Araújo et al. (2010) presented two main reasons for the increase of bacterial adhesion with an increasing roughness: firstly, a rough surface will have a greater surface area which will increase the collision rate and the surface for attachment. Secondly, depressions in rough surfaces provide a favourable site for bacterial colonization because they are protected from shear stress and other inhibiting factors.

Another structural factor is the surface morphology, or configuration. The physical morphology differs from surface roughness. It describes patterns of a material such as a porous surface or a braided surface. Irregularity of material surfaces enhance bacterial adhesion; it was found that porous surfaces are more prone to adhesion than dense materials (Merritt and An, 2000).

Hydrophobic bacteria are more likely to adhere on surfaces, and preferably to hy-

drophobic surfaces. As covered in Section 2.7, several studies have reported hydrophilic materials to be more resistant to adhesion.

Chapter 4

Atomic Force Microscopy

The Atomic Force Microscope (AFM) was invented in 1986 by Binnig, Quate and Gerber (Razatos and Georgiou, 2000). It enables the imaging of surface features at an atomic level. The imaging technique differs from other microscopes. It does not form an image by focusing light or electrons onto a surface like an optical or electron microscope. An AFM consists of a cantilever equipped with a small tip that scans a surface resulting in its topographic map.

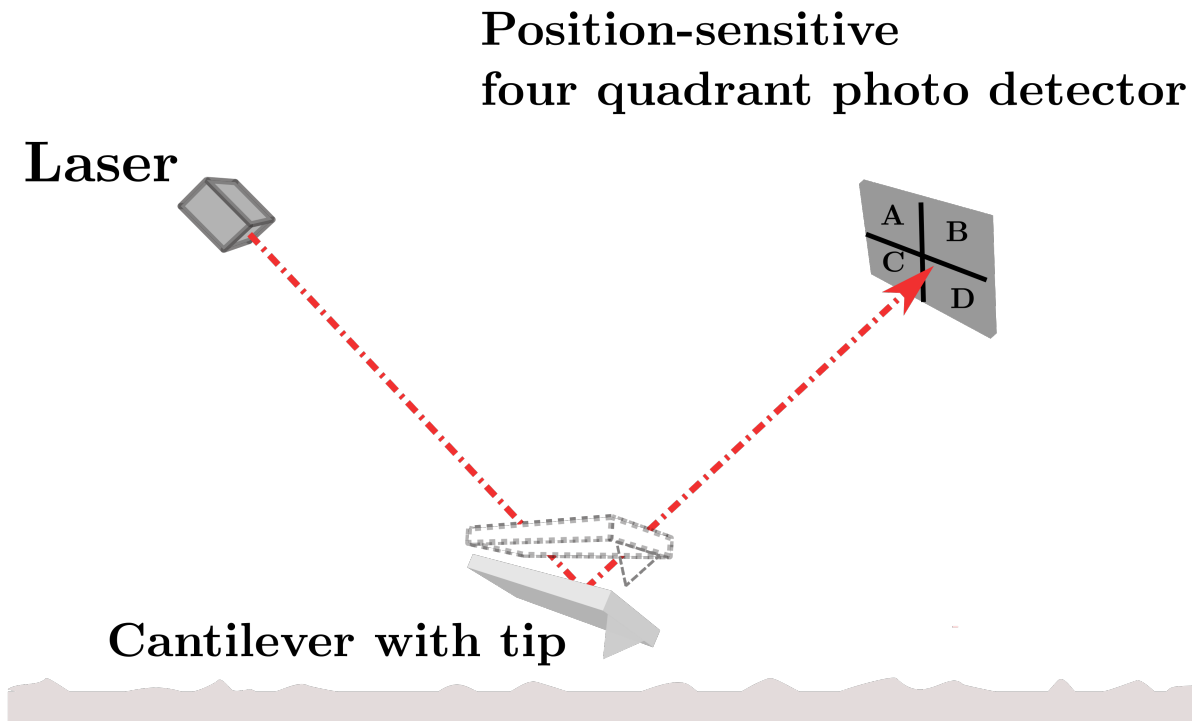


Figure 4.0.1: A schematic illustration of AFM.

As illustrated in Figure 4.0.1, the tip will move across the sample's surface while a laser beam is projected onto the tip. This beam will then be reflected on a photodetector, reading of the tip's position (Eaton and West, 2010).

Eaton and West (2010) defined three basic concepts that control the operation of an AFM: piezoelectric transducer, force transducer and feedback control. The piezoelectric transducer moves the tip over the surface, the force transducer senses the force between the tip and the surface, and the feedback control feeds the signal from the force transducer back in to the piezoelectric in order to maintain a fixed force between the tip and the sample.

The data from an AFM analysis must be treated by an analysis software in order to form an image. AFM can be run in two different modes. For the topographic modes,

the most basic differentiation is the one made between contact mode and tapping mode. Contact mode AFM was the first developed mode. As the name states, the tip is in direct contact with the sample. The tip is dragged across the surface of the sample and its contours are measured. An advantage with contact-mode analysis is that they are rapid and give high resolution. However, the contact between the sample and the tip means that both the sample and the tip might get damaged. Additionally, this technique is highly dependent on the sample's nature.

In tapping mode, also called AC mode, the cantilever is driven to oscillate up and down near its resonance frequency. The oscillation is facilitated by an additional piezoelectric element. When the oscillating probe approaches the surface, interaction forces like Van der Waals, or electrostatic forces will change the amplitude and frequency of the oscillation, decreasing them as it approaches. The oscillation frequency and the method used to detect the changes depends on the type of tapping mode (Eaton and West, 2010).

4.1 Single Cell Force Spectroscopy

Besides imaging surfaces, AFM can also measure adhesion forces; it actually has a sensitivity down to the picoNewton range. This mode is called force spectroscopy. The x-y position of the AFM probe is fixed while varying along the z-axis. While approaching the surface, the tip will deflect because of interaction forces (Eaton and West, 2010). Force measurements with a single cell immobilized on the cantilever are referred to as Single Cell Force Spectroscopy (SCFS). As illustrated with Figure 4.1.1, the cantilever deflection will be read by the photo detector. The deflection, in V , will then be converted to a distance, Δx , through a parameter expressing the cantilever's sensitivity called the Invols. Subsequently, the force can be expressed using the cantilever's spring constant, k , and Hooke's law:

$$F = -k\Delta x \tag{4.1.1}$$

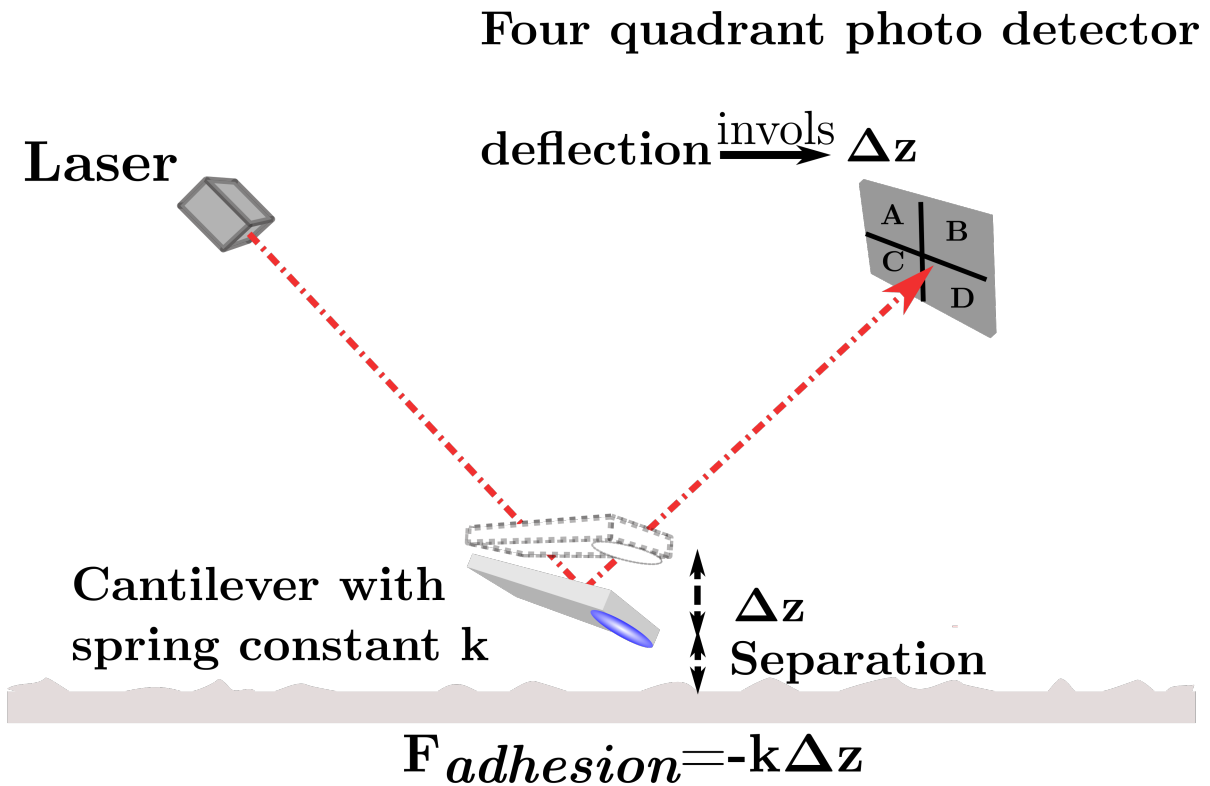


Figure 4.1.1: A schematic illustration of SFCS with an immobilized cell.

Even though the manufacturers give a nominal value for the spring constant, it can vary greatly. Thus, the cantilever must always be calibrated before each experiment. First, the cantilever's sensitivity must be determined. This is done by taking a force curve by pressing the cantilever (without a cell) on a stiff surface. Next, the spring constant is found by measuring the cantilever's thermal fluctuation (noise). The thermal noise method is the most versatile and used method to calibrate the spring constant (Friedrichs et al., 2013).

For SCFS, soft and tipless cantilever should be used. Tipless cantilevers are preferable because they provide a better control as to where the cell is immobilized. When a tip is

present, it is hard to know if it is the tip or the cell that is in contact with the surface. Soft cantilevers allow the detection of very small forces down to the piconewton range (Friedrichs et al., 2013).

To attach a cell to the cantilever, the cantilever's surface must be functionalized with a cell-adhesive substrate. (Friedrichs et al., 2013; Taubenberger et al., 2013). The functionalization implies coating the cantilevers with adhesive reagents. Examples of those are CellTak, a protein derived from the marine mussel *Mytilus edulis*, lectins such as concanavalin A and poly-lysine that due to its positive charge attracts negatively charged cells (Friedrichs et al., 2013).

Usually, it is recommended to have an inverted microscope installed in order to be able to locate a single cell. Figure 4.1.2 illustrates the usual procedure for making a single cell probe. The cantilever is first calibrated without a cell. Subsequently, a cell is located under the optical microscope. The apex of the functionalized cantilever is then navigated above the cell and engaged at a desired force, also called set point. To immobilize bacterial cells, a set point of 1 nN is recommended. Five minutes later, the cantilever is retracted with the cell immobilized on it and measurements can be performed (Zeng et al., 2014).

Various significant parameters can be adjusted during a SCFS experiment such as the contact force, contact time, temperature and retraction speed. The contact force is defined as the force exerted on the cell when in contact. The contact time is the amount of time for at which the cell is pressed on to the surface. With increasing contact time, the detachment force will usually increase since an increasing number of adhesins can interact with the surface. Controlling the temperature can be relevant in many biological experiments such as those involving mammalian cells where a constant temperature of 37°C is required. The retraction speed determines the loading rate at which the bonds are stressed during cell detachment (Taubenberger et al., 2013).

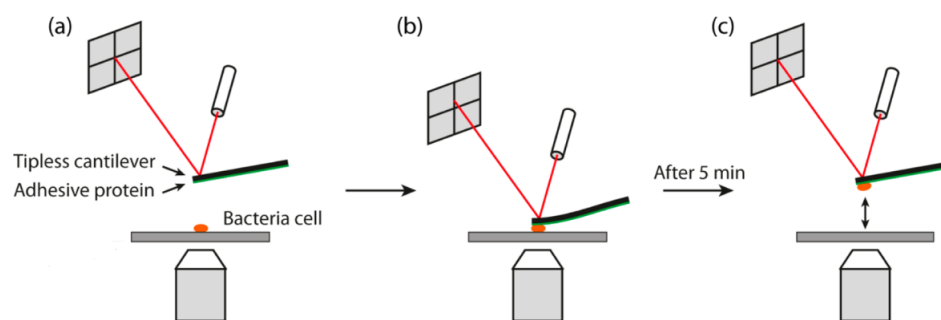


Figure 4.1.2: illustration of the process of making a single-cell bacterial probe (Zeng et al., 2014).

Chapter 5

Methodology

5.1 Membrane Fabrication by Phase Inversion

PSF UF membranes were made using the wet phase-inversion process described in Zodrow et al. (2009). 10 g of PVP (MW: 58.000, Acros Organics) were dissolved in 75 g NMP (99,5 %, Sigma-Aldrich) by stirring at a temperature of 60°C for 2 hours. Subsequently, 15 g PSF (MW: 22.000, Sigma-Aldrich) were added to the solution and stirred at a temperature of 80°C for about 4 to 6 hours. The polymer dope solution was then stored over night in a desiccator to remove any air bubbles.

For the casting, glass plates were wrapped in polyethylene terephthalate (PET) fabric, making sure that the wrinkles forming on it were removed. The PET's function was to provide structural support for the membrane. The fabric was then wetted with NMP and carefully wiped with a tissue to remove any excess solvent.

Around 10 to 15 mL of the dope solution were poured on the plate and spread on the fabric using a casting knife set at a height of 0,25 mm.

The plate was then immediately immersed into a primary precipitation bath containing 2 L of ultra-pure water.

After 10 min, it was subsequently placed in a secondary precipitation bath containing

4 to 6 L of ultra-pure water for 1 hour. The membrane was then cut from the plate and stored in the refrigerator using a container filled with ultra-pure water.

The wet inversion process was covered in details in Section 2.5.1. NMP serves as the solvent, and ultra-pure water is the non-solvent. When immersed in ultra-pure water, NMP will flow through the polymeric layer and create pores, whereas PSF and PVP will precipitate. This is shown in Figure 5.1.1.

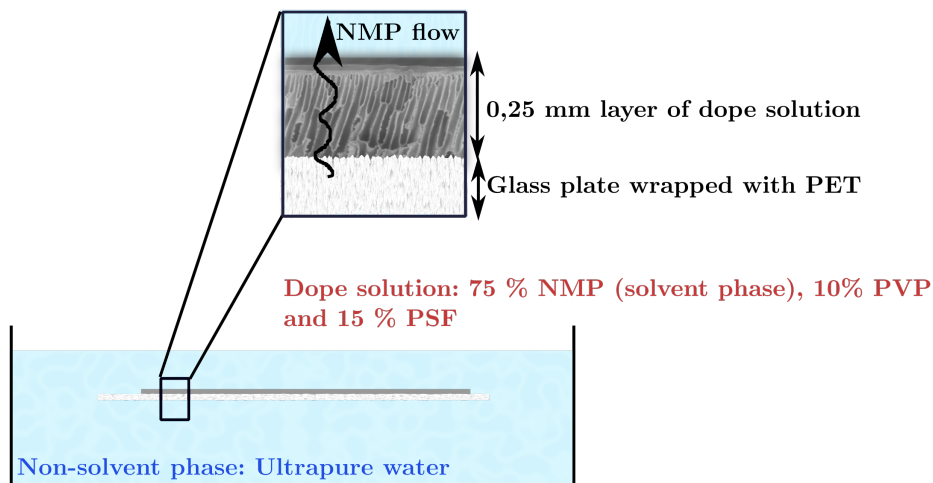


Figure 5.1.1: Illustration of the process of wet phase inversion using NMP as a solvent, and PSF+PVP as polymers.

5.2 Membrane Modification: PDA coating

The membranes were modified by PDA-coating. Before coating, they were thoroughly inspected rejecting those that had pin holes or other defects.

The coating process is shown in Figure 5.2.1.

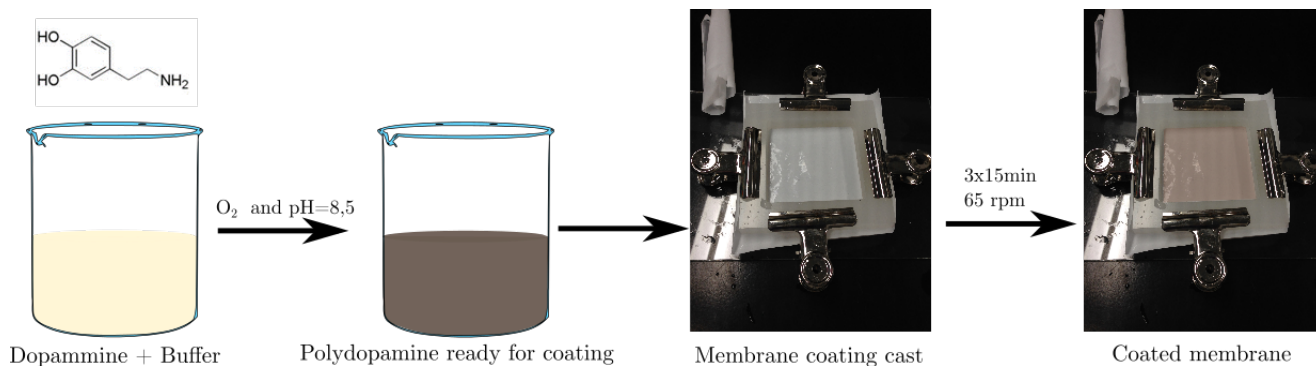


Figure 5.2.1: Illustration of the PDA coating of membranes.

A tris buffer (10 mM) was prepared by diluting Trizma hydrochloride solution (Sigma-Aldrich) in ultra-pure water and adding NaOH until the pH was risen to 8.5. Dopamine hydrochloride (Sigma-Aldrich) was dissolved in the solution at a concentration 4 g/L, turning it a light brown color. The membranes were placed in a frame and the PDA solution was poured on the surface. The frames were stirred for 15 min at 65 rpm. This step was repeated thrice and the membranes were rinsed with ultra-pure water between each step. After coating, the membranes were stored in ultra-pure water in the refrigerator.

5.3 Membrane Characterization

The membranes were characterized both before (PSF) and after coating (PSF-PDA). The hydrophobicity, permeability and roughness were determined.

5.3.1 Hydrophobicity

Water contact angle measurements (Kyowa MCA-3) were used to find the hydrophobicity of the membranes.

Contact angle measurements consist on reading the angle formed between a water droplet

and the measured substrate (as seen in Figure 5.3.1). Small contact angles ($<90^\circ$) correspond to high wettability (hydrophilic), while large contact angles ($>90^\circ$) correspond to low wettability (hydrophobic) (Yuan and Lee, 2013).

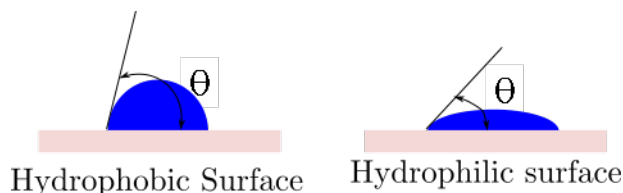


Figure 5.3.1: Illustration of contact angles (θ) formed by a water droplet on a smooth surface.

10 droplets of water were randomly placed on 3 samples of PSF and PSF-PDA membranes. The angle from both the left and right side were measured, providing a total of 60 measurements.

5.3.2 Permeability

To measure the permeability, 25 mm circular membrane samples were mounted into an Amicon 8010 Stirred Cell. The permeate water was weighed every 10 s at pressures of 10, 20, 30, 40 and 50 PSI. The pure water flux (PWF) was then determined using the following equation:

$$J = \frac{\Delta V}{\Delta t A_{mb}} \quad (5.3.1)$$

Where $\frac{\Delta V}{\Delta t}$ is the change of volume over time. The change of volume is determined using a density of water equal to $1 \frac{g}{mL}$. A_{mb} is the membrane's area and is equal to 490.87 mm^2 .

The permeability (A) was then defined using Equation 5.3.2, where $\frac{\Delta J}{\Delta P}$ is the change of the PWF over the change of pressure.

$$A = \frac{\Delta J}{\Delta P} \quad (5.3.2)$$

5.3.3 Roughness

The roughness was determined using AFM (MFP3D-Cypher) in AC mode topography at a rate of 0,5 Hz. The used cantilevers were Tap300Al-G from Budget Sensors. Images of $1\mu\text{m}$ by $1\mu\text{m}$ were obtained. They were then analyzed using the instrument's software (MFP3D 14.13, in Igor Pro 6.37), giving the root-mean-square (RMS) roughness. In total, 6 images of random spots were obtained for PSF membranes and 5 for PSF-PDA membranes.

5.4 Quantification of Adhesion

5.4.1 The Experimental Set-Up

Preparation of the fluid cell

Gram-negative *Pseudomonas fluorescens* (ATCC 13525) were first streaked on agar plates (LB broth with agar, Miller, Sigma-Aldrich) and stored in the refrigerator. A preculture was made by inoculating cells over night in a growth medium, Luria Broth (LB Miller, Sigma-Aldrich), at a temperature of 30°C , while shaking at 125 rpm.

The next day, the preculture was diluted to 2:50 in fresh LB and incubated for 1,5 to 2 hours at a temperature of 30°C and shaken at 175 rpm.

Bacterial cells were harvested at an optical density at 600 nm (OD_{600}) of 0,500 A. They were subsequently centrifuged thrice at 5000 rpm for 1 min. This step is to remove any proteins or other secretions that might be present. After the first centrifuge round, the cells were suspended in Phosphate-buffered saline (PBS, P4417 Sigma-Aldrich).

On an UV/O₃-cleaned glass plate, a small sample of the membrane was glued using epoxy. When the membrane had dried, 13 μL of the suspended cells were deposited next to the membrane and left for 30 min. The plate was then rinsed thoroughly using PBS, making sure that the cells that did not adhere were removed. This step was very

important, because floating cells in the liquid would risk contaminating the cantilever and hinder proper measurements.

The glass was then mounted onto a fluid cell (Fluid Cell Lite, Asylum Research). 300 μL of PBS were added to the cell.

Preparation of bacterial probe

A tipless cantilever (MLCT0, cantilever C. Bruker) was cleaned by UV/O₃ for 10 min. A 4 g/l PDA-solution was prepared as described in Section 5.2. The cantilever was carefully immersed in the solution and was shaken at 65 rpm for 15 min. The cantilever was then rinsed with ultra-pure water and dried under nitrogen flow in a desiccator. The PDA-coating has to be conducted immediately before use, when completely oxidized, PDA lost its adhesiveness and failed to immobilize a bacterial cell.

The cantilever was then mounted onto its holder. Before immersing the cantilever in the fluid cell, small droplets of PBS were put around it to speed up its stabilization in the liquid.

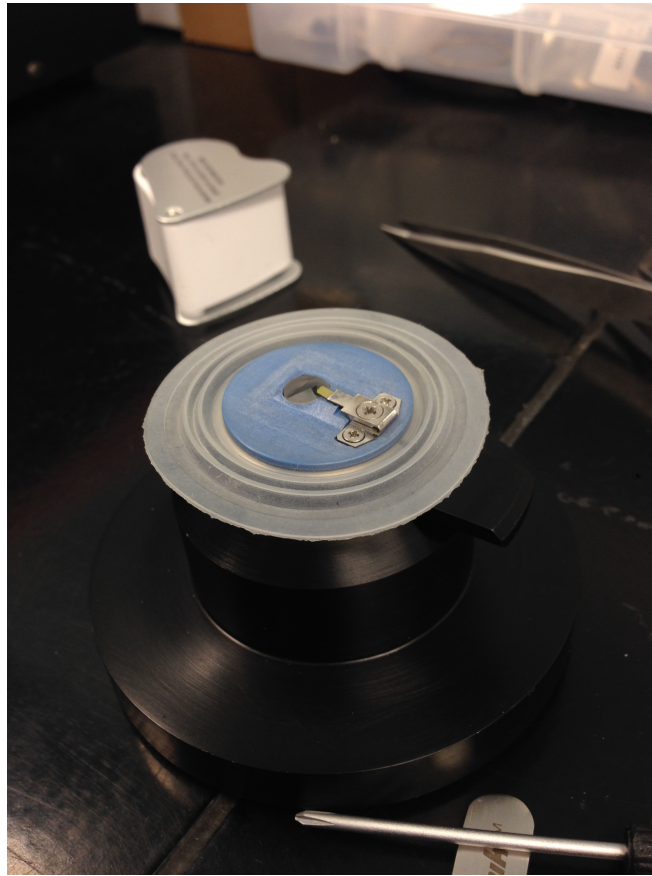


Figure 5.4.1: The cantilever placed in its holder.

When soft cantilevers are entering a liquid, they deflect a lot and then slowly go back to their original position. This stabilization process took about 20 to 45 min. Once the cantilever was stabilized, it was first calibrated without a bacterial cell.

To make a probe, a bacterial cell was located using an inverted optical microscope and a 60x lens (Axio vert A1, Zeiss). The cell had to fulfil certain criteria in order to be a proper candidate:

- Have enough clearance around so that the cantilever could approach it without being contaminated.
- Be between 3 and 8 μm long.
- Not be dividing.

- The long side of the cell had to be oriented parallel to the apex of the cantilever, as shown in Figure 5.4.2.

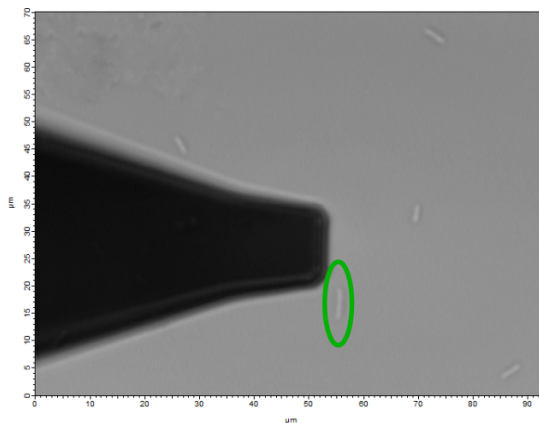


Figure 5.4.2: This picture shows the cantilever and a rod shaped *P.fluorescens* (circled in green) right before immobilization.

The apex of the functionalized cantilever was then navigated above the cell and engaged at a set point of 1 nN for 5 min. It was important to place the bacteria as close to the edge of the cantilever as possible, as shown in Figure 5.4.3, to make sure that the bacteria, and not the cantilever, was in contact with the surface while doing measurements (see Figure 5.4.4). The cantilever was finally retracted with the cell immobilized on it and measurements could be performed.

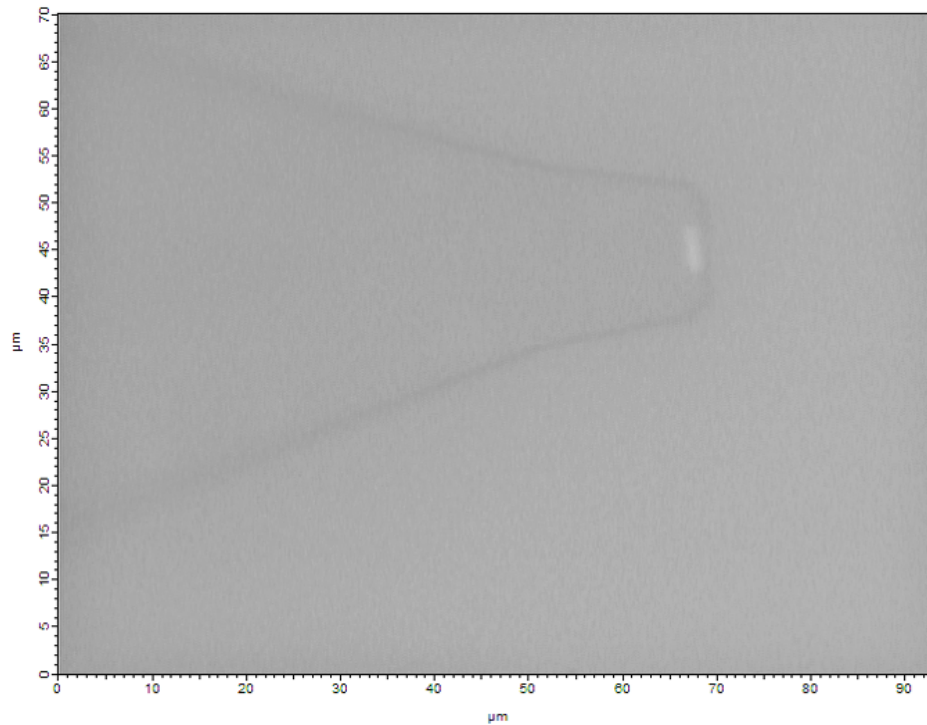


Figure 5.4.3: *P. fluorescens* immobilized on a cantilever looked at through a 60x lens and fluorescent microscopy.

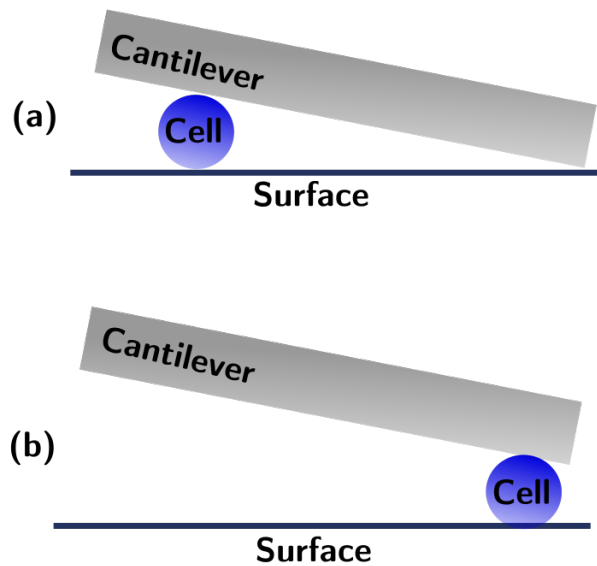


Figure 5.4.4: (a) The cell is placed too far in, and the cantilever is touching the surface when doing measurements. (b) The cell is positioned properly and is the only thing in contact with the surface when doing measurements.

5.4.2 AFM calibration

Triangular cantilevers are prone to optical interference when they are over reflective surfaces. This is because some of the laser beam will spill on the surface and be reflected back to the detector. This reflection will interfere with the measurements giving sinusoidal-shaped force curves (Figure 5.4.5). To avoid this, the laser beam was placed on one of the legs of the triangle in stead of the tip (Figure 5.4.6). Usually, the laser beam should preferably be placed on the tip in order to read of good results. However, the used cantilever was very soft ($k=0.02$ N/m), thus its legs also deflected, making it possible to read of good results.

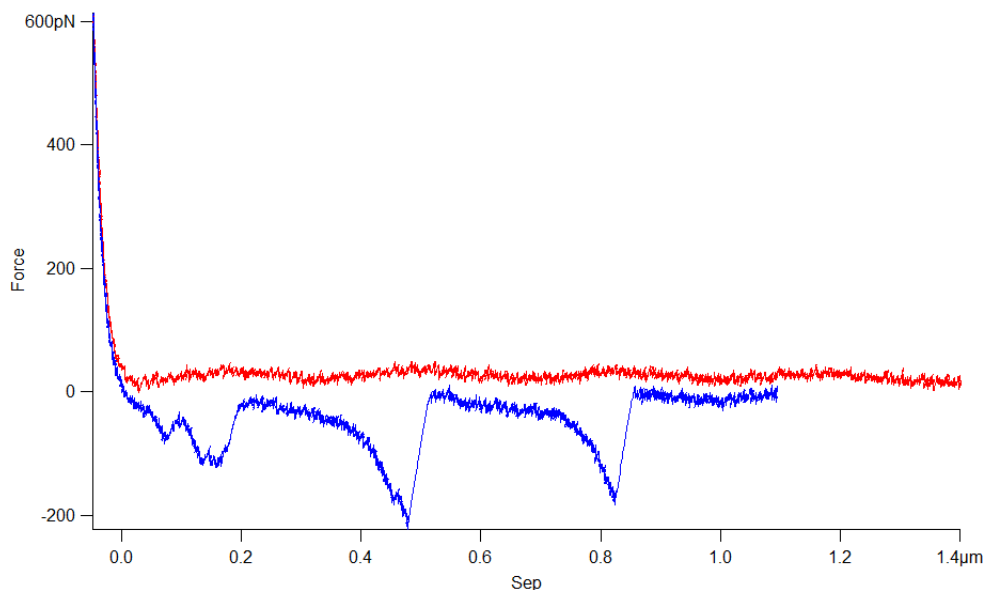


Figure 5.4.5: A force curve taken on a PSF membrane with a bacterial probe, at a force of 600 pN and a contact time of 0s. The red curve shows the extraction, and the blue curve the retraction. The red curve has a sinusoidal shape due to optical interference.

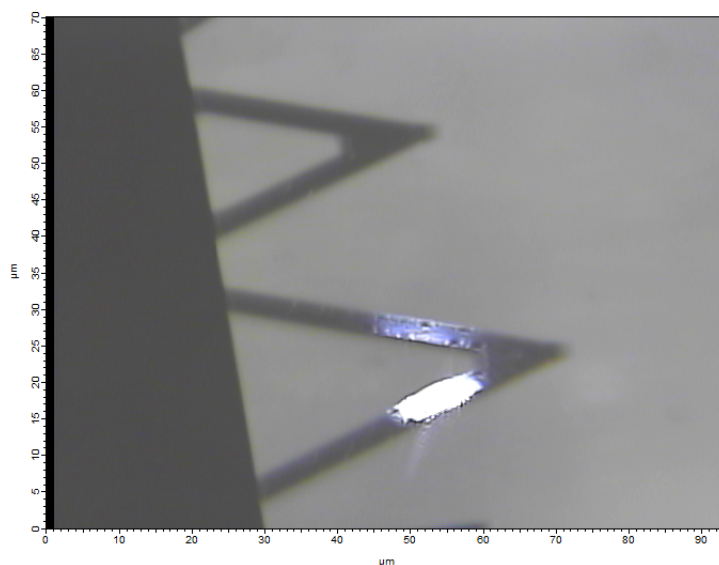


Figure 5.4.6: Cantilever C, MLCT0. The laser beam was placed on the triangle's leg to avoid optical interference

Prior to performing measurements, the following parameters were calibrated over a clean, hard surface without an immobilized cell:

Table 5.4.1: Calibrated parameters

Parameter	Method	Use
Drive Frequency	Thermal Tuning	Used in AC mode for approaching the surface over the membrane. The frequency that the cantilever is driven at by the shake piezo
Drive Amplitude	Manual Tuning	Used in AC mode for approaching the surface over the membrane. It is the voltage applied to the shake piezo.
Virtual Deflection	Untriggered force curve	The virtual deflection is a mechanical coupling of the deflection signal with the Z movement, resulting in a slight slope in the force curve. It must therefore be corrected.
InvOLS	Force curve on glass	Inverse opticallever sensitivity (InvOLS) is a parameter necessary for the algorithm to determine the spring constant
Spring Constant	Thermal Tuning	Used in Hooke's law to calculate the force.

5.4.3 AFM force measurements with bacterial probe

The measurements were conducted in PBS. After calibrating the cantilever and attaching a bacterial cell, the cantilever was moved over the membrane. The surface was approached in AC mode to avoid colliding into it.

Measurements were performed over random spots. On each spot, three curves were collected at a speed of 400 nm/s. The applied force was 600 pN for all the curves, and the contact time varied between 0s, 2s and 5s. Three curves with the same contact time were collected, then the cantilever was moved to a new random spot where the contact time was changed in the order from 0s to 5s, and three new curves were obtained. For each experiment, up to 30 spots were measured giving a maximum of 90 curves (30 curves for each contact time) per experiment. Figure 5.4.7 explains how a force curve was obtained.

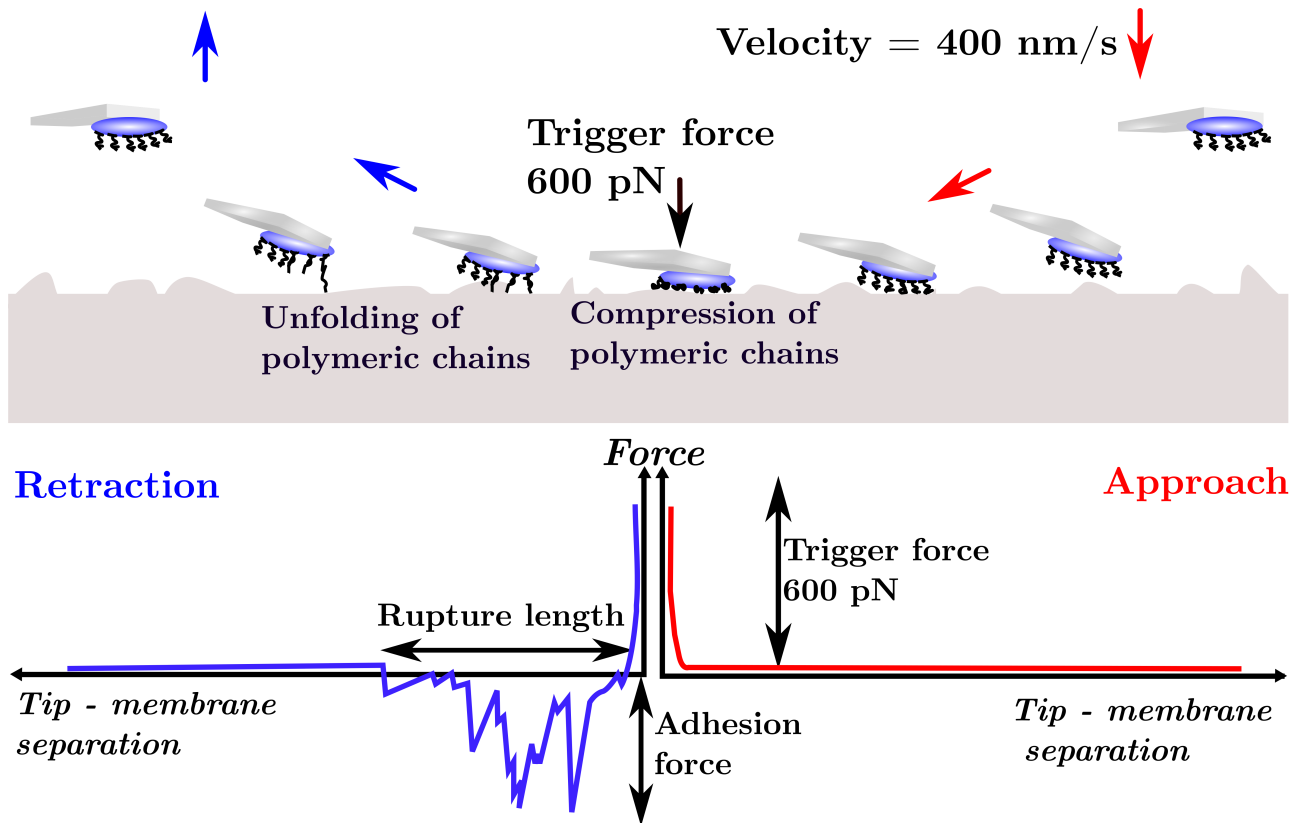


Figure 5.4.7: Illustration explaining how a force curve was obtained.

The cantilever approached the surface (red curve), stayed in contact for a given time and retracted (blue curve).

The most negative peak on the retraction curve is defined as the adhesion force. The rupture length is defined as the length from contact to the last force of adhesion.

5.4.4 Viability assay of the immobilized bacteria

The viability and position of the cell on the cantilever was verified after each experiment by using a LIVE/DEAD BacLight kit (Thermo Fisher Scientific). The kit had two different dyes: one that would only penetrate damaged cell membranes, and another that would penetrate all cell membranes. 2 μL of each dyes were diluted in 300 μL PBS. If the cell's membrane was intact, it emitted a green light when looked at with a fluorescent light. If it was damaged, it emitted a red light. Only results from experiments where the cell was alive (green) and still in its original position were used, the others were discarded. Working with PDA and *P.fluorescens*, around 1 out of 10 experiment was discarded. However, when trying another functionalization technique called silinazation, the cell would be dead 9 out of 10 experiments. This method is therefore not recommended when working with bacterial cells.

5.4.5 Data Analysis

For the data analysis, the software belonging to the AFM (MFP3D 14.13 in Igor Pro 6.37), Origin 2016 and Matlab were used.

Data distribution and experiments

Every force curve was taken at a speed of 400 nm/s and an applied force of 600 pN. The contact time, and the membrane's surface type were the only parameters that were varied. The measured contact times were 0s, 2s and 5s and the membrane types were PSF and PSF-PDA. The forces were obtained over several experiment, Table 5.4.2 shows their distribution and the amount of obtained curves.

Table 5.4.2: Distribution and the amount of obtained force curves.

	With a bacterial probe						Control measurements					
Membrane type	PSF			PSF-PDA			PSF			PSF-PDA		
Contact time	0s	2s	5s	0s	2s	5s	0s	2s	5s	0s	2s	5s
Amount of days	6	5	5	6	6	6	1	1	1	1	1	1
Amount of curves	126	104	102	128	128	125	124	101	98	125	127	126

Modifying the curves

For each measurements, a force curve was obtained. The adhesion force, defined as the lowest peak of the curve (Figure 5.4.8), and the rupture length, defined as the length from contact to the last point of adhesion (Figure 5.4.8), were the desired values.

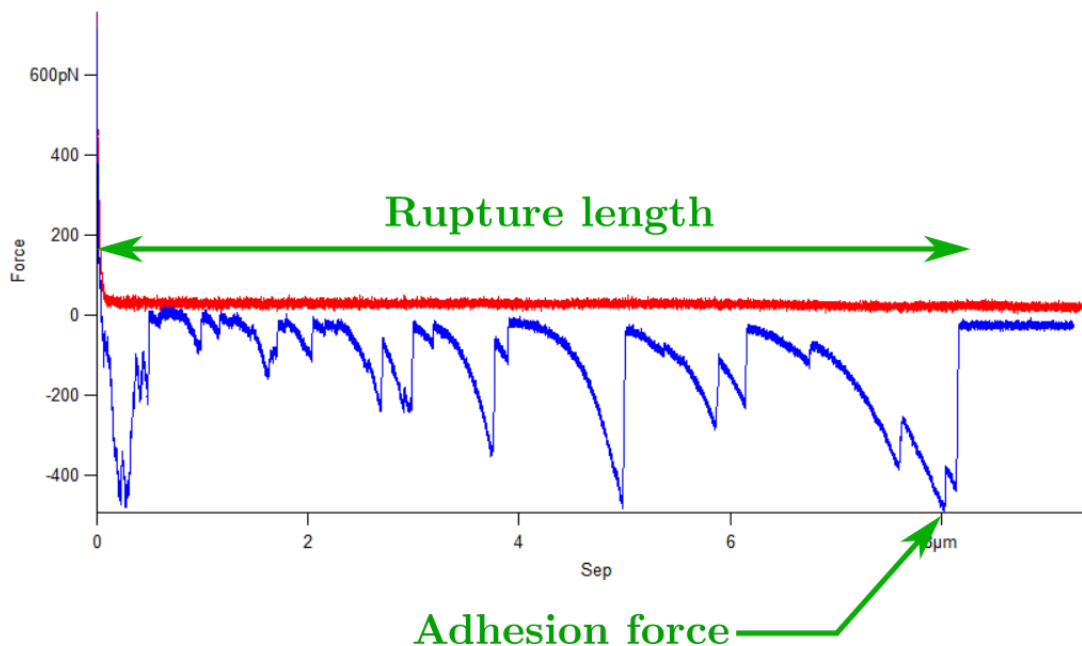


Figure 5.4.8: A force curve taken with a *P.fluorescens* cell at a set point of 600 pN, 5s contact time over a PSF membrane.

However, before finding the rupture length and adhesion force, the curves had to be modified. Figure 5.4.9 illustrates the modifications that were performed.

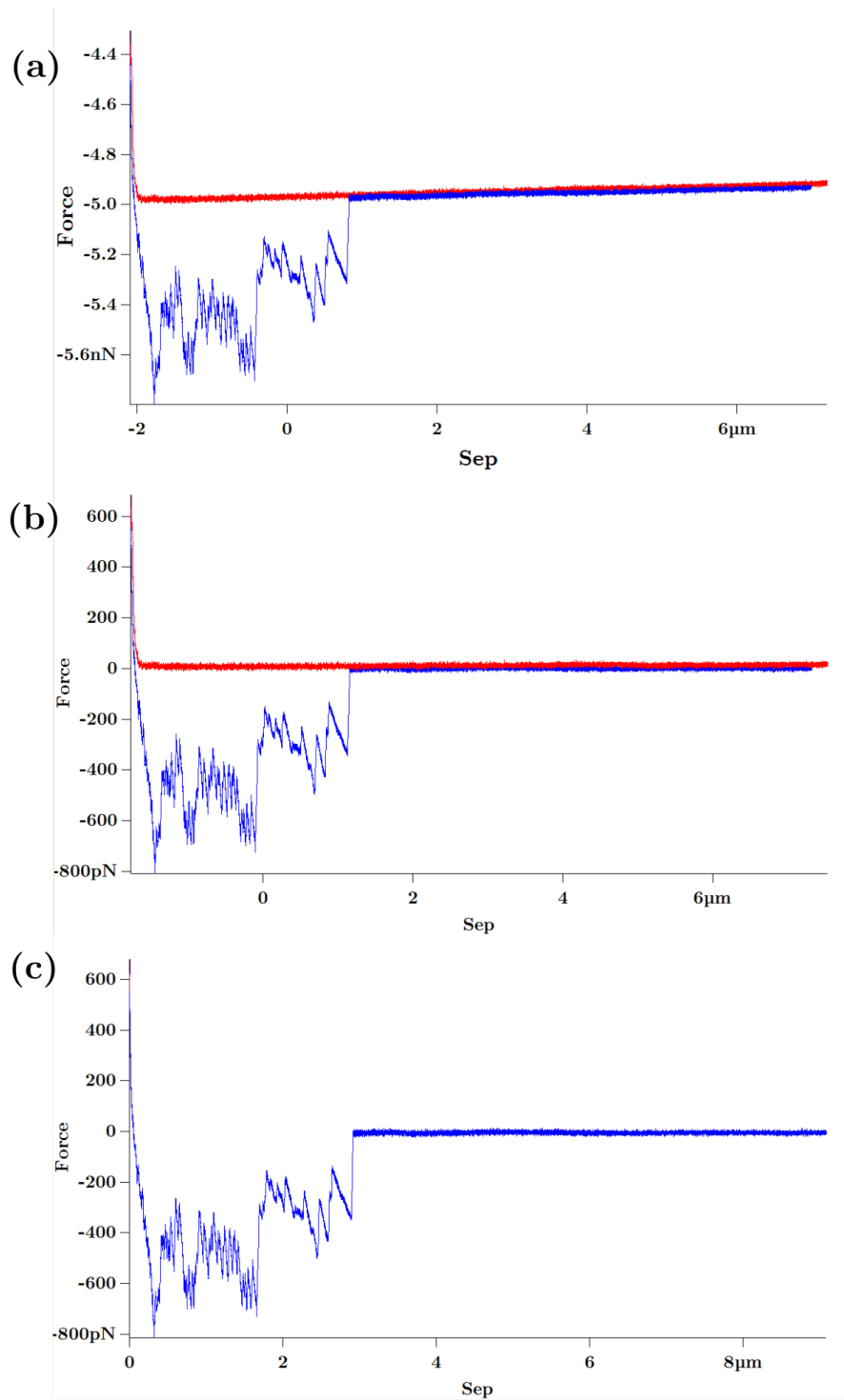


Figure 5.4.9: Illustration of the performed modifications on a force vs. separation curve. The measurement was taken with a *P.fluorescens* cell at a set point of 600 pN, 5s contact time and over a PSF membrane. (a) Raw force vs separation curve. (b) After line subtract (c) Only displaying the retraction after x and y offset.

Sometimes, the curve's baseline can have a slope. This is due to an artifact called virtual deflection. The virtual deflection is a mechanical coupling of the deflection signal with the Z movement, resulting in a slight slope in the force curve. This is normally corrected during calibration, but because of the cantilever's low spring constant, the virtual deflection might still be high. It can be corrected by using the line subtract function in the software. This function subtracts a defined line from the baseline and straightens it. From there, the curves were offset both on the x- and y-axis. This step was extremely important for finding the rupture length and the curves had to be offset one by one for it to be correct.

Adhesion force

The MFP3D software has the ability to batch process several curves. After each experiment, the adhesion forces for each contact time were determined and then extracted as a raw text file. The data was then transferred to the data analysis and graphing software Origin for further analysis that will be presented in the next chapter.

Rupture length

The rupture length was found by using a Matlab script written by Sara Binahmed with the help of the author. This script takes in force vs. separation data in the form of text files and gives out the rupture length. As previously mentioned, the curves must be modified as explained in Section 5.4.5. After each experiment, the data was transferred to Origin for further analysis.

5.4.6 Control Measurements

Control measurements on PSF and PSF-PDA membranes were performed. They were performed using a PDA-coated cantilever without an attached bacterial cell. Measure-

ments were taken at random spots for each contact time.

Chapter 6

Results and Discussion

6.1 Membrane characterization

6.1.1 Hydrophobicity

Figure 6.1.1 presents the mean and standard deviation of the contact angles of the PSF and PSF-PDA membranes. The PSF-PDA membrane is more hydrophilic than the PSF membrane, meaning that the contact angle was reduced.

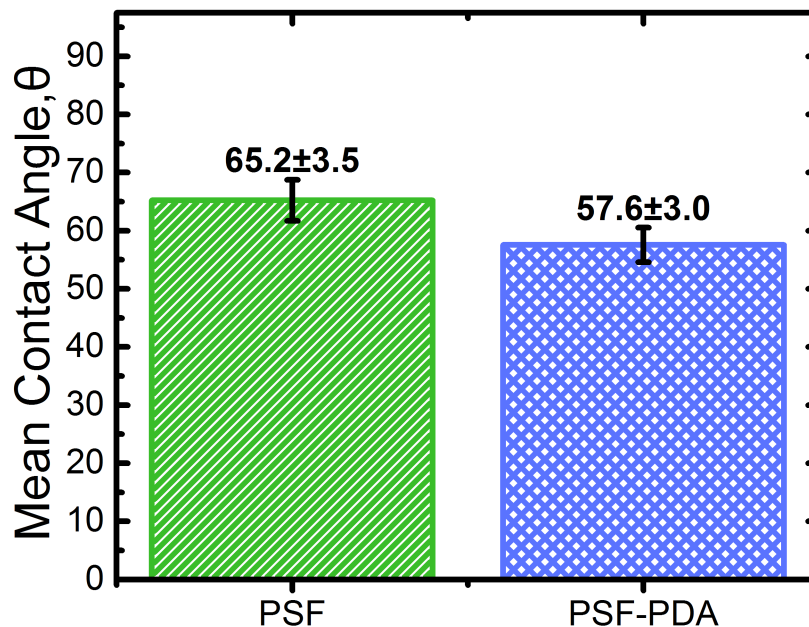


Figure 6.1.1: The mean and standard deviation of contact angle measurements performed on PSF and PSF-PDA membrane. The measurements were performed by Nathan Karp and obtained through personal communication.

A decrease in hydrophobicity is a desired effect when aiming to reduce biofouling because it makes it more difficult for bacterial cells to adhere.

6.1.2 Permeability

When talking about membrane technology, permeability is an important factor. A low permeability means that a higher pressure will be necessary to treat the desired amount of water. A higher pressure means higher operational costs, it is therefore desirable to have a permeability that is as high as possible and still yields good separation.

The permeability of a PSF-PDA sample was measured and compared with PSF samples from the same original membrane. This was done to exclude variance in permeability

Table 6.1.1: Measured permeability of PSF and PSF-PDA samples.

PSF	PSF-PDA
$274 \pm 24, 5 \frac{L}{m^2 h Bar}$	$313 \frac{L}{m^2 h Bar}$

due to differences between different membrane samples. One PSF-PDA sample was measured and compared to 3 PSF samples. The results are shown in Table 6.1.1.

PDA only forms a thin nanolayer on the surface. In their study, Lee et al. (2007) found the thickness of a 2 g/L PDA film to be around 3 nm after an immersion time of 1 hour. It was therefore not expected for the modification to decrease the permeability. Results (Table 6.1.1) indicate that PDA coating does not negatively affect membrane permeability, and may even increase it. This phenomenon could be due to the increasing hydrophilicity making it easier for water molecules to penetrate the pores. However, further replicates would be needed to confirm the reproducibility of this observation.

6.1.3 Roughness

The RMS roughness (R_{RMS}) for both membrane types is shown in Table 6.1.2 and Figure 6.1.2 shows sample images of the membranes.

The surface roughness values for the modified membranes were statistically identical to that of the pristine membranes. Kasemset et al. (2016) obtained comparable results when coating PSF membranes with 4 g/L PDA. However, some previous studies such as Cheng et al. (2012); Ball et al. (2012) showed that PDA modification increased the surface roughness.

Table 6.1.2: R_{RMS} of PSF and PSF-PDA membranes. The roughness was found using AFM in topography mode. 6 1-by-1 μm images were obtained for PSF membranes, and 5 1-by-1 μm images for PSF-PDA

PSF	PSF-PDA
$2,45 \pm 0,32nm$	$3,74 \pm 1,44nm$

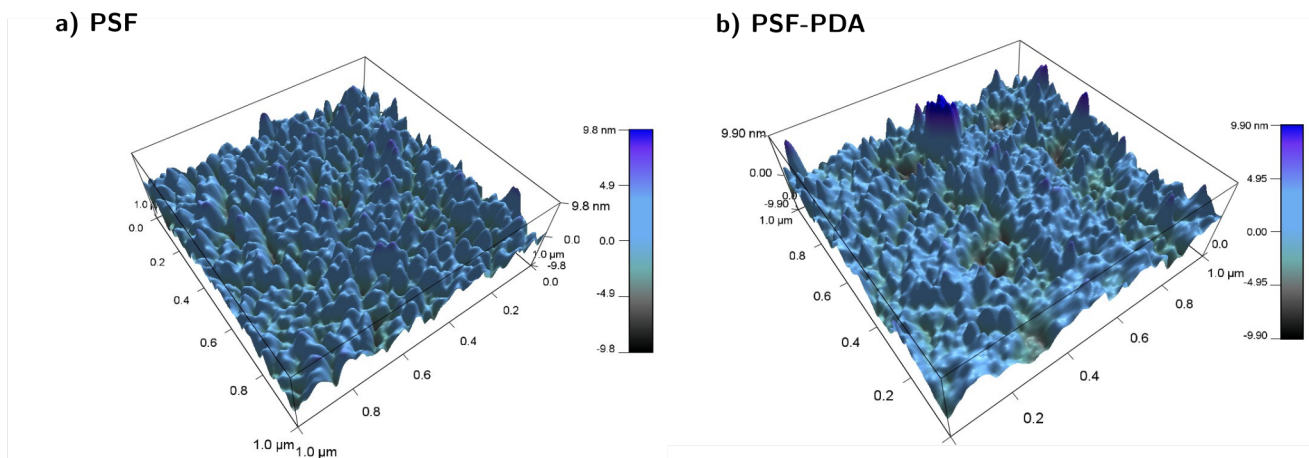


Figure 6.1.2: AFM images of (a) PSF and (b) PSF-PDA membranes.

This increase is due to the deposition of PDA nanoaggregates forming on the surface. These could clearly be observed when scanning over larger areas, such as 10-by-10 μm or 20-by-20 μm (Figure 6.1.3). On the other hand, those larger images could not be used to calculate the R_{RMS} because it was difficult to obtain a good resolution. Whether or not these aggregates could increase the bacterial adhesion by creating protective niches should be investigated, but was not covered in this study.

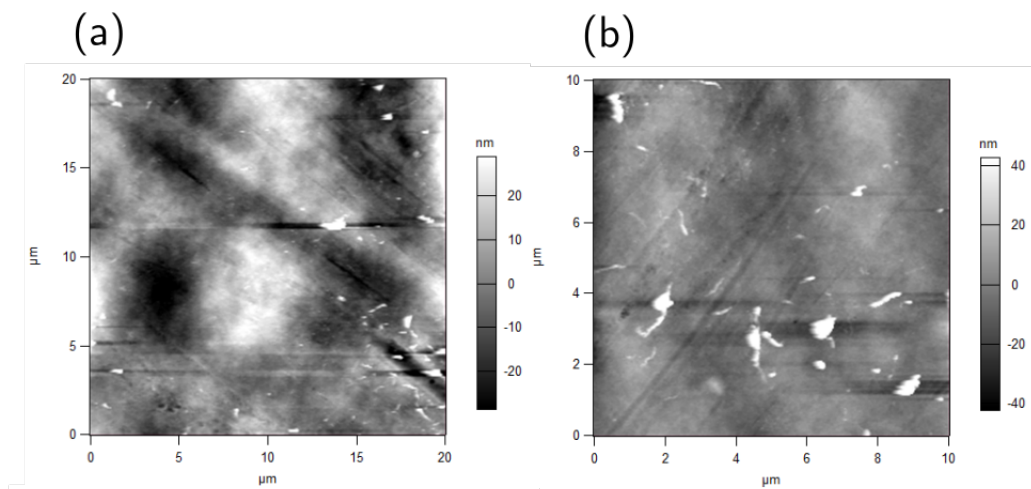


Figure 6.1.3: AFM images of (a) 20-by-20 μm and (b) 10-by-10 μm PSF-PDA membranes. The white spots on the images are PDA nanoaggregates and the black lines are artifacts .

6.2 Quantification of Bacterial Adhesion

6.2.1 Adhesion profiles

A typical retraction curve is shown in Figure 6.2.1. The curves were often composed of consecutive peaks and sometimes long rupture length.

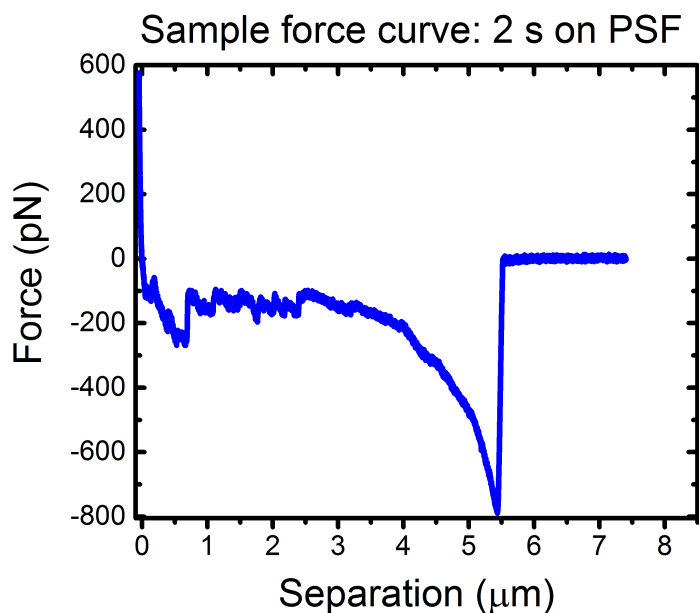


Figure 6.2.1: A force-separation curve obtained with a single *P.fluorescens* cell at a set point of 600 pN, 2s contact time and over a PSF membrane

Although this sample curve has a typical shape, the obtained curves had many different patterns. As described in Section 5.4.3, three measurements were taken at each spot. These three consecutive measurements could give completely different curves. This differs from the expectation for them to be similar given that they were taken at the same location, with the same cell and contact time.

Figure 6.2.2 shows three curves taken at the same spot. The measurements were taken with a single *P.fluorescens* cell at a set point of 600 pN, 0s contact time and over a PSF membrane. In the first curve, the adhesion force (F_{adh}) and rupture length (L_{rup}) are rather low, laying bellow 400 pN and 1 μm . The second measurement showed a slightly higher F_{adh} (400 pN) and a considerably higher L_{rup} of 6 μm . The last curve had a sawtooth pattern giving $F_{adh} = 600\text{pN}$ and $L_{rup} = 1,8\mu\text{m}$. This sawtooth pattern corresponds to the consecutive unbinding of single adhesion molecules (Friedrichs et al., 2013).

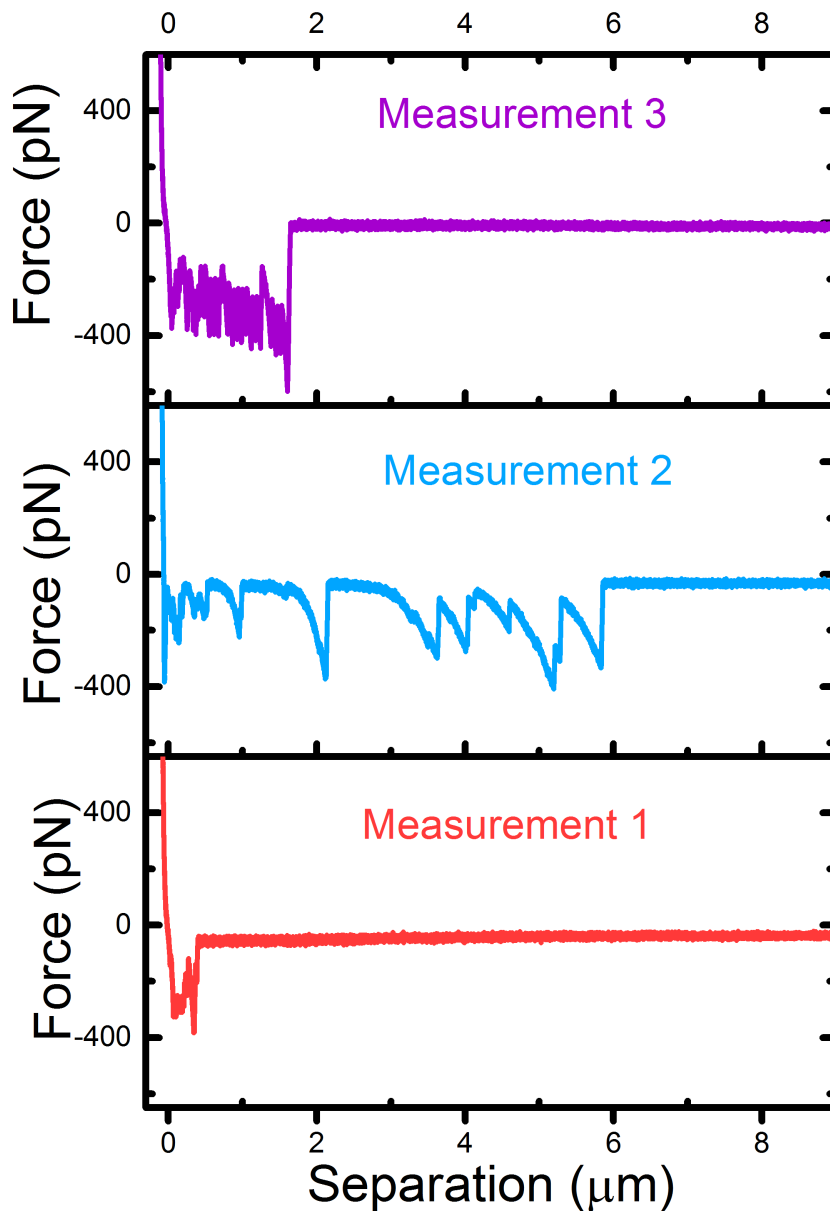


Figure 6.2.2: Three force-separation curves obtained at the same spot with a single *P.fluorescens* cell at a set point of 600 pN, 0s contact time and over a PSF membrane

Although the curves would differ a lot even while measuring with the same parameters, some curves would randomly have the same pattern. A similar manifestation was also observed by Thewes et al. (2015) when performing experiments with the gram-positive

Staphylococcus aureus. This phenomenon could indicate that the binding of a cell to a substrate depends on the orientation of the appendages and molecules mediating adhesion.

5 profiles were identified for PSF-membranes and 4 for PSF-PDA. These patterns are shown in Tables 6.2.1 and 6.2.2.

Table 6.2.1: Typical patterns observed for force-curves on PSF membranes.

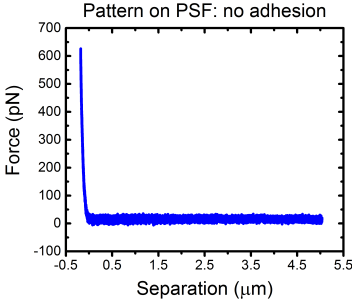
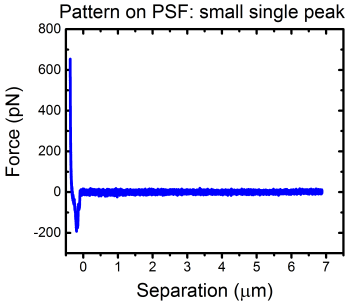
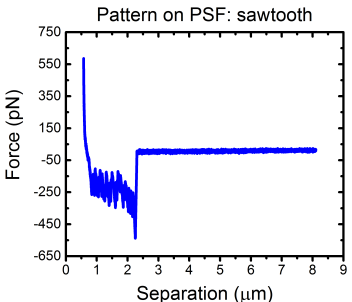
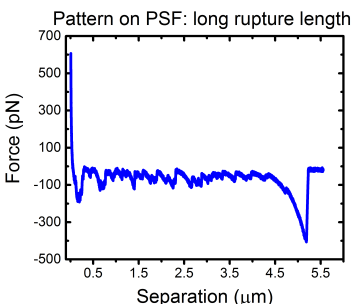
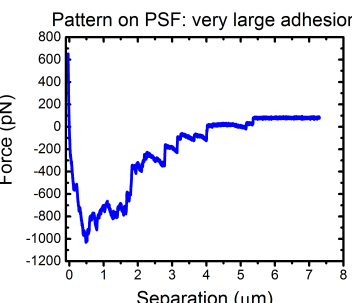
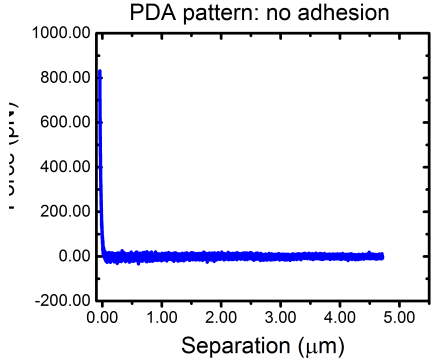
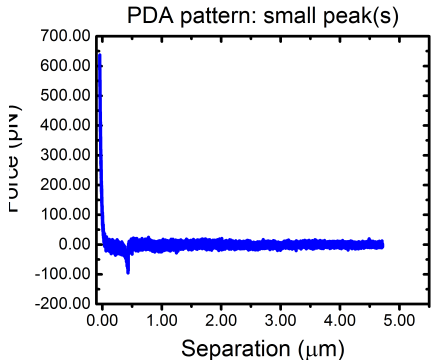
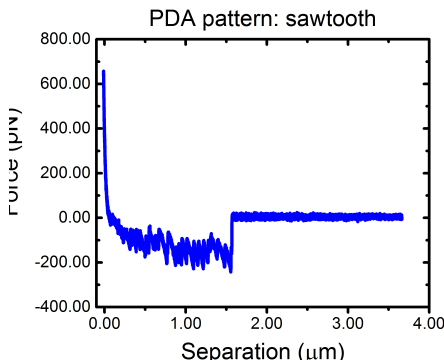
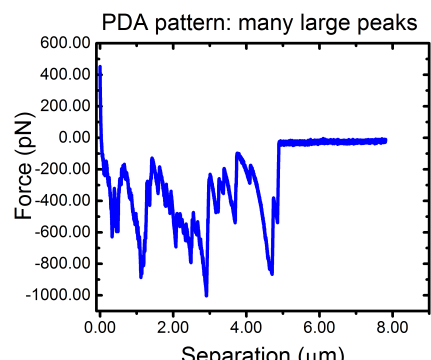
PSF Patterns	Description
 <p>Pattern on PSF: no adhesion</p>	<p>No detectable adhesion was measured.</p> <p>The fluctuation of the curve is caused by the cantilever vibrating due to Brownian motion.</p>
 <p>Pattern on PSF: small single peak</p>	<p>A small adhesion peak with a short rupture length indicates low adhesion. The peak could sometimes be surrounded by other small peaks, these are due to the unbinding of several molecules.</p>
 <p>Pattern on PSF: sawtooth</p>	<p>The sawtooth pattern is usually combined with a medium rupture length and adhesion force.</p> <p>According to (Friedrichs et al., 2013), it corresponds to the consecutive unbinding of single adhesion molecules</p>
 <p>Pattern on PSF: long rupture length</p>	<p>A long rupture length indicates that there are many bonds forming. The long rupture length might be due to extracellular appendages such as pili.</p>
 <p>Pattern on PSF: very large adhesion</p>	<p>Big adhesion peaks indicate that there are very strong bonds forming.</p>

Table 6.2.2: Typical patterns observed for force-curves on PSF-PDA membranes.

PSF-PDA Patterns	Description
 <p>PDA pattern: no adhesion</p>	<p>No detectable adhesion was measured.</p> <p>The fluctuation of the curve is caused by the cantilever vibrating due to Brownian motion.</p>
 <p>PDA pattern: small peak(s)</p>	<p>A small adhesion peak with a short rupture length indicates low adhesion. The peak could sometimes be surrounded by other small peaks, these are due to the unbinding of several molecules.</p>
 <p>PDA pattern: sawtooth</p>	<p>The sawtooth pattern is usually combined with a medium rupture length and adhesion force.</p> <p>According to (Friedrichs et al., 2013), it corresponds to the consecutive unbinding of single adhesion molecules</p>
 <p>PDA pattern: many large peaks</p>	<p>Big adhesion peaks combined with longer rupture length indicate that there are very strong bonds forming.</p>

6.2.2 Statistical significance

As described in Chapter 5, the results describing the adhesion force and rupture length were transferred to Origin for statistical analysis. First, T-test were performed for the F_{adh} and L_{rup} data. The T-tests were performed to find whether or not the populations had statistically different means or not. The obtained data is not normally distributed, but since the population is high, 100, T-tests can be performed (Lumley et al., 2002). This study aims to look at how the substrate (membrane type) and contact time affect the adhesion and rupture length, T-tests were therefore performed as shown in Tables 6.2.3 and 6.2.4. The detailed results can be found in Appendix C.

Table 6.2.3: T-tests of F_{adh} and L_{rup} with regards to contact time. *OK* means that there is a statistically significant difference between the two groups, whereas *Failed* means that there is not a statistically significant difference.

Contact times	PSF		PSF-PDA	
	F_{adh}	L_{rup}	F_{adh}	L_{rup}
0s and 2s	OK	OK	OK	Failed
2s and 5s	OK	Failed	OK	Failed
0s and 5s	OK	OK	OK	Failed

Table 6.2.4: T-tests of F_{adh} and L_{rup} with regards to the membrane type. *OK* means that there is a statistically significant difference between the two groups, whereas *Failed* means that there is not a statistically significant difference.

PSF against PSF-PDA		
Contact time	F_{adh}	L_{rup}
0s	OK	OK
2s	OK	Failed
5s	OK	OK

F_{adh} depends on both the contact time and type of membrane, whereas for L_{rup} , only the results 0-2s on PSF along with 0s and 5s on PSF against PSF-PDA are statistically significant.

6.2.3 Control measurements

Control measurements were performed using a functionalized cantilever over the membrane. No cell was attached. Figures 6.2.3 and 6.2.6 show two sample curves obtained with a set point of 600 pN and a contact time of 2s. Without a cell, the peaks are more prominent, with few sub-peaks.

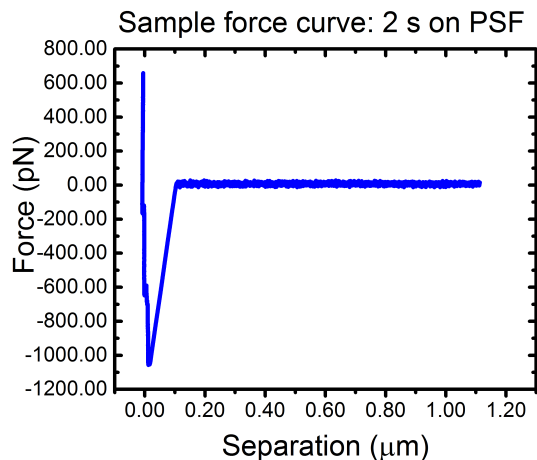


Figure 6.2.3: Force-separation curve obtained at a set point of 600 pN, 2s contact time and over a PSF membrane. No cell was immobilized.

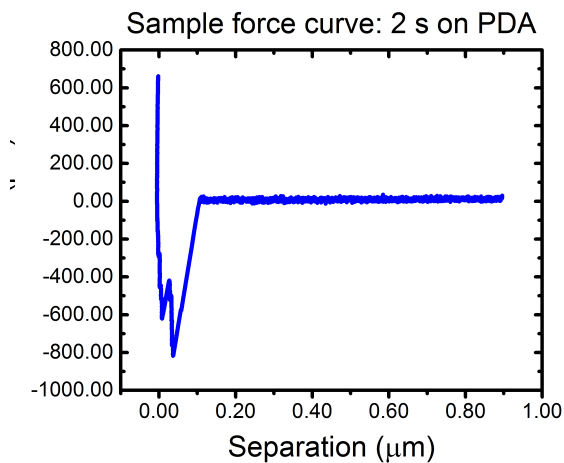


Figure 6.2.4: Force-separation curve obtained at a set point of 600 pN, 2s contact time and over a PSF-PDA membrane. No cell was immobilized.

The mean adhesion force and rupture length are shown bellow. They differ much from the values with an immobilized cell shown in Section 6.2.4.

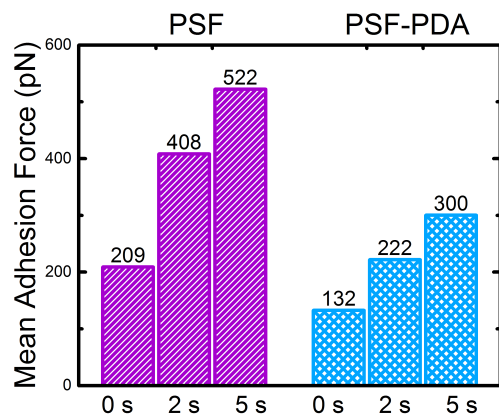


Figure 6.2.5: The mean of F_{adh} for both membrane types and the three contact times. No cell was immobilized.

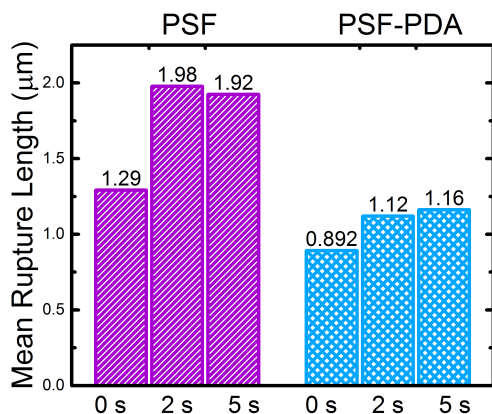


Figure 6.2.6: The mean of L_{rup} for both membrane types and the three contact times. No cell was immobilized.

6.2.4 Adhesion force and rupture length

Figure 6.2.7 and 6.2.8 show normalized histograms on both membrane types of F_{adh} and L_{rup} respectively. Figure 6.2.9 shows the mean of F_{adh} and L_{rup} for the two membrane types and the three contact times.

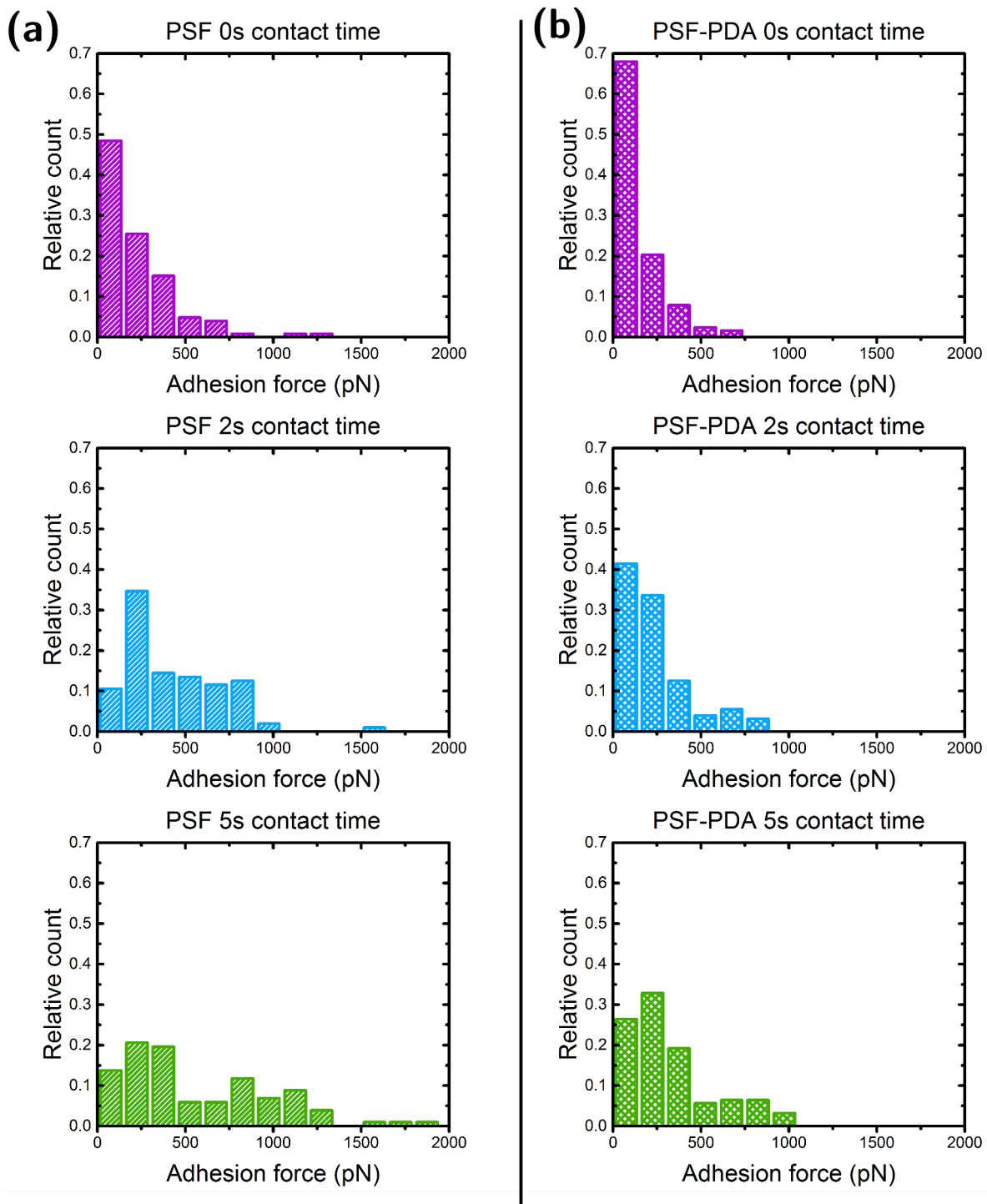


Figure 6.2.7: Normalized histograms of F_{adh} for (a) PSF membrane and (b) PSF-PDA membrane.

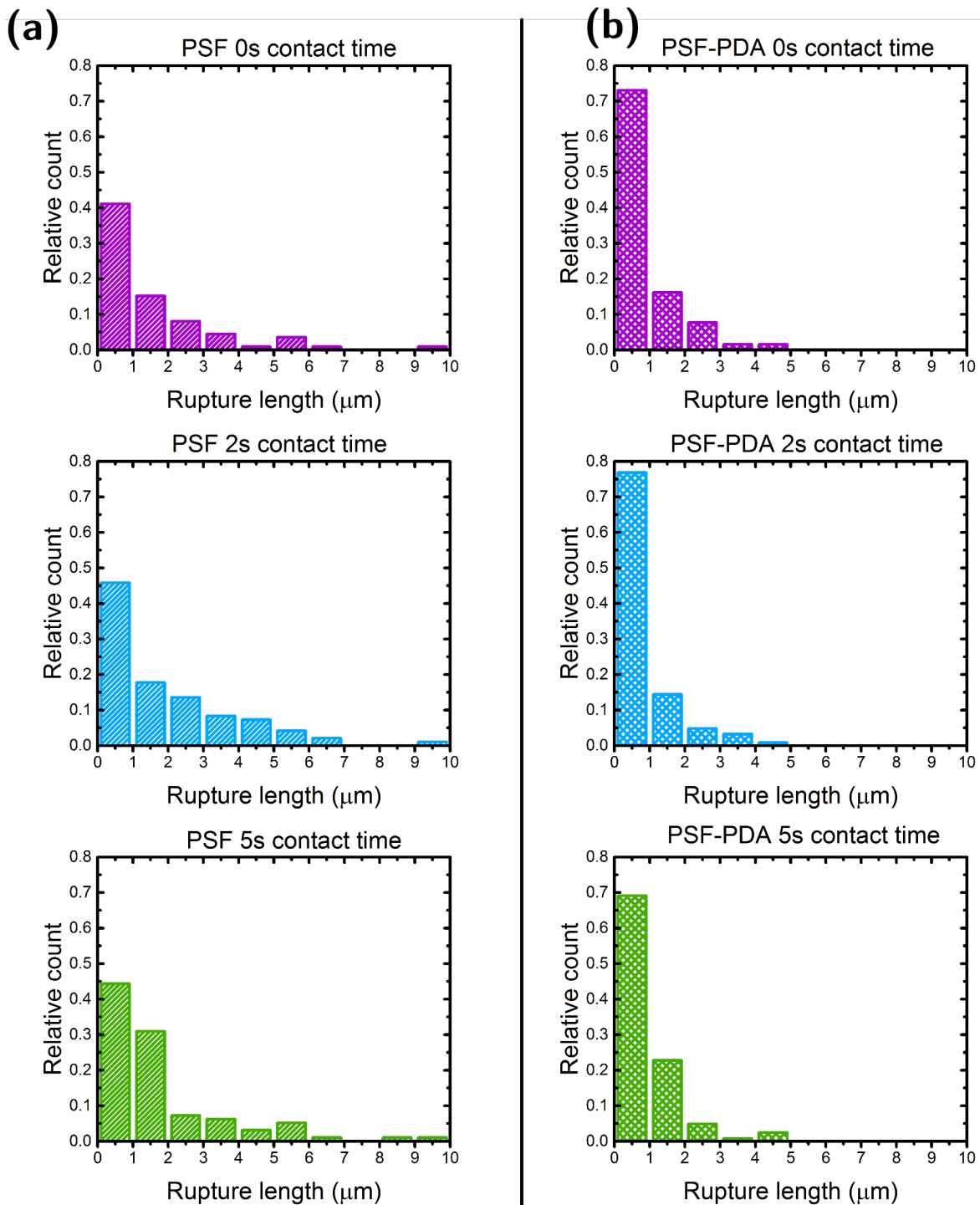


Figure 6.2.8: Normalized histograms of L_{rup} for (a) PSF membrane and (b) PSF-PDA membrane.

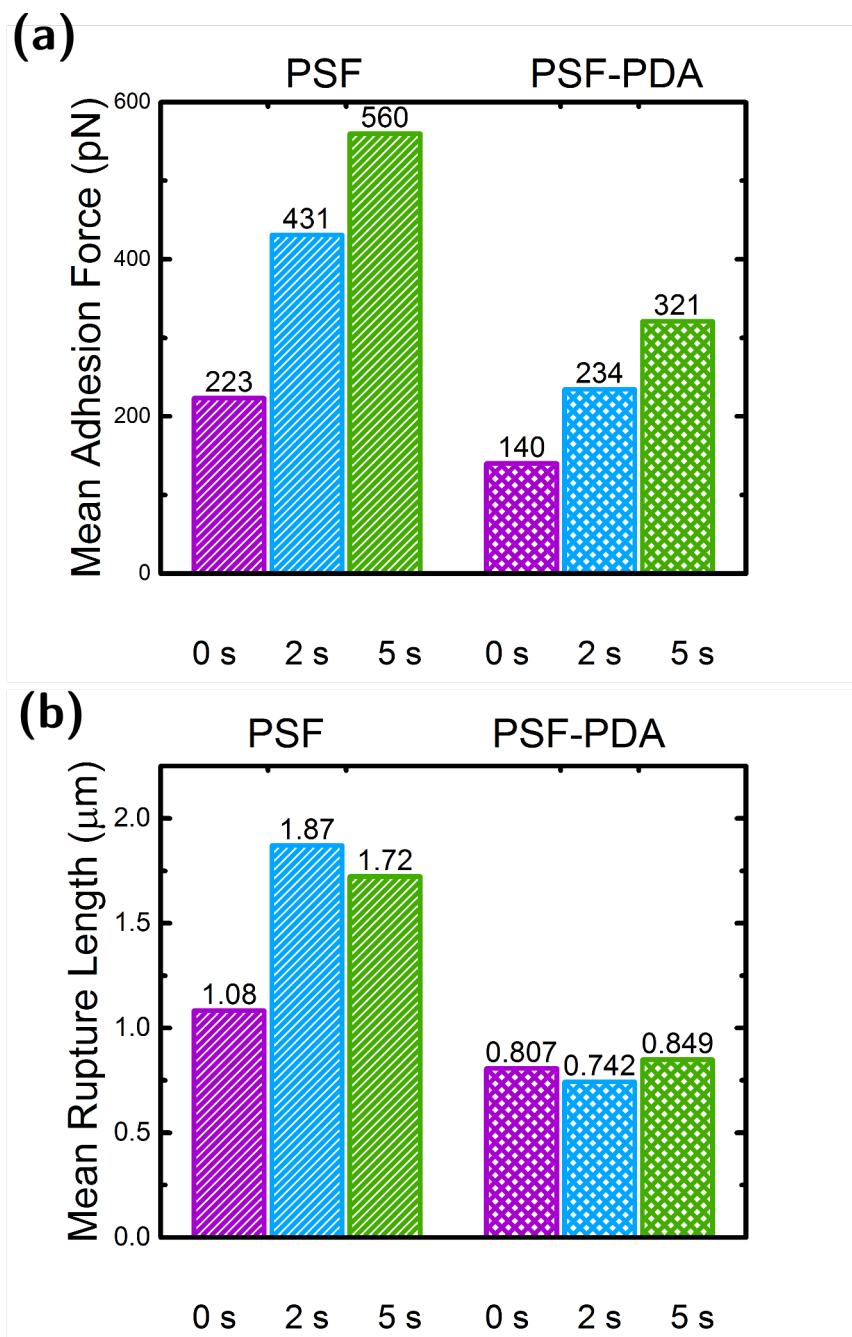


Figure 6.2.9: (a) The mean of F_{adh} for both membrane types and the three contact times. (b) The mean of L_{rup} for both membrane types and the three contact times.

F_{adh} increased gradually with increasing contact times on both membrane types (Figure 6.2.9 (a)). This indicates a bond strengthening over time. When it comes to L_{rup} , not all results are comparable because of the T-tests' outcome. If L_{rup} had changed signif-

icantly as the contact time increased, it would have indicated a sequential involvement of adhesins of different lengths during the bond strengthening. Since it was not the case, one can conclude that bond strengthening does not involve a sequence of different adhesins, but rather an increasing number of adhesins increasing the interaction.

P.fluorescens is a motile strain with both flagella and T4P. As covered in Section 3.1.4, T4P are long, filamentous surface appendages that are located at the cell poles and have several functions including twitching motility and attachment to biotic and abiotic surfaces. *P.fluorescens* was found to have similar T4P as *P.aeruginosa*, a very well-studied Pseudomonas. Whitchurch (2006) concluded that what is known about the biogenesis and function of the T4P of *P.aeruginosa* is applicable to *P.fluorescens*.

In general, the T4P of *P.aeruginosa* are 5-6 nm in diameter and have a hollow core of 1,2 nm. Their length vary a lot due to the fact that they retract, but they can reach up to 10 μm . This extensive length might have contributed to the sometimes long interaction distance between the cell and the membrane.

The PSF-PDA membranes showed clearly lower F_{adh} and L_{rup} . This suggests that weaker bonds were formed and fewer adhesins were able to adhere. This could be due to the increased hydrophilicity of PSF-PDA membranes.

6.2.5 PDA as an anti-foulant

PDA coating showed promising results in a small-scale and over short incubation times. In reality, the bacteria will be in contact with the membrane under higher pressures reaching the order of magnitude of $11 \cdot 10^6$ pN (Appendix B) and with higher incubation time.

The feed water in membrane treatment units is usually polluted. Surface water bodies

often contain high levels of NOM. In Norway, the concentration of NOM in the raw water is often higher than the limit of 25 mgPt/L and is continuously increasing due to climate change (Folkehelseinstituttet, 2009).

NOM on its own is an important foulant, but it also forms a conditioning film enabling the formation of a biofilm, thus it mediates adhesion.

The experiments in this thesis were conducted under highly simplified conditions: no flow, no presence of NOM, a pressure of 600 pN and contact times between 0 and 5 s. Therefore, one cannot immediately conclude that PDA is an effective coating agent for UF membranes. However, the obtained results are promising: the coating reduces the hydrophobicity, increases the permeability and reduces bacterial adhesion. These findings make PDA modification a good candidate for further research that should include testing in bigger scales. It is important to keep in mind that fouling does not necessarily need to be completely eliminated. If the operation cycle can be increased by a couple of hours, it could already save both energy and costs.

Chapter 7

Conclusion and Further Work

7.1 Conclusion

The aim of this thesis was to investigate the following hypothesis:

- PDA modification does not negatively affect the UF membrane's function and performance:
- PDA modification and the contact time have an impact on bacterial adhesion.

The hydrophilicity increased significantly when coating. Not only does this have a positive effect on the reduction of bacterial adhesion, but it also might have contributed in increasing the permeability.

The roughness did not increase much, but when scanning over larger areas, some nanoaggregates could be observed. However, they are still very small and it is unknown if they could increase the bacterial adhesion by creating protective niches where cells could thrive.

The obtained force curves showed that F_{adh} increased with an increasing contact time. The contact time did not have a statistical significant impact on L_{rup} , one can therefore conclude that bond strengthening does not involve a sequence of different adhesins, but

rather an increasing number of adhesins increasing the interaction.

The adhesion force decreased drastically when obtained on modified membranes. These results are promising in regards of using PDA as an anti-foulant on UF membranes.

The tests were performed under highly simplified conditions. One cannot conclude that PDA will be effective in reducing biofouling under real conditions, but one should rather conclude with the fact that PDA is a good candidate for reducing biofouling and should be investigated further.

As a summary, the following conclusions can be drawn in regards to the original hypothesis:

- PDA coating did not negatively affect the membrane's function and performance and actually improved important parameters such as the permeability and hydrophilicity.
- Both the contact time and PDA coating affected the force of adhesion. The rupture length, on the other hand, was only partially affected by the coating and not by the contact time.

7.2 Recommendations for Further Work

For further research, the following should be done:

- Perform more permeability tests to have more comparable results and exclude possible sources of error such as the difference in permeability being due to membrane artifacts and not the coating itself.
- Perform rejection tests to see if the coating has any effect.
- Add NOM to the fluid cell to mimic the formation of a conditioning film.

- If the results still are promising, a small-scale pilot project using PDA-coated membranes should be tested.

Bibliography

- Araújo, E. A., de Andrade, N. J., da Silva, L. H. M., de Carvalho, A. F., de Sá Silva, C. A., and Ramos, A. M. (2010). Control of microbial adhesion as a strategy for food and bioprocess technology. *Food and bioprocess technology*, 3(3):321–332.
- Ball, V., Del Frari, D., Toniazzo, V., and Ruch, D. (2012). Kinetics of polydopamine film deposition as a function of ph and dopamine concentration: Insights in the polydopamine deposition mechanism. *Journal of colloid and interface science*, 386(1):366–372.
- Belfort, G., Davis, R. H., and Zydney, A. L. (1994). The behavior of suspensions and macromolecular solutions in crossflow microfiltration. *Journal of Membrane Science*, 96(1):1–58.
- Boland, T., Latour, R. A., and Stutzenberger, F. J. (2000). *Molecular basis of bacterial adhesion*, pages 29–41. Springer.
- Chakrabarty, B., Ghoshal, A., and Purkait, M. (2008). Preparation, characterization and performance studies of polysulfone membranes using pvp as an additive. *Journal of Membrane Science*, 315(1):36–47.
- Characklis, W., Bryers, J. D., et al. (2009). Bioengineering report: Fouling biofilm development: A process analysis. *Biotechnology and bioengineering*, 102(2):309–347.
- Cheng, C., Li, S., Zhao, W., Wei, Q., Nie, S., Sun, S., and Zhao, C. (2012). The hydrodynamic permeability and surface property of polyethersulfone ultrafiltration

- membranes with mussel-inspired polydopamine coatings. *Journal of membrane science*, 417:228–236.
- Corcoran, E. (2010). *Sick water?: the central role of wastewater management in sustainable development: a rapid response assessment*. UNEP/Earthprint.
- Craig, L. and Li, J. (2008). Type iv pili: paradoxes in form and function. *Current opinion in structural biology*, 18(2):267–277.
- Dufrêne, Y. F. (2015). Sticky microbes: forces in microbial cell adhesion. *Trends in microbiology*, 23(6):376–382.
- Eaton, P. and West, P. (2010). *Atomic force microscopy*. Oxford University Press, Oxford.
- Escobar, I. C., Hoek, E. M., Gabelich, C. J., DiGiano, F. A., and et al. (2005). Committee report: Recent advances and research needs in membrane fouling. *American Water Works Association. Journal*, 97(8):79–89,14.
- Folkehelseinstituttet (2009). Rapport 2009:2. Miljø og helse – en forskningsbasert kunnskapsbase. Technical report.
- Friedlander, R. S., Aizenberg, J., and Vogel, N. (2015). Role of flagella in adhesion of escherichia coli to abiotic surfaces. *Langmuir*, 31(22):6137–6144.
- Friedrichs, J., Legate, K. R., Schubert, R., Bharadwaj, M., Werner, C., Müller, D. J., and Benoit, M. (2013). A practical guide to quantify cell adhesion using single-cell force spectroscopy. *Methods*, 60(2):169–178.
- Garrett, T. R., Bhakoo, M., and Zhang, Z. (2008). Bacterial adhesion and biofilms on surfaces. *Progress in Natural Science*, 18(9):1049–1056.
- Geise, G. M., Lee, H., Miller, D. J., Freeman, B. D., McGrath, J. E., and Paul, D. R. (2010). Water purification by membranes: The role of polymer science. *Journal of Polymer Science Part B: Polymer Physics*, 48(15):1685–1718.

- Glucina, K., Laine, J., and Durand-Bourlier, L. (1998). Assessment of filtration mode for the ultrafiltration membrane process. *Desalination*, 118(1):205–211.
- Goren, S. L. (1979). The hydrodynamic force resisting the approach of a sphere to a plane permeable wall. *Journal of Colloid and Interface Science*, 69(1):78–85.
- Guillen, G. R., Pan, Y., Li, M., and Hoek, E. M. (2011). Preparation and characterization of membranes formed by nonsolvent induced phase separation: a review. *Industrial & Engineering Chemistry Research*, 50(7):3798–3817.
- Gutman, J., Herzberg, M., and Walker, S. (2014). Biofouling of reverse osmosis membranes: Positively contributing factors of sphingomonas. *Environmental Science Technology*, 48(23):13941.
- Haaf, F., Sanner, A., and Straub, F. (1985). Polymers of n-vinylpyrrolidone: synthesis, characterization and uses. *Polymer Journal*, 17(1):143–152.
- Hand, D. W., Crittenden, J. C., Trussell, R. R., Tchobanoglous, G., and Howe, K. J. (2012). Principles of water treatment.
- Hem, L. J. and Thorsen, T. (2008). Driftserfaringer med membranfiltrering. Technical report.
- Isaacson, R. E. (1985). *Pilus Adhesins*, pages 307–336. Springer US, Boston, MA.
- Jucker, C. and Clark, M. M. (1994). Adsorption of aquatic humic substances on hydrophobic ultrafiltration membranes. *Journal of Membrane Science*, 97:37–52.
- Kasemset, S., He, Z., Miller, D. J., Freeman, B. D., and Sharma, M. M. (2016). Effect of polydopamine deposition conditions on polysulfone ultrafiltration membrane properties and threshold flux during oil/water emulsion filtration. *Polymer*, 97:247–257.
- Lee, H., Dellatore, S. M., Miller, W. M., and Messersmith, P. B. (2007). Mussel-inspired surface chemistry for multifunctional coatings. *science*, 318(5849):426–430.

- Lumley, T., Diehr, P., Emerson, S., and Chen, L. (2002). The importance of the normality assumption in large public health data sets. *Annual review of public health*, 23(1):151–169.
- Lynge, M. E., van der Westen, R., Postma, A., and Städler, B. (2011). Polydopamine—a nature-inspired polymer coating for biomedical science. *Nanoscale*, 3(12):4916–4928.
- Machenbach, I. (2007). *Drinking water production by coagulation and membrane filtration*. Thesis. Avhandling (dr.ing.) - Norges teknisk-naturvitenskapelige universitet, Trondheim, 2007.
- Madigan, M. T., Martinko, J. M., Brock, T. D., Bender, K. S., Buckley, D. H., and Stahl, D. A. (2015). *Brock biology of microorganisms*. Pearson, Harlow, 14th ed., global ed. edition. Brock, Thomas D. Biology of microorganisms.
- Mattick, J. S. (2002). Type iv pili and twitching motility. *Annual Reviews in Microbiology*, 56(1):289–314.
- Merritt, K. and An, Y. H. (2000). *Factors influencing bacterial adhesion*, pages 53–72. Springer.
- Miller, D. J., Araújo, P. A., Correia, P. B., Ramsey, M. M., Kruithof, J. C., van Loosdrecht, M. C., Freeman, B. D., Paul, D. R., Whiteley, M., and Vrouwenvelder, J. S. (2012). Short-term adhesion and long-term biofouling testing of polydopamine and poly (ethylene glycol) surface modifications of membranes and feed spacers for biofouling control. *water research*, 46(12):3737–3753.
- Monks, K. (2014). From toilet to tap: Getting a taste for drinking recycled waste water.
- Mulder, J. (1991). *Basic principles of membrane technology*. Springer Science & Business Media.
- O’Toole, G. A. and Kolter, R. (1998). Flagellar and twitching motility are necessary

- for pseudomonas aeruginosa biofilm development. *Molecular microbiology*, 30(2):295–304.
- Ou, J. T. and Anderson, T. F. (1970). Role of pili in bacterial conjugation. *Journal of bacteriology*, 102(3):648–654.
- Parker, D., Bussink, J., Grampel, H. T., Wheatley, G. W., Dorf, E.-U., Ostlinning, E., Reinking, K., Schubert, F., Jünger, O., and Wagener, R. (2002). Polymers, high-temperature. *Ullmann's Encyclopedia of Industrial Chemistry*.
- Pendergast, M. M. and Hoek, E. M. (2011). A review of water treatment membrane nanotechnologies. *Energy & Environmental Science*, 4(6):1946–1971.
- PUB (2015). Newater.
- Razatos, A. P. and Georgiou, G. (2000). *Evaluating bacterial adhesion using atomic force microscopy*, pages 285–296. Springer.
- Richard, W. B. et al. (2004). Membrane technology and applications. *John Wiley & Sons Ltd*.
- Ridgway, H. and Flemming, H.-C. (1996). *Membrane Biofouling, Chap 6*. Water Treatment Membrane Processes. McGraw-Hill, New York.
- Strathmann, H. and Kock, K. (1977). The formation mechanism of phase inversion membranes. *Desalination*, 21(3):241–255.
- Taubenberger, A. V., Hutmacher, D. W., and Muller, D. J. (2013). Single-cell force spectroscopy, an emerging tool to quantify cell adhesion to biomaterials. *Tissue Engineering Part B: Reviews*, 20(1):40–55.
- Thewes, N., Thewes, A., Loskill, P., Peisker, H., Bischoff, M., Herrmann, M., Santen, L., and Jacobs, K. (2015). Stochastic binding of staphylococcus aureus to hydrophobic surfaces. *Soft matter*, 11(46):8913–8919.

- United-Nations (2010). The human right to water and sanitation.
- Van de Witte, P., Dijkstra, P., Van den Berg, J., and Feijen, J. (1996). Phase separation processes in polymer solutions in relation to membrane formation. *Journal of Membrane Science*, 117(1):1–31.
- Van Loosdrecht, M., Lyklema, J., Norde, W., Schraa, G., and Zehnder, A. (1987). The role of bacterial cell wall hydrophobicity in adhesion. *Applied and environmental microbiology*, 53(8):1893–1897.
- Whitchurch, C. B. (2006). Biogenesis and function of type iv pili in pseudomonas species. In *Pseudomonas*, pages 139–188. Springer.
- Wood, T. L., Guha, R., Tang, L., Geitner, M., Kumar, M., and Wood, T. K. (2016). Living biofouling-resistant membranes as a model for the beneficial use of engineered biofilms. *Proceedings of the National Academy of Sciences*, 113(20):E2802–E2811.
- Yuan, Y. and Lee, T. R. (2013). Contact angle and wetting properties. In *Surface science techniques*, pages 3–34. Springer.
- Zeng, G., Müller, T., and Meyer, R. L. (2014). Single-cell force spectroscopy of bacteria enabled by naturally derived proteins. *Langmuir : the ACS journal of surfaces and colloids*, 30(14):4019.
- Zodrow, K., Brunet, L., Mahendra, S., Li, D., Zhang, A., Li, Q., and Alvarez, P. J. (2009). Polysulfone ultrafiltration membranes impregnated with silver nanoparticles show improved biofouling resistance and virus removal. *Water research*, 43(3):715–723.
- Ødegaard, H., Norheim, B., and Norsk Vann, B. A. (2012). *Vann- og avløpsteknikk*. VA-teknikk. Norsk Vann, Hamar.

Appendix A

Protocols for conducted laboratory work

A.1 Protocol for fabricating and modifying the polymeric membranes

A.1.1 Making the dope solution

Information

The fabrication is done over two days. The dope solution has to rest over night in a desiccator in order for the gas bubbles to disappear.

Necessary equipment:

- Ultra-pure water
- Glass plates
- A magnetic stirrer and heater
- Polysulfone (PSf, MW: 22,000, Sigma-Aldrich)

- Poly(vinylpyrrolidone (PVP, MW: 58,000, Acros Organics)
- N-methyl-2-pyrrolidone (NMP, 99.5%, Sigma-Aldrich)

First, the dope solution must be prepared. With a syringe, take out 75 g of NMP and put it in a flask with a stirring-magnet. Place the flask on the magnetic stirrer and heater and add 10 g of PVP. Turn the heat up to about 60°C while stirring. It should take about two hours to dissolve.

When the PVP is completely dissolved, add 15 g of PSF and turn up the heat to 80°C. PSF should be kept away from water because it might precipitate in the dope solution. It is therefore recommended to reserve a spatula for PSF only and keep it in the desiccator. The PSF will need about four hours to dissolve.

When the dope solution is done, it should be a homogeneous, viscous and transparent solution. Small air bubble might be present in the solution. To remove them, keep the solution overnight in the desiccator. Do not tighten the cap of the flask completely in order to let the air escape. The flask should also be wrapped in aluminium foil to protect the solution from light.

A.1.2 Making the membranes

Information

100 ml of dope solution is enough to make about 9 membranes.

Necessary equipment:

- Ultra-pure water
- Glass plates
- 2 containers or more big enough for the glass plate to be immersed
- Polyethylene terephthalate (PET) fabric
- Dope solution
- Casting blade
- A container to store the membranes
- Box cutter
- 15mL of N-methyl-2-pyrrolidone (NMP, 99.5%, Sigma-Aldrich)
- A glass pipette

Start by wrapping the glass plates with PET and remove all the wrinkles. To attach the PET, use a tape that will resist water or else, it might leak some color in the water. Pour 2L of ultra-pure water in a primary bath. Zero out the casting blade and set it at 0.25 mm.

Using a syringe, take out about 15 mL of NMP. With a glass pipette, wet the fabric with NMP. Start by adding a few drops first, making sure not to soak it completely. The whole fabric should be wetted, make sure there are no dry spots. To make sure that there not too much NMP on the fabric, wipe it a little bit with a Kim wipe and go over it with an air flow, if available.

Pour some solution on top of the glass plate, and spread it with the casting blade. Directly take the glass plate and immerse it for 10 min in the primary bath. After 10 min, immerse the membrane in a secondary bath with about 4 L of ultra-pure water for 1 hour. When finished, cut out the membrane with a cutting knife and store it in a container filled with ultra-pure water. The membranes should be stored in the refrigerator.

In order to make several membranes after each other, clean the blade, zero it and prepare everything for a new membrane while the previous one is in the primary bath. It is recommended to have 3 to 4 secondary baths in order to be able to make the membranes without interruption.

A.1.3 Coating the membranes with Polydopamine

Information

The membranes should not be coated immediately after being fabricated. They should rest at least over night in the refrigerator.

Necessary equipment:

- pH meter
- Membrane casting frame with clamps
- A glass plate to provide support while cutting
- A box cutter
- A magnetic stirrer
- A 500 mL beaker
- Ultra-pure water
- Trizma Hydrochloride solution (Sigma Aldrich, T3038)
- NaOH, 1M (Sigma Aldrich, 71463)
- Dopamine Hydrochloride (Sigma Aldrich, H8502) (Should be stored in a refrigerator and in a dry place)

Clean a small glass plate with ultra-pure water and acetone in order to have a surface to cut and work on. With a lamp, check that the membranes do not have holes or other defaults. Place the membrane on the clean glass plate with the active layer facing down and cut out a piece fitting the frame. Place the membrane and tighten with clamps as illustrated in figure A.1.1. If there are some small undamaged pieces left, save them in a falcon tube for later characterization of pristine membranes.

The synthesis of PDA involves the reaction of dopamine with HCl and Trizma at a pH of 8.5. For the coating, assume a necessary dose of approximately 30 mL per membrane.

Add 495 mL of ultra-pure water for 5 mL of Trizma. While stirring, check the pH with a pH meter. With a pipette, add drops of NaOH until the pH reaches 8,5.

On a weighting paper, weigh 2 g of the dopamine powder and add it to the solution while stirring. The powder should dissolve completely.

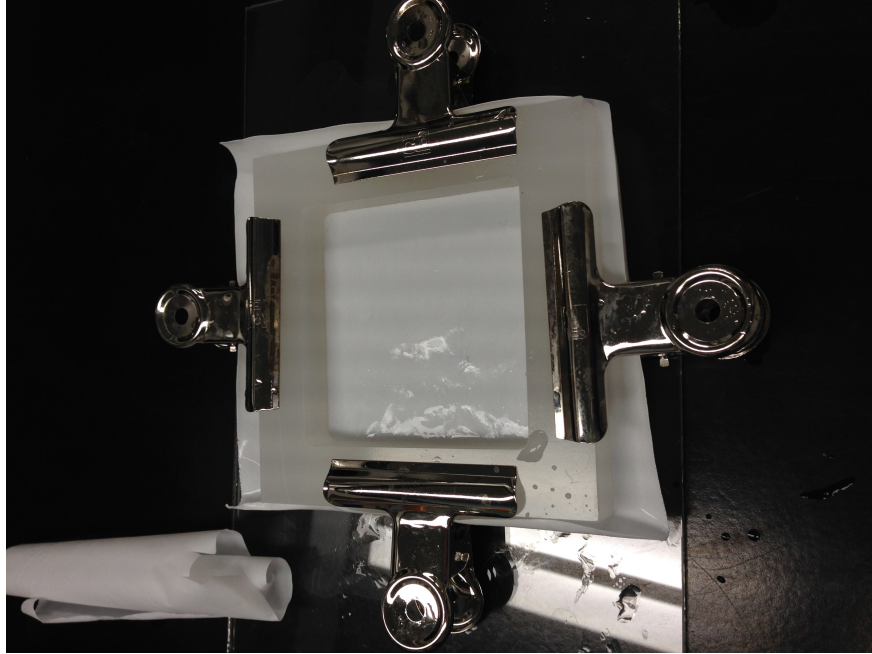


Figure A.1.1: The membranes in the casting frame

Pour some of the PDA solution in each frame and put on a shaker at 65 rpm for 15 min. This step should be repeated three times and the membranes must be rinsed thoroughly with ultra-pure water over a waster beaker between each round.

Store the coated membranes in the refrigerator, in a flask filled with ultra-pure water.

A.2 Protocol for bacterial culture

A.2.1 Preparing the culture

Information

The Luria broth (LB), flask and tips for the pipette must be autoclaved prior to this preparation.

Necessary equipment:

- Spray bottle with Ethanol
- Pipette + autoclaved tips
- Autoclaved flask
- Autoclaved LB
- Autoclaved piece of aluminium foil
- Cultured agar plate
- Incubator
- UV vacuum hood

Start with sterilizing the incubator by spraying it with ethanol and turn it on the following settings: 125 rpm and $T=37\text{ }^{\circ}\text{C}$. Spray the UV vacuum hood with ethanol and turn on the UV light, close it and leave it for five minutes. Before use, turn off the UV light.

Put all the needed equipment under the hood and try to keep your hands under the hood as much as possible.

Pour 50 mL of LB into the flask and put the cap back on to avoid any contamination.



Figure A.2.1: The Necessary equipment

Open the dish with the cultured agar plate. With the pipette tip, scrap an untouched colony. Remember to never scrap twice!

Drop the pipette tip inside the flask and close it.

Remember to seal the Petri dish with Parafilm.

Take all the used equipment out of the hood, and sterilize it again with ethanol.

Place the flask in the incubator over night, and cover it with aluminium foil to make sure there is oxygen getting in

Remember to put the Petri dish back in the refrigerator, always with the agar-side up.

It is recommended to autoclave all the equipment needed for the following day.

A.2.2 Diluting the solution

Information

This preparation demands approximately 15 min and the bacteria 1,5-2 hours to grow. It must be done prior to the AFM experiment and requires autoclaved material.

Necessary equipment:

- Spectrophotometer and two adsorption cells
- Autoclaved tips + pipette (1 mL)
- Autoclaved LB
- Autoclaved flask
- Ultra-pure water
- Two bacterial waste beakers, one for liquids and one for pipette tips.

First, fill up the flask with 50 mL of LB. Next, create a blank adsorption cell using LB (see A.2.2). Measure it as the blank on the spectrophotometer.

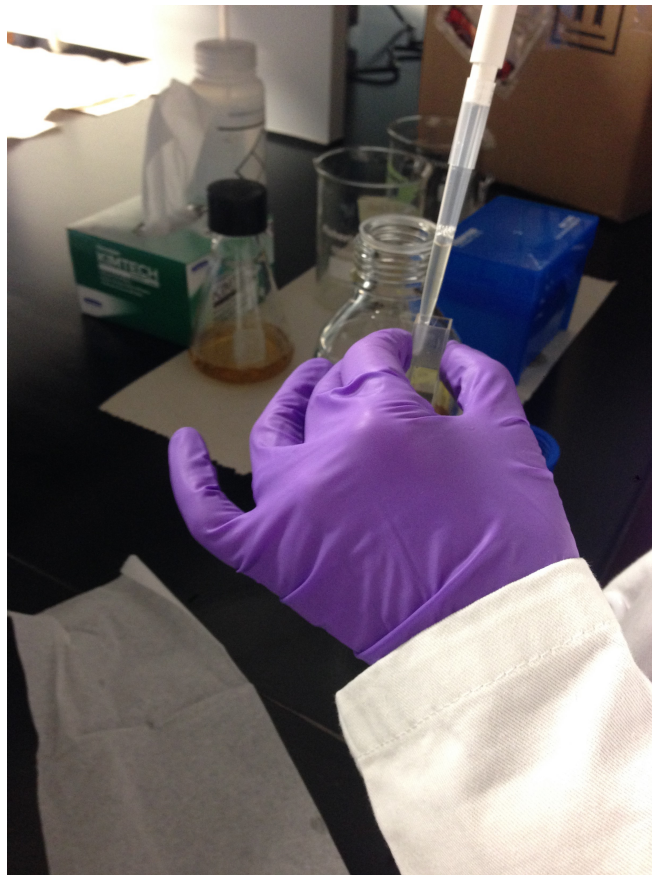


Figure A.2.2: Blank LB

Now, measure the bacteria culture that stayed in the incubator over night. Write down the absorbance and transmittance.

Take 2 mL of the cultured bacteria and put it in the new flaks. Measure the optical density (OD) and write down the time of dilution.

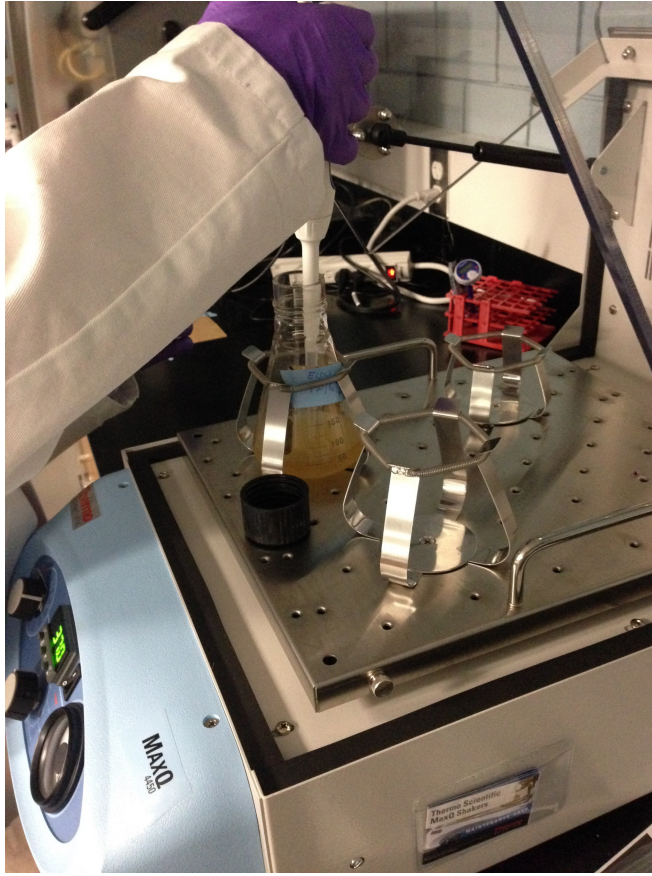


Figure A.2.3: Taped flask in the incubator

Put the new flask in the incubator and increase the speed to 175 rpm. It might be useful to secure the flask by taping it to the incubator (as seen in figure A.2.3) in order to prevent spill.

The bacteria will take approximately 1,5-2 hours to grow. It should be collected at an optical OD_{600} (absorbance) of 0,500 A.

Clean the adsorption cells with DI over a waste beaker

A.2.3 Collecting the bacteria and preparing the fluorescent dye

Information

Check the *OD* regularly as described in A.2.2. When the OD_{600} reaches 0,8 A, the bacteria are ready to be collected.

Remember to take the fluorescent dye kit out of the freezer!

Necessary equipment:

- Two autoclaved centrifuge tube
- Autoclaved Phosphate-buffered saline, (PBS, P4417 Sigma-Aldrich)
- LIVE/DEAD® BacLight™ Bacterial Viability Kit, for microscopy (ThermoFisher)
- Autoclaved pipette tips (1000 μ L, 200 μ L, 1 μ L)

Collect 1 mL of bacteria in a centrifuge tube. Place it in a centrifuge, and run for 1 min (remember to put a tube filled with PBS on the opposite side to create a counterweight in the centrifuge).

Empty the liquid in a waste beaker, and fill the tube with PBS. Vortex until the bacteria is dissolved and centrifuge again. This step should be repeated twice.

To prepare the fluorescent dye, centrifuge both tubes for 1 min. Take 2 μ L of each tube, along with 300 μ L of PBS and put them in a centrifuge tube. Vortex until well-mixed.

The tube should be stored in a dark place while waiting to be used.

A.3 Protocol for preparing the probe

Information

In order for the bacterial cells to adhere, the cantilever has to be coated with a solution of Polydopamine. The preparation of this solution is similar to the one described in A.1.3.

Necessary equipment:

- pH meter
- Ultra-pure water
- A vortex stirrer
- A 25 mL graduated cylinder
- A 10 mL graduated cylinder
- A 20 mL beaker
- Trizma Hydrochloride solution (Sigma Aldrich, T3038)
- NaOH, 1M (Sigma Aldrich, 71463)
- Dopamine Hydrochloride (Sigma Aldrich, H8502) (Should be stored in the refrigerator and in a dry place.)
- A small 20 mL flask
- An AFM probe (MLCTO-10)
- UV/O₃- oxidizer (BioForce, UV/Ozone procleaner plus)

First, start by placing the AFM probe in the UV/O₃ oxidizer for 20 min. When it is done, place the probe on a small glass plate.

Mix 19.8 mL ultra-pure water and 200 μ L Trizma in the beaker. Turn on the pH meter, and wait for it to stabilize. It should stabilize around 8.

With a pipette, add 20 μL of NaOH to the beaker. Measure the pH. It should increase to approximately 8,5.

Pour 10 mL of the prepared solution into a cylinder and later in the vial. You can pour the rest of the solution in another vial in case it is needed for later experiments.

Take the Dopamine Hydrochloride out of the refrigerator and add 40 mg to the vial containing the solution. Mix good with the vortex stirrer making sure that all the powder is dissolved.

Pour the Polydopamine solution into a weighing dish, and carefully soak the AFM probe (see A.3.1).



Figure A.3.1: AFM probe soaked in Polydopamine

Place the weighing dish on a shaker at 75 rpm for 15 min.

When the probe is ready, take it carefully out of the solution. Make sure that the cantilever doesn't break off!



Figure A.3.2: Desiccator with Nitrogen flow

Place the probe in a similar plate filled with ultra-pure water in order to rinse it. Then put the cantilever on the glass plate, and put it in a desiccator under Nitrogen flow until dried (see figure A.3.2).

A.4 Protocol for gluing the sample of membrane

Necessary equipment:

- Autoclaved Petri dish
- glass plate
- Quick dry Epoxy
- Nitrogen gas
- Tweezers and scissors

First, the glass plate, the Petri dish and a piece of the membrane must be dried with Nitrogen gas. It is very important that they are completely dry, because the presence of water may decrease the efficiency of the epoxy.

While holding the membrane with tweezers, cut off the parts that have been damaged or touched. The piece to be glued should not be too big.

In a dish, put a drop of the epoxy resin and a drop of the hardener and stir. With a needle, deposit a small amount of glue on the glass plate. It should be glued slightly to the right. Gently put the membrane on the plate. Do not apply any force on the membrane using tweezers or other sharp objects. In stead, use one of the membrane pieces that are leftover and put it on top of the glued membrane while pressing gently. Leave the membrane to dry for approximately 10 min.

A.5 Protocol for determining the flux and permeability of a membrane

Information

Use the provided excel-sheet. Cut a pristine sample and a PDA sample from the same membrane to make sure the results are comparable. It is very important that your sample does not contain pin holes or any other defects that might lead to the water leaking through!

Necessary equipment:

- Timer
- Ultra-pure N_2 tank
- Amicon 8010 Stirred Cell
- A small Erlenmeyer flask
- A scale
- Ultra-pure water
- 2,5 cm circular membrane disk
- A clean glass plate
- Tweezers
- Box cutter
- A stirring plate

First, start by cutting the membrane to a 2,5 cm circular disk. To do it, either make a template with a piece of paper, or use one of the commercial membrane disks we have. Put the membrane with the active side down on a clean glass plate and, using the box cutter, cut around the template.

Once you have your disk, place it in its holder using tweezers (see Figure A.5.1). Put the rubber ring on top. Make sure you don't touch or damage the membrane.

Screw on the container and put in the stirrer. Fill up the container with around 10 mL of ultra-pure water.

Put on the cap with the valve opened. Make sure the valve faces the same side as the tube coming out of the cell and close it.

Put the cell in its holder as shown in Figure A.5.1 and place the end of the tube in the Erlenmeyer flask and put it on the scale. Put the cell on the stirring plate and turn it on.

Take the tube coming from the nitrogen tank and screw it on the cap of the cell.

Before starting the measurements, the membrane has to be conditioned. Open the nitrogen tank (top valve). Then, open the small valve that let's air in the cell. Before you do that, make sure that the pressure regulating valve is almost loose. When air starts floating in the cell, increase the pressure to 50 psi. Run the whole container and repeat this step 3 times.

Once the membrane is conditioned, the measurements can start. Start with a pressure of 10 psi followed by 20,30,40 and 50 psi.

If there is enough water left, you can go directly from one pressure to another without un-mounting the whole system and carry on your measurements. Just make sure that you write the correct weight at time 0 (the weight will not be 0!).

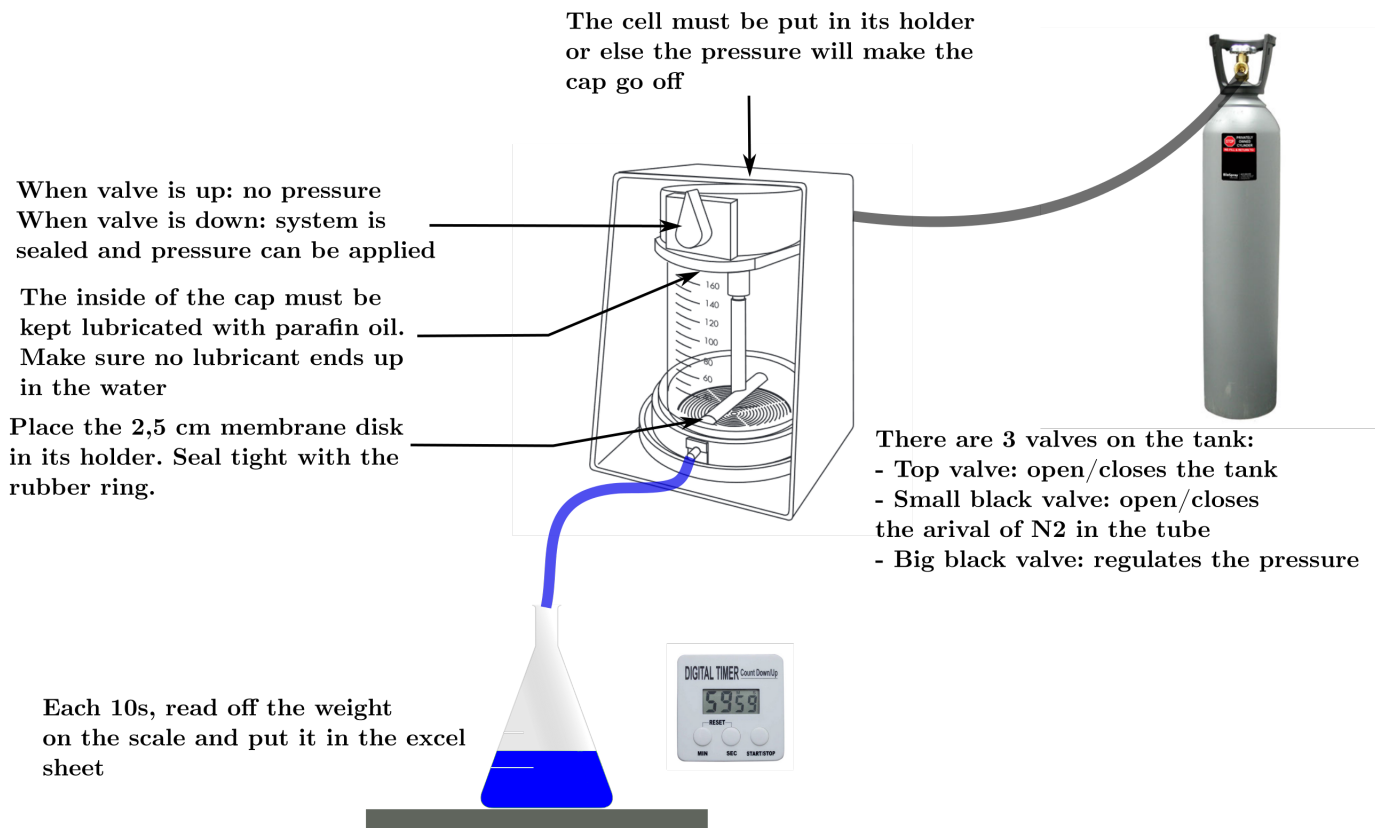


Figure A.5.1: The set-up for determining the flux and permeability.

Appendix B

Pressure on a single cell on a membrane surface

According to Goren (1979), the hydrodynamic force on spherical particle close to the membrane is computed as:

$$F = 6\pi\mu U a \phi \quad (\text{B.0.1})$$

where U is the velocity of fluid passing through membrane, a is the radius of sphere, μ the dynamic viscosity of water (10^{-3} Pas) and ϕ is the hydrodynamic correction factor because of the presence of the membrane.

$$\phi = \left[\frac{2Ka}{3} + (1,072^2) \right]^{\frac{1}{2}} \quad (\text{B.0.2})$$

K is the hydrodynamic resistance of the membrane defined as:

$$K = A_{mb}\mu \quad (\text{B.0.3})$$

A_{mb} is the permeability of the membrane.

*APPENDIX B. PRESSURE ON A SINGLE CELL ON A MEMBRANE SURFACE*104

The cell was simplified to a sphere with a radius of $2 \mu\text{m}$, the velocity $0,27 \text{ m/s}$ and the permeability $210 \frac{\text{L}}{\text{m}^2\text{hbar}}$.

The pressure was found to be $11 \cdot 10^6 \text{pN}$.

Appendix C

T-tests

Two sample t Test (17.07.2016 20:29:41)

Notes

X-Function	Two sample t Test
User Name	Anissa
Time	17.07.2016 20:29:41
Data Filter	No

Input Data

	Data	Range
1st Data Range	[Dataforprist]Prist 600"IC"Adhesion 0s"	[1*:141*]
2nd Data Range	[DataforPDA]PDA 600"IC"Adhesion 0s"	[1*:128*]

Descriptive Statistics

	N	Mean	SD	SEM	Median
"Adhesion 0s"	126	223.19863	215.03447	19.15679	162.9425
	128	140.08649	133.20826	11.77406	94.65025
Difference		83.11214		22.40677	
Overall	254	181.31534	182.99365	11.48204	121.1605

Standard Error of Mean (SEM) of difference is computed under the condition that equal variance is assumed.

t-Test Statistics

	t Statistic	DF	Prob> t
Equal Variance Assumed	3.70924	252	2.55738E-4
Equal Variance NOT Assumed (Welch Correction)	3.69621	208.054	2.79874E-4

Null Hypothesis: mean1-mean2 = 0
 Alternative Hypothesis: mean1-mean2 <> 0
 At 0.05 level, when equal variance is assumed, Mean1 - Mean2 is significantly different from 0
 At 0.05 level, when equal variance is NOT assumed, Mean1 - Mean2 is significantly different from 0

Two sample t Test (17.07.2016 20:32:04)

Notes

X-Function	Two sample t Test
User Name	Anissa
Time	17.07.2016 20:32:04
Data Filter	No

Input Data

	Data	Range
1st Data Range	[Dataforprist]"Prist 600"!G"Adhesion 2s"	[1*:141*]
2nd Data Range	[DataforPDA]"PDA 600"!G"Adhesion 2s"	[1*:128*]

Descriptive Statistics

	N	Mean	SD	SEM	Median
"Adhesion 2s"	104	430.86068	274.41163	26.90827	335.0875
	128	234.42102	193.19822	17.07647	191.1555
Difference		196.43966		30.77169	
Overall	232	322.48018	252.3535	16.56782	251.49

Standard Error of Mean (SEM) of difference is computed under the condition that equal variance is assumed.

t-Test Statistics

	t Statistic	DF	Prob> t
Equal Variance Assumed	6.38378	230	9.43322E-10
Equal Variance NOT Assumed (Welch Correction)	6.16389	179.10953	4.57661E-9

Null Hypothesis: mean1-mean2 = 0
 Alternative Hypothesis: mean1-mean2 <> 0
 At 0.05 level, when equal variance is assumed, Mean1 - Mean2 is significantly different from 0
 At 0.05 level, when equal variance is NOT assumed, Mean1 - Mean2 is significantly different from 0

Two sample t Test (17.07.2016 20:32:28)

Notes

X-Function	Two sample t Test
User Name	Anissa
Time	17.07.2016 20:32:28
Data Filter	No

Input Data

	Data	Range
1st Data Range	[Dataforprist]"Prist 600"!K"Adhesion 5s"	[1*:109*]
2nd Data Range	[DataforPDA]"PDA 600"!K"Adhesion 5s"	[1*:125*]

Descriptive Statistics

	N	Mean	SD	SEM	Median
"Adhesion 5s"	102	559.84559	419.6475	41.55129	416.4215
	125	320.93207	244.19772	21.84171	254.734
Difference		238.91352		44.63778	
Overall	227	428.28528	354.40937	23.52298	316.502

Standard Error of Mean (SEM) of difference is computed under the condition that equal variance is assumed.

t-Test Statistics

	t Statistic	DF	Prob> t
Equal Variance Assumed	5.35227	225	2.13674E-7
Equal Variance NOT Assumed (Welch Correction)	5.08953	154.89432	1.02751E-6

Null Hypothesis: mean1-mean2 = 0
 Alternative Hypothesis: mean1-mean2 <> 0
 At 0.05 level, when equal variance is assumed, Mean1 - Mean2 is significantly different from 0
 At 0.05 level, when equal variance is NOT assumed, Mean1 - Mean2 is significantly different from 0

Two sample t Test (17.07.2016 20:35:28)

Notes

X-Function	Two sample t Test
User Name	Anissa
Time	17.07.2016 20:35:28
Data Filter	No

Input Data

	Data	Range
1st Data Range	[prstinematlab]prist_data_mata b!A"Rupture length 0s"	[1*:112*]
2nd Data Range	[PDAdatamatlab]pda_data_mat lab!A"Rupture length 0s"	[1*:130*]

Descriptive Statistics

	N	Mean	SD	SEM	Median
"Rupture length 0s"	112	1.08216	1.63377	0.15438	0.30716
	130	0.807	0.83932	0.07361	0.41716
Difference		0.27516		0.16374	
Overall	242	0.93435	1.2749	0.08195	0.40204

Standard Error of Mean (SEM) of difference is computed under the condition that equal variance is assumed.

t-Test Statistics

	t Statistic	DF	Prob> t
Equal Variance Assumed	1.68044	240	0.09417
Equal Variance NOT Assumed (Welch Correction)	1.60885	160.09446	0.10962

Null Hypothesis: mean1-mean2 = 0
 Alternative Hypothesis: mean1-mean2 <> 0
 At 0.05 level, when equal variance is assumed, Mean1 - Mean2 is NOT significantly different from 0
 At 0.05 level, when equal variance is NOT assumed, Mean1 - Mean2 is NOT significantly different from 0

Two sample t Test (17.07.2016 20:35:47)

Notes

X-Function	Two sample t Test
User Name	Anissa
Time	17.07.2016 20:35:47
Data Filter	No

Input Data

	Data	Range
1st Data Range	[prstinematlab]prist_data_matab!C"Rupture length 2s"	[1*:96*]
2nd Data Range	[PDAdatamatlab]pda_data_matlab!C"Rupture length 2s"	[1*:125*]

Descriptive Statistics

		N	Mean	SD	SEM	Median
"Rupture length 2s"		96	1.87056	1.86533	0.19038	1.386
		125	0.74227	0.80487	0.07199	0.416
	Difference		1.12828		0.18588	
	Overall	221	1.23239	1.4771	0.09936	0.51923

Standard Error of Mean (SEM) of difference is computed under the condition that equal variance is assumed.

t-Test Statistics

	t Statistic	DF	Prob> t
Equal Variance Assumed	6.06986	219	5.57863E-9
Equal Variance NOT Assumed (Welch Correction)	5.54342	122.19641	1.74056E-7

Null Hypothesis: mean1-mean2 = 0
 Alternative Hypothesis: mean1-mean2 <> 0
 At 0.05 level, when equal variance is assumed, Mean1 - Mean2 is significantly different from 0
 At 0.05 level, when equal variance is NOT assumed, Mean1 - Mean2 is significantly different from 0

Two sample t Test (17.07.2016 20:36:09)

Notes

X-Function	Two sample t Test
User Name	Anissa
Time	17.07.2016 20:36:09
Data Filter	No

Input Data

	Data	Range
1st Data Range	[prstinematlab]prist_data_mata b!E"Rupture length 5s"	[1*:97*]
2nd Data Range	[PDAdatamatlab]pda_data_mat lab!E"Rupture length 5s"	[1*:123*]

Descriptive Statistics

		N	Mean	SD	SEM	Median
"Rupture length 5s"		97	1.72264	1.78152	0.18089	1.41
		123	0.84899	0.86124	0.07766	0.547
	Difference		0.87364		0.18283	
	Overall	220	1.23419	1.4119	0.09519	0.6715

Standard Error of Mean (SEM) of difference is computed under the condition that equal variance is assumed.

t-Test Statistics

	t Statistic	DF	Prob> t
Equal Variance Assumed	4.77852	218	3.2441E-6
Equal Variance NOT Assumed (Welch Correction)	4.43811	131.14193	1.90517E-5

Null Hypothesis: mean1-mean2 = 0
 Alternative Hypothesis: mean1-mean2 <> 0
 At 0.05 level, when equal variance is assumed, Mean1 - Mean2 is significantly different from 0
 At 0.05 level, when equal variance is NOT assumed, Mean1 - Mean2 is significantly different from 0

Two sample t Test (17.07.2016 20:15:50)

Notes

X-Function	Two sample t Test
User Name	Anissa
Time	17.07.2016 20:15:50
Data Filter	No

Input Data

	Data	Range
Group Range	[prstinematlab]prist_data_mata b!A"Rupture length 0s"	[1*:112*]
Data Range	[prstinematlab]prist_data_mata b!C"Rupture length 2s"	[1*:96*]

Descriptive Statistics

	N	Mean	SD	SEM	Median	
"Rupture length 0s"	112	1.08216	1.63377	0.15438	0.30716	
"Rupture length 2s"	96	1.87056	1.86533	0.19038	1.386	
	Difference	-0.7884		0.24262		
	Overall	208	1.44604	1.7842	0.12371	0.53383

Standard Error of Mean (SEM) of difference is computed under the condition that equal variance is assumed.

t-Test Statistics

	t Statistic	DF	Prob> t
Equal Variance Assumed	-3.2495	206	0.00135
Equal Variance NOT Assumed (Welch Correction)	-3.21657	190.5111	0.00152

Null Hypothesis: mean1-mean2 = 0
 Alternative Hypothesis: mean1-mean2 <> 0
 At 0.05 level, when equal variance is assumed, Mean1 - Mean2 is significantly different from 0
 At 0.05 level, when equal variance is NOT assumed, Mean1 - Mean2 is significantly different from 0

Two sample t Test (17.07.2016 20:16:15)

Notes

X-Function	Two sample t Test
User Name	Anissa
Time	17.07.2016 20:16:15
Data Filter	No

Input Data

	Data	Range
Group Range	[prstinematlab]prist_data_mata b!C"Rupture length 2s"	[1*:96*]
Data Range	[prstinematlab]prist_data_mata b!E"Rupture length 5s"	[1*:97*]

Descriptive Statistics

	N	Mean	SD	SEM	Median
"Rupture length 2s"	96	1.87056	1.86533	0.19038	1.386
"Rupture length 5s"	97	1.72264	1.78152	0.18089	1.41
Difference		0.14792		0.26255	
Overall	193	1.79621	1.82044	0.13104	1.41

Standard Error of Mean (SEM) of difference is computed under the condition that equal variance is assumed.

t-Test Statistics

	t Statistic	DF	Prob> t
Equal Variance Assumed	0.56341	191	0.57381
Equal Variance NOT Assumed (Welch Correction)	0.56328	190.39558	0.57391

Null Hypothesis: mean1-mean2 = 0
 Alternative Hypothesis: mean1-mean2 <> 0
 At 0.05 level, when equal variance is assumed, Mean1 - Mean2 is NOT significantly different from 0
 At 0.05 level, when equal variance is NOT assumed, Mean1 - Mean2 is NOT significantly different from 0

Two sample t Test (17.07.2016 20:16:35)

Notes

X-Function	Two sample t Test
User Name	Anissa
Time	17.07.2016 20:16:35
Data Filter	No

Input Data

	Data	Range
Group Range	[prstinematlab]prist_data_mata b!E"Rupture length 5s"	[1*:97*]
Data Range	[prstinematlab]prist_data_mata b!A"Rupture length 0s"	[1*:112*]

Descriptive Statistics

	N	Mean	SD	SEM	Median	
"Rupture length 5s"	97	1.72264	1.78152	0.18089	1.41	
"Rupture length 0s"	112	1.08216	1.63377	0.15438	0.30716	
	Difference	0.64047		0.23633		
	Overall	209	1.37942	1.72968	0.11964	0.573

Standard Error of Mean (SEM) of difference is computed under the condition that equal variance is assumed.

t-Test Statistics

	t Statistic	DF	Prob> t
Equal Variance Assumed	2.71009	207	0.00729
Equal Variance NOT Assumed (Welch Correction)	2.69326	196.58053	0.00769

Null Hypothesis: mean1-mean2 = 0
 Alternative Hypothesis: mean1-mean2 <> 0
 At 0.05 level, when equal variance is assumed, Mean1 - Mean2 is significantly different from 0
 At 0.05 level, when equal variance is NOT assumed, Mean1 - Mean2 is significantly different from 0

Two sample t Test (17.07.2016 20:17:00)

Notes

X-Function	Two sample t Test
User Name	Anissa
Time	17.07.2016 20:17:00
Data Filter	No

Input Data

	Data	Range
Group Range	[Dataforprist]Prist 600!C"Adhesion 0s"	[1*:141*]
Data Range	[Dataforprist]Prist 600!G"Adhesion 2s"	[1*:141*]

Descriptive Statistics

	N	Mean	SD	SEM	Median
"Adhesion 0s"	126	223.19863	215.03447	19.15679	162.9425
"Adhesion 2s"	104	430.86068	274.41163	26.90827	335.0875
Difference		-207.66205		32.28053	
Overall	230	317.09799	264.26939	17.42541	223.389

Standard Error of Mean (SEM) of difference is computed under the condition that equal variance is assumed.

t-Test Statistics

	t Statistic	DF	Prob> t
Equal Variance Assumed	-6.43304	228	7.27103E-10
Equal Variance NOT Assumed (Welch Correction)	-6.28691	193.01295	2.11345E-9

Null Hypothesis: mean1-mean2 = 0
 Alternative Hypothesis: mean1-mean2 <> 0
 At 0.05 level, when equal variance is assumed, Mean1 - Mean2 is significantly different from 0
 At 0.05 level, when equal variance is NOT assumed, Mean1 - Mean2 is significantly different from 0

Two sample t Test (17.07.2016 20:17:20)

Notes

X-Function	Two sample t Test
User Name	Anissa
Time	17.07.2016 20:17:20
Data Filter	No

Input Data

	Data	Range
Group Range	[Dataforprist]"Prist 600"IG"Adhesion 2s"	[1*:141*]
Data Range	[Dataforprist]"Prist 600"IK"Adhesion 5s"	[1*:109*]

Descriptive Statistics

	N	Mean	SD	SEM	Median
"Adhesion 2s"	104	430.86068	274.41163	26.90827	335.0875
"Adhesion 5s"	102	559.84559	419.6475	41.55129	416.4215
Difference		-128.98491		49.30991	
Overall	206	494.727	358.85533	25.00264	376.6495

Standard Error of Mean (SEM) of difference is computed under the condition that equal variance is assumed.

t-Test Statistics

	t Statistic	DF	Prob> t
Equal Variance Assumed	-2.6158	204	0.00957
Equal Variance NOT Assumed (Welch Correction)	-2.60559	173.54717	0.00997

Null Hypothesis: mean1-mean2 = 0
 Alternative Hypothesis: mean1-mean2 <> 0
 At 0.05 level, when equal variance is assumed, Mean1 - Mean2 is significantly different from 0
 At 0.05 level, when equal variance is NOT assumed, Mean1 - Mean2 is significantly different from 0

Two sample t Test (17.07.2016 20:17:40)

Notes

X-Function	Two sample t Test
User Name	Anissa
Time	17.07.2016 20:17:40
Data Filter	No

Input Data

	Data	Range
Group Range	[Dataforprist]"Prist 600"!"K"Adhesion 5s"	[1*:109*]
Data Range	[Dataforprist]"Prist 600"!"C"Adhesion 0s"	[1*:141*]

Descriptive Statistics

		N	Mean	SD	SEM	Median
"Adhesion 5s"		102	559.84559	419.6475	41.55129	416.4215
"Adhesion 0s"		126	223.19863	215.03447	19.15679	162.9425
	Difference		336.64697		43.01057	
	Overall	228	373.80385	363.26217	24.05762	229.911

Standard Error of Mean (SEM) of difference is computed under the condition that equal variance is assumed.

t-Test Statistics

	t Statistic	DF	Prob> t
Equal Variance Assumed	7.82707	226	1.91343E-13
Equal Variance NOT Assumed (Welch Correction)	7.35765	143.26967	1.3325E-11

Null Hypothesis: mean1-mean2 = 0
 Alternative Hypothesis: mean1-mean2 <> 0
 At 0.05 level, when equal variance is assumed, Mean1 - Mean2 is significantly different from 0
 At 0.05 level, when equal variance is NOT assumed, Mean1 - Mean2 is significantly different from 0

Two sample t Test (17.07.2016 20:13:28)

Notes

X-Function	Two sample t Test
User Name	Anissa
Time	17.07.2016 20:13:28
Data Filter	No

Input Data

	Data	Range
Group Range	[PDAdatamatlab]pda_data_mat lab!A"Rupture length 0s"	[1*:130*]
Data Range	[PDAdatamatlab]pda_data_mat lab!C"Rupture length 2s"	[1*:125*]

Descriptive Statistics

	N	Mean	SD	SEM	Median
"Rupture length 0s"	130	0.807	0.83932	0.07361	0.41716
"Rupture length 2s"	125	0.74227	0.80487	0.07199	0.416
Difference		0.06473		0.10305	
Overall	255	0.77527	0.82164	0.05145	0.416

Standard Error of Mean (SEM) of difference is computed under the condition that equal variance is assumed.

t-Test Statistics

	t Statistic	DF	Prob> t
Equal Variance Assumed	0.6281	253	0.5305
Equal Variance NOT Assumed (Welch Correction)	0.62862	252.99838	0.53016

Null Hypothesis: mean1-mean2 = 0
 Alternative Hypothesis: mean1-mean2 <> 0
 At 0.05 level, when equal variance is assumed, Mean1 - Mean2 is NOT significantly different from 0
 At 0.05 level, when equal variance is NOT assumed, Mean1 - Mean2 is NOT significantly different from 0

Two sample t Test (17.07.2016 20:13:52)

Notes

X-Function	Two sample t Test
User Name	Anissa
Time	17.07.2016 20:13:52
Data Filter	No

Input Data

	Data	Range
Group Range	[PDAdatamatlab]pda_data_mat lab!C"Rupture length 2s"	[1*:125*]
Data Range	[PDAdatamatlab]pda_data_mat lab!E"Rupture length 5s"	[1*:123*]

Descriptive Statistics

	N	Mean	SD	SEM	Median
"Rupture length 2s"	125	0.74227	0.80487	0.07199	0.416
"Rupture length 5s"	123	0.84899	0.86124	0.07766	0.547
Difference		-0.10672		0.10583	
Overall	248	0.7952	0.83333	0.05292	0.468

Standard Error of Mean (SEM) of difference is computed under the condition that equal variance is assumed.

t-Test Statistics

	t Statistic	DF	Prob> t
Equal Variance Assumed	-1.00836	246	0.31427
Equal Variance NOT Assumed (Welch Correction)	-1.00781	244.28695	0.31454

Null Hypothesis: mean1-mean2 = 0
 Alternative Hypothesis: mean1-mean2 <> 0
 At 0.05 level, when equal variance is assumed, Mean1 - Mean2 is NOT significantly different from 0
 At 0.05 level, when equal variance is NOT assumed, Mean1 - Mean2 is NOT significantly different from 0

Two sample t Test (17.07.2016 20:15:17)

Notes

X-Function	Two sample t Test
User Name	Anissa
Time	17.07.2016 20:15:17
Data Filter	No

Input Data

	Data	Range
Group Range	[PDAdatamatlab]pda_data_matlab!E"Rupture length 5s"	[1*:123*]
Data Range	[PDAdatamatlab]pda_data_matlab!A"Rupture length 0s"	[1*:130*]

Descriptive Statistics

	N	Mean	SD	SEM	Median
"Rupture length 5s"	123	0.84899	0.86124	0.07766	0.547
"Rupture length 0s"	130	0.807	0.83932	0.07361	0.41716
Difference		0.04199		0.10692	
Overall	253	0.82742	0.84862	0.05335	0.468

Standard Error of Mean (SEM) of difference is computed under the condition that equal variance is assumed.

t-Test Statistics

	t Statistic	DF	Prob> t
Equal Variance Assumed	0.39273	251	0.69485
Equal Variance NOT Assumed (Welch Correction)	0.39245	249.35083	0.69506

Null Hypothesis: mean1-mean2 = 0
 Alternative Hypothesis: mean1-mean2 <> 0
 At 0.05 level, when equal variance is assumed, Mean1 - Mean2 is NOT significantly different from 0
 At 0.05 level, when equal variance is NOT assumed, Mean1 - Mean2 is NOT significantly different from 0

Two sample t Test (17.07.2016 20:11:16)

Notes

X-Function	Two sample t Test
User Name	Anissa
Time	17.07.2016 20:11:16
Data Filter	No

Input Data

	Data	Range
1st Data Range	[DataforPDA]PDA 600!C"Adhesion 0s"	[1*:128*]
2nd Data Range	[DataforPDA]PDA 600!G"Adhesion 2s"	[1*:128*]

Descriptive Statistics

	N	Mean	SD	SEM	Median
"Adhesion 0s"	128	140.08649	133.20826	11.77406	94.65025
"Adhesion 2s"	128	234.42102	193.19822	17.07647	191.1555
Difference	128	-94.33453		20.74209	-60.94675
Overall	256	187.25375	172.22222	10.76389	138.815

Standard Error of Mean (SEM) of difference is computed under the condition that equal variance is assumed.

t-Test Statistics

	t Statistic	DF	Prob> t
Equal Variance Assumed	-4.54798	254	8.39317E-6
Equal Variance NOT Assumed (Welch Correction)	-4.54798	225.49147	8.84372E-6

Null Hypothesis: mean1-mean2 = 0
 Alternative Hypothesis: mean1-mean2 <> 0
 At 0.05 level, when equal variance is assumed, Mean1 - Mean2 is significantly different from 0
 At 0.05 level, when equal variance is NOT assumed, Mean1 - Mean2 is significantly different from 0

Two sample t Test (17.07.2016 20:12:22)

Notes

X-Function	Two sample t Test
User Name	Anissa
Time	17.07.2016 20:12:22
Data Filter	No

Input Data

	Data	Range
Group Range	[DataforPDA]PDA 600!G*Adhesion 2s"	[1*:128*]
Data Range	[DataforPDA]PDA 600!K*Adhesion 5s"	[1*:125*]

Descriptive Statistics

	N	Mean	SD	SEM	Median
"Adhesion 2s"	128	234.42102	193.19822	17.07647	191.1555
"Adhesion 5s"	125	320.93207	244.19772	21.84171	254.734
Difference		-86.51105		27.64899	
Overall	253	277.16363	223.67853	14.06255	222.455

Standard Error of Mean (SEM) of difference is computed under the condition that equal variance is assumed.

t-Test Statistics

	t Statistic	DF	Prob> t
Equal Variance Assumed	-3.1289	251	0.00196
Equal Variance NOT Assumed (Welch Correction)	-3.12035	235.87355	0.00203

Null Hypothesis: mean1-mean2 = 0
 Alternative Hypothesis: mean1-mean2 <> 0
 At 0.05 level, when equal variance is assumed, Mean1 - Mean2 is significantly different from 0
 At 0.05 level, when equal variance is NOT assumed, Mean1 - Mean2 is significantly different from 0

Two sample t Test (17.07.2016 20:12:53)

Notes

X-Function	Two sample t Test
User Name	Anissa
Time	17.07.2016 20:12:53
Data Filter	No

Input Data

	Data	Range
Group Range	[DataforPDA]*PDA 600*!C*Adhesion 0s"	[1*:128*]
Data Range	[DataforPDA]*PDA 600*!K*Adhesion 5s"	[1*:125*]

Descriptive Statistics

	N	Mean	SD	SEM	Median
"Adhesion 0s"	128	140.08649	133.20826	11.77406	94.65025
"Adhesion 5s"	125	320.93207	244.19772	21.84171	254.734
Difference		-180.84558		24.65367	
Overall	253	229.43707	215.62281	13.55609	162.181

Standard Error of Mean (SEM) of difference is computed under the condition that equal variance is assumed.

t-Test Statistics

	t Statistic	DF	Prob> t
Equal Variance Assumed	-7.33544	251	3.04931E-12
Equal Variance NOT Assumed (Welch Correction)	-7.28832	190.80548	8.09356E-12

Null Hypothesis: mean1-mean2 = 0
 Alternative Hypothesis: mean1-mean2 <> 0
 At 0.05 level, when equal variance is assumed, Mean1 - Mean2 is significantly different from 0
 At 0.05 level, when equal variance is NOT assumed, Mean1 - Mean2 is significantly different from 0